

TECHNISCHE UNIVERSITÄT MÜNCHEN
Lehrstuhl für Proteomik und Bioanalytik

Development and application of small molecule probes for
kinase affinity purification and quantitative chemical proteomics

Xin Ku

Vollständiger Abdruck der von der Fakultät Wissenschaftszentrum Weihenstephan
für Ernährung, Landnutzung und Umwelt der Technischen Universität München zur
Erlangung des akademischen Grades eines

Doktors der Naturwissenschaften

genehmigten Dissertation.

Vorsitzender: Univ.-Prof. Dr. D. Haller

Prüfer der Dissertation: 1. Univ.-Prof. Dr. B. Küster

2. Univ.-Prof. Dr. D. Langosch

Die Dissertation wurde am 08.05.2014 bei der Technischen Universität München
eingereicht und durch die Fakultät Wissenschaftszentrum Weihenstephan für
Ernährung, Landnutzung und Umwelt am 11.06.2014 angenommen.SSS

Table of content

Chapter I	General Introduction	1
Chapter II	Characterization of the binding profile of a small molecule pan-kinase inhibition probe VI16743	35
Chapter III	A chemical probe for quantitative proteomic profiling of fibroblast growth factor receptor and its inhibitors	51
Chapter IV	An affinity probe targeting VEGF receptors for kinase inhibitor selectivity profiling by chemical proteomics	85
Summary		115
Zusammenfassung		117
Acknowledgements		121
List of Publications		123
Curriculum Vitae		125

Chapter I

General Introduction

1.1 Targeted cancer therapy

Cancer refers to a broad group of diseases characterized by the failure in the regulation of many cell activities, which can ultimately results in uncontrolled proliferation of cells and the spread of these cells to other organs through the blood and lymph systems (Matthews and Gerritsen, 2011). It is nowadays the major cause of death worldwide: about 14.1 million new cancer cases and 8.2 million cancer deaths occurred in 2012 (Siegel et al., 2013; WHO, 2013). Therefore, considerable efforts have been devoted to elucidate the molecular mechanism of cancer development and to provide therapeutic strategies. Today, although we have not improved the mortality rate or survival time for metastatic cancer as much as we would have expected (Comis, 2003; Halnan, 1999; Sudhakar, 2009), we do have dramatically broaden and deepen our understanding of cancer biology, identified some characteristics as well as pathways of different tumor entities , and created great prospects. This knowledge is now being used to generate specific tumor treatments, termed targeted therapy, by selectively targeting certain proteins which are differentially expressed or abnormal in the cancer cells, compared to normal cells or tissues (Sawyers, 2004).

Targeted therapy refers to the use of pharmaceutical agents that affect a single or a group of specific molecular target(s) with significant biological functions in cancer cells or tumor microenvironment (Fedorov et al., 2010; Hait and Hambley, 2009; Sawyers, 2004). In contrast, non-targeted therapeutics are drugs usually identified by phenotypic screening of natural products or chemical libraries against cancer cell lines or established animal models without a prior knowledge of targets (Fishman and Porter, 2005; Galmarini et al., 2012). These drugs often react on the downstream consequences of the activated signaling pathways, e.g., DNA synthesis and microtubule assembly (DeVita and Chu, 2008; Verrill, 2009). Since the affected biological processes may or may not be abnormal in malignant compared to normal tissues, untargeted therapies often involve higher risk of toxicity than targeted ones (al-Tweigeri et al., 1996; Carroll et al., 2012).

Targeted therapy encompasses a wide variety of approaches. Major strategies target either tumor antigens by monoclonal antibodies (mAbs) (Kohler and Milstein, 1975) or tumor associated proteins by small molecule drugs (Zhang et al., 2009). Both of them are crucial signaling molecules affecting a variety of activities in cancer cells including cell

growth, survival, proliferation and migration (Katzel et al., 2009; Sawyers, 2004). Therapeutic antibodies are widely investigated for the treatment of different types of cancers during the past decades (Carter, 2001). In spite of the great success in antibody drug development, several obstacles must be acknowledged, for instance, the choice of antigen (Carter, 2006; Parker et al., 1990), immunogenicity of antibodies, the difficulties in delivery and penetration into solid tumors (Butowski and Chang, 2005), antibody half-lives and the high manufacturing costs. Meanwhile, with a growing understanding of tumor pathology at molecular and systems level (Galmarini et al., 2012; Gashaw et al., 2011), more and more critical signaling events for cancer cells have been discovered and characterized. This knowledge has significantly enhanced our opportunity to develop the other important targeted therapeutics: small molecule inhibitors (Hait and Hambley, 2009; Zhang et al., 2009). Unlike mAbs, small molecule agents can penetrate into cancer cells through plasma membranes and interact with the cytoplasmic domain of cell-surface protein targets or other intracellular signaling macromolecules (Dancey and Sausville, 2003; Imai and Takaoka, 2006). In addition, small molecule drugs offer manufacturing and delivery advantages over protein-based drugs as well as patient preference for oral administration (e.g., tablet or capsule) over an injectable antibody therapeutic. Meanwhile, distinct from mAbs, small molecule drugs are not potentially immunogenic and do not suffer from rapid clearance by human antibodies (Baselga, 2001; Goldberg, 2005). Owing to the aforementioned advantages, small molecule chemical agents have become the vast majority of drugs in the global marketplace, as well as the potential new drug entities in preclinical developments and clinical trials. Protein kinases, proved to be very good targets for small molecule inhibitors in targeted cancer therapy (Baselga, 2006), have become one of the largest classes of potential drug targets for the pharmaceutical industry (Hopkins and Groom, 2002; Pearson and Fabbro, 2004) and will be discussed in the next section.

1.2 Protein kinases and their inhibitors

Protein kinases are important mediators of a wide range of cellular functions, regulating diverse processes like proliferation, migration, metabolism and apoptosis. Comprehensive analysis of the human genome revealed 518 kinase genes, a number amounting to approximately 1.7% of all human genes (Manning et al., 2002). These identified protein kinases can be roughly grouped into a total of seven families, based on their sequence similarities among the catalytic domains (Figure 1A) (Manning et al.,

2002). Alterations in these enzymes have been causally linked to numerous pathological disorders especially cancer. Therefore they have demonstrated very promising prospect for targeted treatment, holding approximately 20% of all druggable targets in the pharmaceutical industry (Levitzki, 1999; Matthews and Gerritsen, 2011).

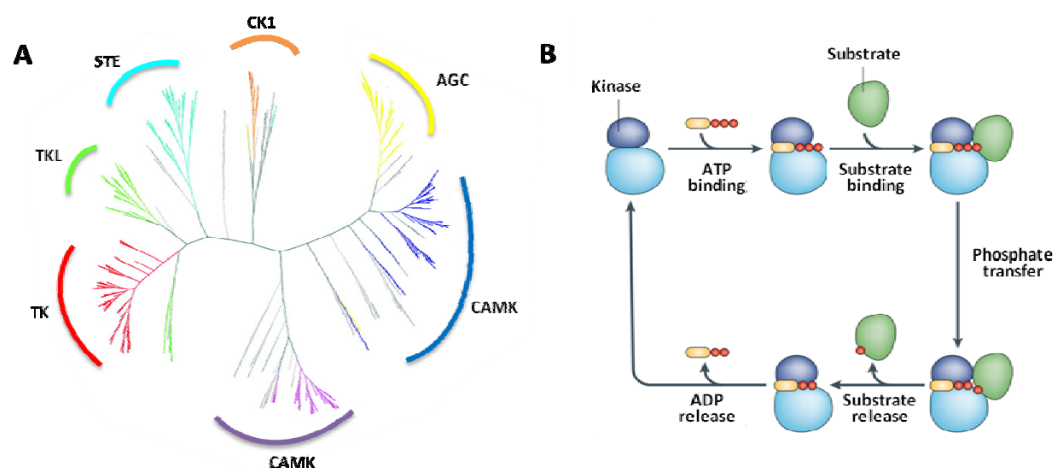


Figure 1 | Classification of protein kinases and the catalytic cycle for substrate phosphorylation by a kinase.

(A) Dendrogram of the human kinome. Major groups are labeled and colored, adapted from (Manning et al., 2002). (B) The catalytic cycle of a kinase, adapted from (Ubersax and Ferrell, 2007). ATP binds to the kinase followed by the substrate protein binding. After binding, the γ -phosphate of ATP (red) is transferred to a Ser, Thr or Tyr residue of the substrate. After being phosphorylated, the substrate is released from the kinase followed by the release of ADP from the active site. Some kinases bind to their protein substrates before binding ATP and others release ADP before releasing the protein substrate.

Protein kinases catalyze phosphorylation reactions by transferring a γ -phosphate group from high energy donor adenosine-triphosphate (ATP) to a substrate protein (Figure 1B). Based on the amino acid residue of the substrate protein they phosphorylate, most protein kinases can be classified as serine/threonine kinases and tyrosine kinases. All protein kinases have a similar protein folding that consists of two lobes: one lobe mainly consists of β -sheets and the other lobe mainly of α -helices. An ATP-binding cleft constituting the active site locates between these two lobes (Johnson et al., 1998; Manning et al., 2002; Traxler and Furet, 1999). Besides, a conserved activation loop is also expected to present in all protein kinases, which is important in regulating kinase activity and is marked by a conserved DFG motif (which refer to one-letter amino acid abbreviations) at the start of the activation loop (Baselga, 2006; Grant, 2009; Zhang et al.,

2009). Movement of the activation loop from DFG-in to DFG-out conformation usually brings an additional hydrophobic binding site directly adjacent to the ATP binding site.

The ubiquitous existence of the ATP binding pocket across kinases has inspired the pharma community to develop small molecule kinase inhibitors. By mimicking the hydrogen bonds that are normally formed by the adenine ring of ATP (Liu and Gray, 2006; Traxler and Furet, 1999), small molecules are able to compete with the ATP to bind the kinase and block the kinase activity, thus inhibiting the phosphorylation cascades in cancer cells. The early developments of small molecule kinase inhibitors often suffered from drawbacks such as lack of potency, specificity and bioavailability for clinical utility due to our blindness to the binding details (Butowski and Chang, 2005; Imai and Takaoka, 2006). Nowadays, utilizing state of art techniques such as molecular modeling, X-ray crystallography or protein NMR, medicinal chemists are better guided to establish the structure activity relationship (SAR) between the compound and the target. These technology advances have greatly influenced the preclinical drug discovery pipeline, leading to the discovery of thousands of potent kinase inhibitors. The first small molecule kinase drug Imatinib (Gleevec, Novartis), targeting the Bcr-Abl kinase, was proved for the treatment of cancer in 2001 (Savage and Antman, 2002). To date, the development of small molecule kinase inhibitors has become a leading strategy for targeted cancer therapy (Baselga, 2006). About 20 kinase inhibitors have been approved by the US FDA till 2014 (Table 1) and hundreds more are in different clinical trials.

Table 1 | Current status of approved small molecule kinase inhibitors with target, indication, company and year of approval.

Drug	Target	Indication	Company	Year
Imatinib	ABL1/2, PDGFR, KIT	CML, CMML, GIST	Novartis	2001
Everolimus	mTOR	Transplantation	Novartis	2003
Gefitinib	EGFR	NSCLC	AstraZeneca	2003
Erlotinib	EGFR	NSCLC, pancreatic cancer	OSI/Roche	2004
Sorafenib	VEGFR2, PDGFR, KIT, FLT3, BRAF	RCC	Onyx and Bayer	2005
Sunitinib	VEGFR1-3, KIT, PDGFR, RET, CSF1R, FLT3	RCC, GIST	Pfizer	2006
Fasudil	Rho	Pulmonary hypertension	Asahi Kasei	2006
Lapatinib	EGFR, ERBB2	Breast cancer	GSK	2007
Dasatinib	ABL1/2, PDGFR, KIT, SRC	CML	Bristol Myers	2007
Nilotinib	ABL1/2, PDGFR, KIT	CML	Novartis	2007
Critozinib	MET, ALK	NSCLC	Pfizer	2011
Vandetanib	RET, VEGFR1/2, FGFR, EGFR	MTC	AstraZeneca	2011
Ruxolitinib	JAK2	IMF	Incyte /Novartis	2011
Vemurafenib	BRAF mutant	Metastatic melanoma	Plexxikon/ Roche	2011
Ponatinib	VEGFR, FGFR, FLT3, TIE	CML, ALL	Ariad	2012
Pazopanib	VEGFR1-3, PDGFR, KIT	RCC	GSK	2012
Axitinib	VEGFR1-3, KIT, PDGFR, CSF1R, FLT3	RCC	Pfizer	2012
Bosutinib	Bcr-Abl, SRC	CML	Pfizer	2012
Regorafenib	VEGFR2, TIE2	Colorectal	Bayer	2012
Afatinib	Her2, EGFR	NSCLC	Boehringer Ingelheim	2013
Ibrutinib	BTK	MCL	Pharmacyclics/J&J	2013

1.3 Angiogenesis and related inhibitors

There are several ways through which the functions of protein kinases can be altered, and all of them lead eventually to the dysregulation of usually well-orchestrated pathways. These variations are usually acquired over a long period of time and lead the normal cells to acquire certain phenotypes which were summarized by Hanahan and Weinberg as the 6 hallmarks of cancer (Figure 2) (Hanahan and Weinberg, 2000, 2011). Each of these hallmarks is a certain biological ability that tumor cells acquire during their multistep development from normal cells.

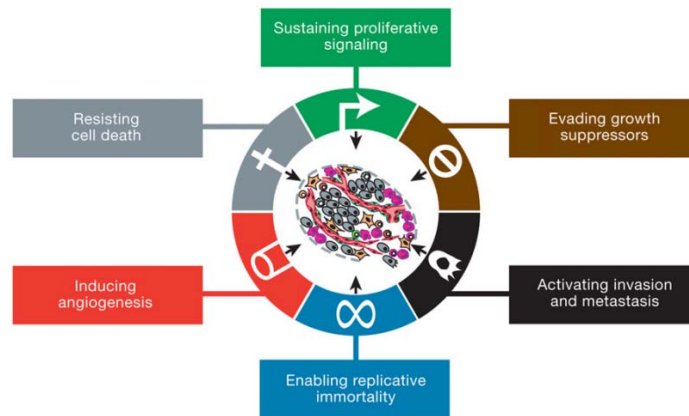


Figure 2 | The six hallmarks of cancer, adapted from (Hanahan and Weinberg, 2000).

Angiogenesis, one of the six hallmarks of cancer, refers to the formation of new blood vessels from pre-existing vessels (Cross and Claesson-Welsh, 2001). Physiological angiogenesis is required for many biological processes such as embryonic development, wound healing and the menstrual cycle (Cross and Claesson-Welsh, 2001; Lieu et al., 2011). Several pathological conditions, such as tumor progression, rheumatoid arthritis and diabetes are also characterized by excessive angiogenesis where vessels develop in an uncontrolled or disorganized manner (Moreira et al., 2007). Judah Folkman first suggested that tumor growth was dependent on angiogenesis in 1971, hypothesizing that the size of tumors would be limited in the absence of angiogenesis (Folkman, 1971). It has been shown that cancer cells can acquire the ability to disturb the balance between proangiogenic effects and antiangiogenic effects, thereby promoting angiogenesis.

A number of signaling molecules have been identified as contributing to the vascular recruitment and development, including the growth factors VEGF, PDGF, FGF, HGF and their corresponding receptors (Lieu et al., 2011; Moreira et al., 2007). Basic fibroblast growth factor (bFGF or FGF-2) was the first identified angiogenesis promoting molecule (Cross and Claesson-Welsh, 2001; Shing et al., 1984), the biological effects of which are mediated by four structurally related receptor tyrosine kinases, namely FGFR-1, -2, -3, and -4. A number of studies have shown that FGFR-1 and FGFR-2 are required for the development and maintenance of the vasculature in the embryo (Deng et al., 1994; Xu et al., 1998). Disruption of the gene encoding FGFR-3 may result in mice with skeletal abnormalities (Colvin et al., 1996), whereas the consequence of inactivation of gene

encoding FGFR-4 has not yet been well understood. Another very important endothelial cell mitogen is the vascular endothelial growth factor (VEGF) family, which renders the microvasculature hyper permeable to allow the circulation of macromolecules (Senger et al., 1983) and promotes angiogenesis (Folkman and Klagsbrun, 1987). These biological effects of VEGFs are mediated via three specific cell surface-expressed receptor tyrosine kinases, VEGFR-1 (Flt-1), VEGFR-2 (KDR or Flk-1) and VEGFR-3 (Flt-4). FGFRs and VEGFRs share many similarities in their structures. Both of them consist of an extracellular ligand binding region and a transmembrane domain followed by an intracellular kinase domain (Shibuya et al., 1999; Taipale et al., 1999).

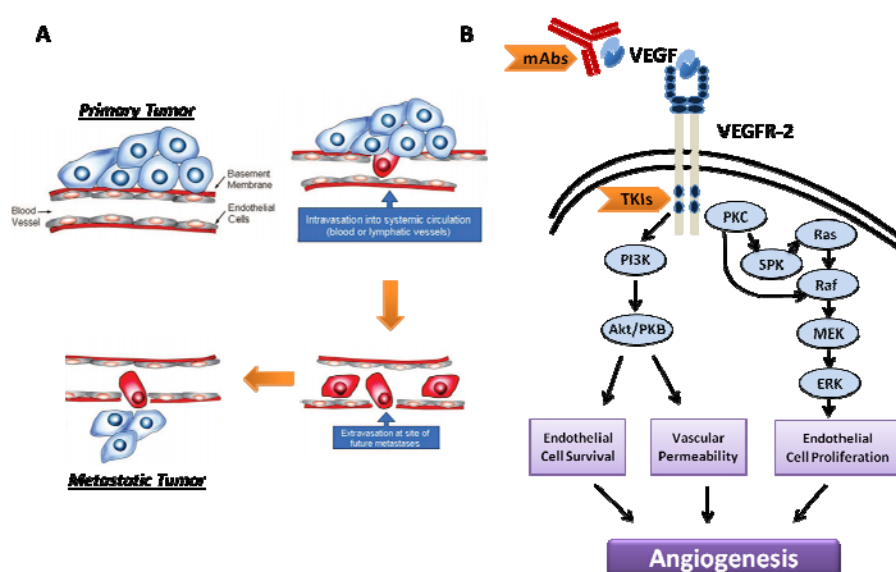


Figure 3 | Schema of the complex metastatic process of tumor cells and the VEGFR mediated signaling pathways.

(A) Metastatic process of tumor cells, adapted from (Dotan et al., 2009). (B) The VEGF/VEGFR signaling pathway. Binding of the ligand (VEGF) to its receptors activate downstream signaling pathways which lead to the promotion of angiogenesis, adapted from (Rini, 2007).

The activation mechanism of VEGFRs and FGFRs share many similarities. Both of them are triggered by ligand binding followed by receptor dimerization which initiates the intermolecular autophosphorylation of specific tyrosine residues within the dimeric complex (Hennequin et al., 1999). Several intracellular signaling cascades are known to be activated further, including the phosphoinositide 3-kinase (PI3K)/Akt pathway (Ferrara, 2004; Ivy et al., 2009) and the Ras-Raf-MEK-ERK pathway (Klint and Claesson-Welsh, 1999; Rini, 2007) (Figure 3). These pathways play important roles in

commanding endothelial cell survival and proliferation as well as vascular permeability, all of which can greatly influence angiogenesis (Cross and Claesson-Welsh, 2001; Cross et al., 2003; Moreira et al., 2007). Therefore, targeting the VEGFRs and FGFRs is regarded as a very promising strategy for inhibiting angiogenesis and tumor growth (Ferrara, 2004; Moreira et al., 2007). In addition, because the angiogenesis related proteins (receptors or ligands) are mainly present in endothelial cells, targeting these proteins reduces the risk of adverse effects that are caused by targeting proteins that are present in a wide range of cells (Kerbel and Folkman, 2002). Furthermore, endothelial cells are relatively stable, quiescent in adults and have a lifespan of many years. Thus, targeting the endothelial cells should provide an anti-cancer treatment that is less likely to trigger treatment-induced resistance (Ferrara, 2005; Gasparini et al., 2005). Owing to these advantageous characteristics, angiogenesis pathways have become very promising targets for cancer therapy.

Therapeutic inhibition of the aforementioned angiogenesis targets may be achieved either via monoclonal antibodies targeting the various ligands (VEGFs, FGFs) (Halin and Neri, 2001; Hicklin et al., 2001), or via intracellular inhibition of the corresponding receptors by small molecule tyrosine kinase inhibitors (TKIs) (Zhang et al., 2009) (Figure 3B). So far, 8 oral angiogenesis inhibitors, representing more than 1/3 of all kinase drugs, have been approved by the US FDA for the clinical treatment of various cancers (Table 1) and many more are under clinical trials. Data from clinical applications already showed excellent application outcomes of these small molecules for oncology treatment (Planchard, 2011; Savas et al., 2013). However, there are still some obstacles to overcome, such as the occurrence of some severe or even life-threatening adverse effects (Chen and Cleck, 2009; Rini, 2007). This field is currently under very active investigation. With a better understanding of the modes of action of these inhibitors, the outcome of cancer treatment via angiogenesis inhibition will be enhanced.

1.4 Selectivity and off-targeting of angiogenesis drugs

As previously described, aberrant kinase function of the VEGF and FGF signaling pathway is highly associated with tumorigenesis and metastasis, which provide a rationale for targeting the VEGF and FGF receptors in the treatment of cancers. However, with expanded clinical experience with the VEGFR and FGFR inhibitors, a number of diverse adverse effects were observed in wound healing and tissue repair as well as in

the cardiovascular and renal systems, which resulted in large numbers of withdrawals or discontinuations of the drugs tested in clinical trials (Chen and Cleck, 2009). Some adverse events are very mild and predictable, which result from angiogenesis inhibition. However, some angiogenesis TKIs are also associated with variable additional “off-target” toxic effects due to their additional inhibitions of other proteins. As mentioned before, small molecule kinase inhibitors are usually ATP-mimics and the ATP binding pockets are highly conserved across more than 2000 ATP-binding proteins including more than 500 protein kinases. Thus, the small molecule kinase inhibitors are usually found to target several other ATP binding proteins. On the other hand, most tumors, particularly solid tumors, are multifactorial and are frequently linked to defects in more than one signaling pathway (Hanahan and Weinberg, 2000, 2011). Therefore, multi-target drugs may also be advantageous for solid tumors by opening up application areas or preventing drug resistance over single-target agents (Hait and Hambley, 2009; Scagliotti and Govindan, 2010). For example, Imatinib was first discovered as a potent Bcr-Abl kinase inhibitor and was approved for the treatment of Chronic Myelogenous Leukemia (CML). However, it was later identified to have great potencies against c-Kit and PDGFR, which resulted in additional applications for the treatment of gastrointestinal tumors (GIST) (Croom and Perry, 2003) and myeloproliferative diseases (Apperley et al., 2002). As the medical and pharmaceutical communities are moving toward personalized medical care, understanding a drug target spectrum as thoroughly as possible is an essential step to fully exploit its therapeutic potential and minimize the toxicity. There are a number of assay platforms developed to serve this purpose. However, many of these assays employ recombinant proteins, which have obvious disadvantages such as not able to reflect the real binding in cells. Recently, chemical proteomics has emerged as a comprehensive and unbiased approach for target profiling under close to physiological conditions and will be briefly reviewed in the following section.

1.5 Mass spectrometry-based chemical proteomics for target profiling

1.5.1 Chemical proteomics

The term proteomics refers to “the large-scale study of the proteome, particularly with regard to expression, structure, function, modifications, interactions, and the changes therein in different environments and conditions” (Mallick and Kuster, 2010). Attributing to the availability of gene and genome sequence databases and the development of ionization techniques for macromolecules, protein or peptide sequencing via tandem mass spectrometry has become one of most comprehensive and versatile tools in proteomics (Mallick and Kuster, 2010; Schirle et al., 2012). These technique advances led to the discovery of numerous protein expression changes that correlate with tumorigenesis (Aebersold and Mann, 2003; Pandey and Mann, 2000). However, determining the relevance of these expression changes with the biological pathways they affect has been hindered by our limited understanding of the proteome and its myriad of functions as well as the modes of the regulation. Recently, diversification of the experimental approaches with a shift from complex unfractionated protein samples to the investigation of subproteomes has been a general trend in proteomics (Angel et al., 2012; Daub et al., 2008; Kruse et al., 2011; Yates et al., 2009). This is significantly promoted by enrichment techniques that allow quantitative or qualitative characterization of lower abundant proteins. Examples include the focused analysis of protein sets that share certain types of post translational modifications, such as “phosphoproteomics” (Daub et al., 2008; Li et al., 2010) and the assignment of proteins to particular subcellular structures, such as nuclei, mitochondria, etc., in an approach termed subcellular proteomics (Boisvert et al., 2010; Dreger, 2003). Recently, the application of chemically engendered probes to enrich protein targets or entire subproteome (e.g. kinases, proteases, phosphatases) from native biological samples has been introduced and summarized under the term chemical proteomics (Bantscheff and Drewes, 2012; Kruse et al., 2008; Oda et al., 2003). Combining affinity purification and advanced mass spectrometry, chemical proteomics provides a comprehensive profile of small molecule-target interactions and enabled a multitude of investigations which are of great value to the drug discovery pipelines (Schirle et al., 2012).

Chemical proteomic approaches encompass a variety of experimental procedures, which can be roughly grouped into two sections, activity- and affinity-based chemical proteomics (Rix and Superti-Furga, 2009), featuring different application possibilities. While both of them can provide valuable information on the identification and quantification of protein expression changes, each approach has distinct advantages and disadvantages, which will be discussed in the next section.

1.5.2 Activity- and affinity-based chemical proteomic

Activity-based chemical proteomic (ABPP) detects members of a class of enzymes which is usually known to be active under certain conditions—for example, in a disease (Cravatt et al., 2008; Nomura et al., 2010). Based on the enzymatic activity of the target protein class, ABPP utilizes a chemical probe to covalently bind the target enzymes and to detect the interactions. These probes are based on compounds that can irreversibly modify their cellular protein targets, thus directly report protein–ligand interactions in native biological samples (Cravatt et al., 2007; Simon and Cravatt, 2010). Typical ABPP probes usually consist of two key elements: a reactive group for binding and covalently labeling the active site of many members of a given enzyme family (or families), and a reporter tag for the detection, enrichment and identification of probe-labeled enzymes in proteomes (Cravatt et al., 2008; Lenz et al., 2011; Nomura et al., 2010) (Figure 4A).

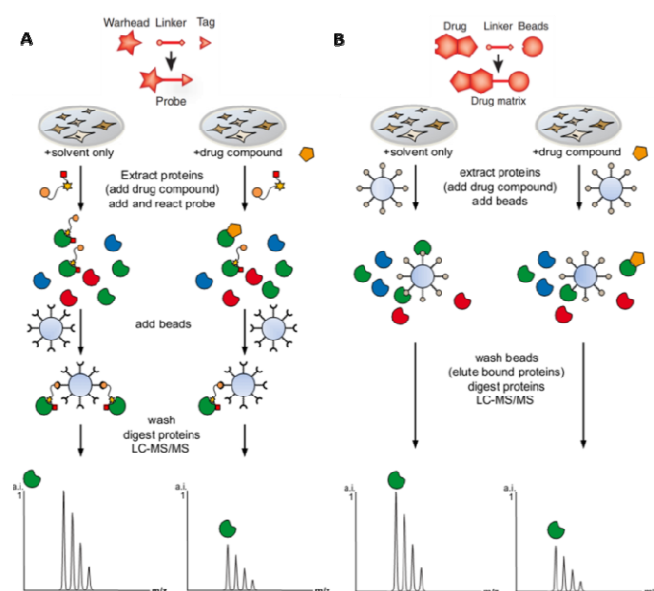


Figure 4 | Comparison of general workflows of activity- and affinity-based chemical proteomics, adapted from (Bantscheff and Drewes, 2012) and (Rix and Superti-Furga, 2009).

(A) Activity-based chemical proteomics: A bifunctional reactive probe is designed to specifically target the active site of an enzyme family. The workflow starts from the incubation of protein lysates with the probe to covalently attach to its target. Then the probe and targets are purified using affinity chromatography. (B) Affinity-based chemical proteomics: The drug of interest is immobilized on a bio-compatible matrix. The immobilized compound is subsequently incubated with a protein extract to specifically enrich the target proteins via affinity-based binding. In both cases, purified proteins are identified and quantified by mass spectrometry.

One of the most important considerations in ABPP is the design of the probes. The introduction of a chemically “tractable” tag is required for the parent bioactive compound. This tag must not or minimally disturb the binding in situ, while it should also feature a handle for the subsequent in vitro protein enrichment and other downstream applications. Terminal alkynes are the most frequently used tags because they are relatively stable and can efficiently react with a variety of azide-containing reporters (Huisgen, 2003; Rix and Superti-Furga, 2009; Simon and Cravatt, 2010), owing to the well-known “click chemistry” (Sharpless and Manetsch, 2006). In conjunction with a range of data acquisition techniques such as gel- and MS-based methods (Lenz et al., 2011; Wang et al., 2012), these probes have enabled the identification of a wide range of enzyme families, including many that have crucial roles in cancer, such as kinases (Cohen et al., 2007; Patricelli et al., 2007), proteases (Kato et al., 2005; Saghatelian et al., 2004), phosphatases (Kumar et al., 2004), histone deacetylases (Salisbury and Cravatt, 2007, 2008) and hydrolases (Kidd et al., 2001; Simon and Cravatt, 2010). ABPP can be used for the identification of new proteins with the defined biochemical activity. It can also be applied to determine the selectivity profile of drugs for a given enzyme family, by pretreatment of the lysate with the drug of interest and subsequent identification of the remaining enzymes (Gillet et al., 2008). Importantly, activity-based probes can be applied for in vivo labeling (Speers and Cravatt, 2004, 2009). Although these probes generally focus only on the active kinases, they are of great value for characterizing dysregulated enzymatic activities in various cancer models (Cravatt et al., 2008; Nomura et al., 2010).

Affinity-based chemical proteomics is another important application of chemical proteomics, which utilizes bioactive small molecules immobilized on a matrix to specifically enrich the binding partners (Bantscheff and Drewes, 2012; Rix et al., 2012). As most bioactive compounds, especially drugs or drug candidates, bind to their protein

targets in a non-covalent fashion, therefore in affinity-based approaches, physical interactions (e.g. Van der Waals and/or hydrophobic interactions) are observed. The compound of interest (whose bioactivity is typically known) is coupled covalently to an inert and biocompatible matrix (such as sepharose beads) via an appropriate linker (Figure 4B) (Bantscheff et al., 2007a; Rix et al., 2012; Rix et al., 2007). In contrast to ABPP, the affinity-based approach allows the identification of binders of unexpected biochemical classes, including proteins even without enzymatic function, and can therefore be used to find entirely novel targets. Recently, affinity-based proteome wide profiling of bioactive compounds *in vivo* was introduced. In 2012, Dasatinib was converted to its corresponding cell-permeable probes by replacing the non-essential hydroxyethylpiperazinyl group in the drug with a terminal alkyne-containing a photo-cross linker, the resulting probe was found to retain most of the original drug's biological activities after administration into cancer cells (Chan et al., 2012). This study is the first demonstration that a small molecule drug could be comprehensively profiled in live cells.

Meanwhile, some challenges and difficulties have to be noticed. First of all, chemical synthesis of a suitable functionalized analog of the compound will generally be required (for subsequent immobilization or detection) and is usually the rate-determining step of the workflow. To guide the structure modification so that the functionalized molecule could retain similar biological activity properties, detailed information about the structure activity relationships of a compound is necessary. Second, a high background level is often observed as a result of non-specific binding, because some proteins are either very abundant or prone to interact generically with hydrophobic or charged surfaces (Bantscheff and Drewes, 2012; Rix and Superti-Furga, 2009; Schirle et al., 2012). Third, membrane proteins (especially those with several transmembrane domains) remain a challenge for this technology, as these proteins require special solubilization conditions so as to obtain their native conformation (Bantscheff et al., 2007a; Daub et al., 2008; Rix and Superti-Furga, 2009).

1.5.3 Drug-target profiling using chemical proteomics

As mentioned before, small molecule kinase inhibitors are expected to bind or modulate more than one protein, which can induce desirable or undesirable consequences (additional applications or toxic side effects). In order to provide evidence-based

guidance for the management of off-target effects as well as more effective and precise treatment, it is of great significance to establish reliable and comprehensive strategies for the identification of drug target profiles. However, this level of information was not achievable in the past in drug discovery partly because of the lack of competent technology. Although some progresses have been made for the prediction of small molecule selectivity profile by molecular modeling (Sciabola et al., 2008), drug discovery traditionally relies more on experimental methods that can screen compounds against a range of proteins to assess their selectivity profiles (Anastassiadis et al., 2011; Karaman et al., 2008). These tools for target identification of bioactive compounds are mostly in vitro-based, using assay panels comprising a set of potential target proteins in isolation (Anastassiadis et al., 2011; Karaman et al., 2008). In most cases recombinant proteins or protein fragments are used instead of the full-length endogenous protein. These recombinant proteins do not necessarily reflect the conformation and activity of the target in its physiological context due to the lack of regulatory domains and interacting proteins, and the possibility of protein misfolding and the expression of incorrect post-translational modifications (PTMs). Hence, data generated in such assays may not be predictive for the efficacy of a compound in cell-based or in vivo models (Bantscheff and Drewes, 2012; Schirle et al., 2012; Zinn et al., 2012). Besides, these assays cannot identify unexpected drug-target interactions (Schirle et al., 2012). Chemical proteomic approaches alleviate this problem to some extent by providing a direct approach, to comprehensively study drug target profiles by exposing the drug to the whole proteome as expressed under physiological context and quantitatively analyzing the interacting partners by advanced mass spectrometry techniques. Nowadays, the main applications of chemoproteomic-based target identification can be grouped into two categories: drug-centric target identification and binding mode-centric drug selectivity profiling (Schirle et al., 2012).

Drug-centric target identification can be carried out by either affinity based proteomics or activity based proteomics. The bioactive molecule of interest is functionalized with a suitable affinity tag (e.g., biotin) or immobilized on a bio-compatible matrix. The resulting probe is then incubated with cell extracts, and bound proteins are identified using mass spectrometry (Bantscheff et al., 2009; Oda et al., 2003; Rix and Superti-Furga, 2009). However, as discussed in the previous section, due to unspecific binding or high background level, some identified “targets” are constantly detected in independent experiments using different probes. These “targets” should be tagged as “false-positive”

identifications and neglected for further analysis (Trinkle-Mulcahy et al., 2008). An elaborate but very laborious strategy to avoid false discovery is to generate both active and inactive analogs of the probe (Oda et al., 2003). Real targets can be short-listed by comparison of the captured proteins from parallel experiments using active and inactive probes. Affinity based competition binding experiments provide a very efficient and labor-saving methodology in addressing false-positive targets. In this approach, an affinity probe is incubated with and without the parent bioactive compound (unmodified) in cell extract respectively (Ong et al., 2009). The binding of true targets to the affinity matrix should be significantly reduced compared to vehicle control, whereas the nonspecific binders do not show this behavior.

Binding mode-centric drug selectivity profiling highlights the establishment of the selectivity profile of a drug across a certain protein target class (kinases, proteases, etc.). Similar to drug-centric target profiling, this can also be achieved by competitive binding assays using either affinity (Bantscheff et al., 2009; Hall, 2006; Rix and Superti-Furga, 2009) or activity based probes (Cravatt et al., 2008; Nomura et al., 2010). However, in selectivity profiling, the drug of interest is typically used as a competitor (over a range of concentrations, see Figure 5, exemplified by affinity based approach) and does not have to be chemically modified. The proteins in the target class usually share a similar binding site (such as ATP binding site) and the employed chemical probes ideally bind to all members of that target class. By quantifying the amount of proteins (affected by drug doses) captured by the affinity matrix or activity probe, the affinity of the compound to all members of the target class can be determined (Bantscheff et al., 2011; Sharma et al., 2009). One such elaborate and successful application is the Kinobeads technology introduced by Bantscheff et al in 2007 (Bantscheff et al., 2007a). Kinobeads are affinity resins consisting of several immobilized chemical probes, which can reversibly bind the highly conserved ATP pockets in native proteins. In our group, the first published version of Kinobeads (containing 7 probes) was optimized into a mixture of five immobilized non-selective kinase inhibitors (Figure 6) after careful optimization. These probes accomplished the enrichment of a broad range of about 350 different kinases and over 2000 additional ATP and nucleotide binding proteins from different cell lines (Moghaddas Gholami et al., 2013), such as chaperones, ATPases, transporters and metabolic enzymes, making the Kinobeads approach a highly valuable tool for kinome research.

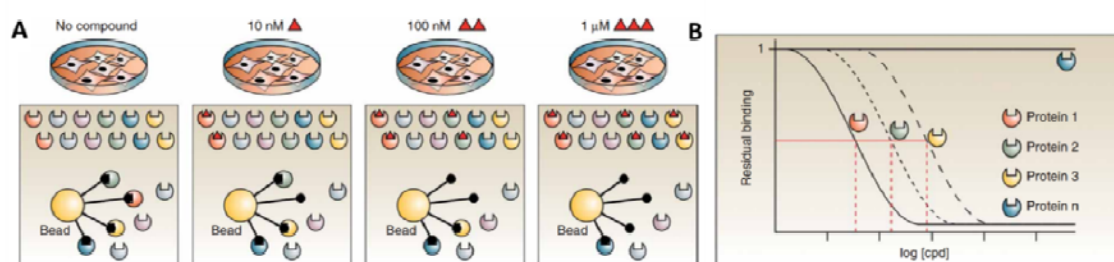


Figure 5 | Overview of the affinity based chemical proteomics assay for drug selectivity profiling, adapted from (Bantscheff et al., 2007a).

(A) Either lysates or cells are treated with vehicle and with drug over a range of concentrations (upper panel). Subsequently, the immobilized probes are added and compete with the “free” drug for ATP-binding or related ligand-binding sites of its targets (lower panels). (B) Samples are digested and analyzed by LC-MS/MS. For each peptide detected, the decrease of signal intensity compared to the vehicle control reflects competition by the “free” drug for its target.

Both drug-centric and binding-mode centric profiling are very powerful and relatively unbiased approaches for the characterization of drug-protein interaction profiles, since all proteins are assayed under close to physiological conditions (e.g., use of relevant cell lines or tissues; proteins at endogenous expression levels and with natural modifications) within only one experiment. In spite of these advantages, some challenges must be acknowledged, notably the incomplete coverage of many proteins that are clinically relevant due to the lack of efficient probes. It should also be noted that, although chemical proteomic experiments can efficiently shortlist target candidates, evidences from cell-based or in vivo assays to validate these targets are still needed.

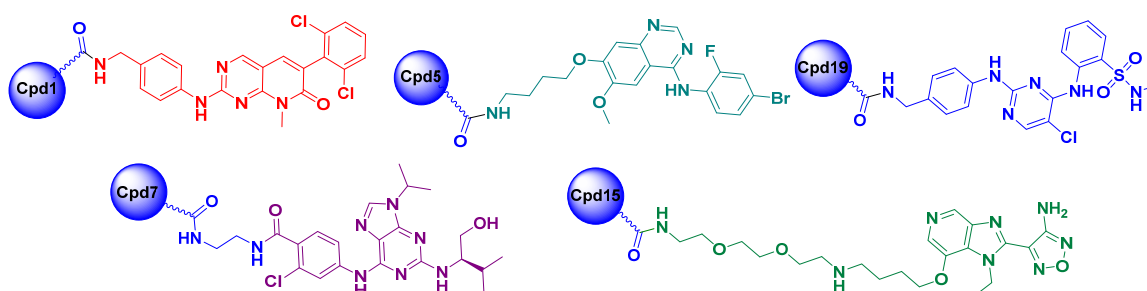


Figure 6 | Immobilized Kinobead compounds. Coupling densities were optimized for each compound and the beads were combined in equal amount to give the probe matrix (Kinobeads) for large kinome profiling.

1.6 Mass spectrometry

Chemical proteomics has become a very active investigation area owing to the outstanding progresses achieved in mass spectrometry (MS) during recent years. These advances in high resolution mass spectrometry offer great opportunity for accurate and systematic analyses of protein and peptides in complex biological samples (Aebersold and Mann, 2003; Mallick and Kuster, 2010). So far, MS-based proteomics has achieved identification and quantification of more than 10,000 proteins from a single cell line (Beck et al., 2011; Nagaraj et al., 2011). In addition, mass spectrometry also provides comprehensive information of proteins on a higher complexity level such as post-translational modifications (Mann and Jensen, 2003; Zaia, 2004) including phosphorylation, acetylation, methylation, glycosylation and ubiquitination. Owing to such distinct advantages, mass spectrometry has become a dominant technique for proteomic research.

1.6.1 Instrumentation

A typical mass spectrometer generally consists of three parts: an ion source to produce the gas-phase ions, a mass analyzer to separate the ionized analytes according to their mass-to-charge ratio (m/z), and a detector that registers the number of ions at each m/z value. Ionization is commonly achieved by either matrix-assisted laser desorption/ionization (MALDI) (Karas and Hillenkamp, 1988) or electrospray ionization (ESI) (Fenn et al., 1989). Once the peptides or proteins are ionized, they are transferred into the mass analyzer via the electric potential differences between the ion source and mass analyzer, and subsequently separated according to their different mass-to-charge ratios. Alternatively, to acquire more structural information, an extra collision cell is implemented in the tandem mass spectrometer, where the peptides or proteins can be fragmented by different dissociation methods. The resulting fragment ions are subsequently separated in the mass analyzer. In the end, all separated ions with different mass-to-charge ratio can be detected by the detectors and translated into a mass spectrum, plotting the signal intensities against m/z values.

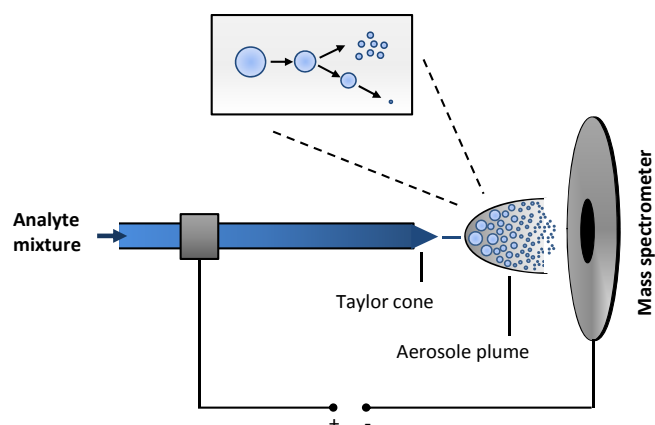


Figure 7 | Electro spray ionization (ESI) techniques, adapted from (Steen and Mann, 2004).

Before they are subjected to LC-MS/MS analysis, proteins are usually digested into peptides using a sequence-specific protease. The most commonly used enzyme is trypsin, which specifically cleaves proteins on the carboxyl-terminal side of lysine and arginine residues (Leiros et al., 2004). The complexity of the resulting peptide mixture is often beyond the processing capacity of mass spectrometers, for this reason, reverse phase liquid chromatography using volatile solvents (water, acetonitrile, organic acids, etc) is usually online coupled to tandem mass spectrometers (LC-MS/MS) (Thakur et al., 2011). The peptides are initially protonated under aqueous acidic conditions and then eluted in the presence of increasing percentage of organic solvent according to their hydrophobic properties.

Gentle ionization methods such as electro spray ionization (ESI) (Fenn et al., 1989) greatly facilitate the measurement of large biomolecules. The eluted peptide mixtures are directly sprayed into an electric field from a fine capillary on which a high voltage is applied (Figure 7). The ionization process starts from the creation of an electrically charged spray (Taylor Cone). Then small charged droplets are formed (Wilm, 2011). The continuous evaporation of solvent results in the increase of the surface charge density of the droplet. When the Coulomb repulsion overcomes the surface tension of a droplet, it begins to break into smaller highly charged droplets. At last, only one remaining analyte is obtained as the final gas phase ions by constant repeat of breakdown of charged droplet as described before (charge residue model, CRM) (Wilm, 1994) and/or the ejection of individual analyte ions from the droplet surface (ion evaporation model, IEM) (Iribarne, 1976; Nguyen and Fenn, 2007). The development of nanoESI

(nanoelectrospray), which features rather low flow rates (nL/min), has significantly enhanced the ionization efficiency and thereby improves the sensitivity of methods (Yates et al., 2009).

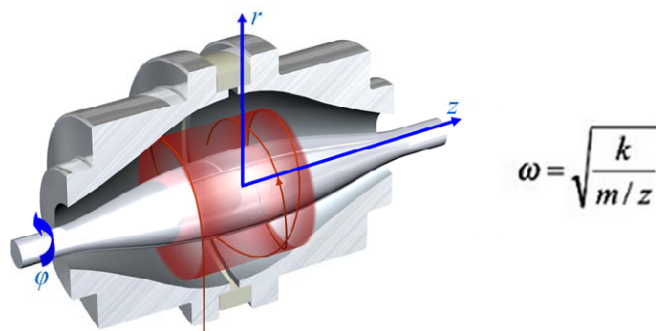


Figure 8 | A cut away model of Orbitrap mass analyzer and the formula which axial oscillation frequency follows, adapted from (Scigelova and Makarov, 2006).

The progress in mass spectrometry has also been driven by the development of a range of powerful mass analyzers. They can be categorized into two major types: the scanning mass spectrometers, such as quadrupole (Q) and time-of-flight (TOF) analyzers, and the trapping mass spectrometers, such as ion traps (linear and 3D), Orbitrap and Fourier-transform ion cyclotron resonance (FT-ICR) analyzer. Each analyzer displays particular characteristics, such as resolution, mass accuracy, mass range, sensitivity and analysis speed (Han et al., 2008; Yates et al., 2009). Orbitrap mass analyzer and the corresponding mass spectrometry, developed by Makarov in 2000 (Makarov, 2000), have become the leading players in proteomics (Scigelova and Makarov, 2006; Zubarev and Makarov, 2013) and have been used for all the projects in this thesis. In Orbitraps, the generated ions are injected and trapped in an electrostatic field generated by an outer barrel-like electrode and a central spindle electrode (Figure 8). The ions circle around the central spindle in harmonic oscillations with a certain frequency which is inversely proportional to the square root of m/z . The axial oscillation is recorded and converted into a mass spectrum by Fourier transformation. The Orbitrap recognizes these oscillations with a very high accuracy (1-2 ppm) which results in very precise molecular masses.

1.6.2 Protein Identification and quantification

High resolution mass spectrometry enables the application of tandem MS/MS for peptide identification, attributing to the fact that peptides usually fragment along the backbones upon addition of energy in a collision cell. For this purpose, two or more mass spectra are usually required. The first (full scan) mass spectrum is generated from the precursor ions to determine the m/z values of the intact peptides. For the second mass spectrum, the precursors of interest are isolated, fragmented and the various fragment ions are recorded. Fragmentation of the precursor ion of the full MS results in the generation of b- (N-terminal) and y-ions (C-terminal) (Johnson et al., 1987; Roepstorff and Fohlman, 1984) (Figure 9) and the differences between this ions series allows for the determination of the amino acid sequence.

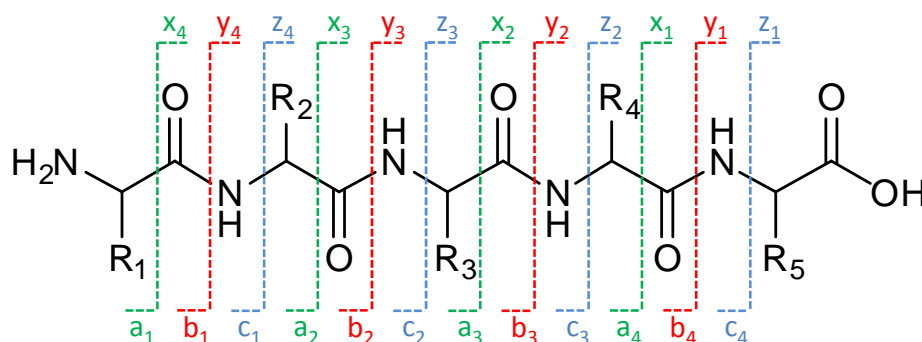


Figure 9 | Peptide fragmentation nomenclature according to Roepstorff and Fohlmann, adapted from (Roepstorff and Fohlman, 1984).

N-terminal fragments are named a_n, b_n, c_n ions and C-terminal fragments are x_n, y_n and z_n ions.

Database searching is the most commonly applied strategy for peptide and protein identification in large scale proteomic studies. The experimental fragmentation spectra of a peptide are compared with theoretically generated fragment spectra for each peptide in the protein sequence database. The peptide is then assigned based on the best match between predicted and observed spectrum, defined by database dependent scores and user specific parameters. Once the peptides have been identified, they can be assigned to proteins. The quality of protein identification is assessed by the use of target-decoy searches (Fitzgibbon et al., 2008; Nesvizhskii and Aebersold, 2005). All tandem spectra are searched against the target (forward peptide sequences) and a decoy (reversed or randomized sequences) database (Nesvizhskii et al., 2007). With the

assumption that any matches in the decoy search are false assignments, the corresponding false-discovery rate (FDR) can be computed (Lenz et al., 2011).

In recent years, obtaining quantitative data for identified proteins has been of great interest in order to compare their abundances under different physiological conditions or in diverse biological systems. Two different methods can be generally applied for this purpose, stable isotope labeling and label free approaches (Bantscheff et al., 2012; Bantscheff et al., 2007b). The isotope labelling can be achieved as an internal standard metabolically, chemically and enzymatically, or, as an external standard using spiked synthetic peptides (Aebersold and Mann, 2003; Bantscheff et al., 2007b; Heck and Krijgsveld, 2004). Quantification is achieved by the comparison of mass spectrometric signal intensities between the same peptide which were differently labeled. This approach offers accurate quantification with dynamic ranges of one to two logs (Bantscheff and Kuster, 2012; Bantscheff et al., 2012). Recently, label free quantification has received more and more attention. Two different strategies can be distinguished: spectral counting and precursor ion intensity comparison of peptides belonging to the same protein. Spectral counting is based on the observation that the number of tandem mass spectra collected for peptides of a protein increases with protein abundance (Bylund et al., 2002; Jaitly et al., 2006). In precursor ion intensity comparison, the area of extracted ion intensity chromatograms for the same peptide in different samples is integrated and compared (Bondarenko et al., 2002; Wiener et al., 2004). Label-free approaches are the least accurate among the mass spectrometric quantification techniques since variations from different steps of the workflow are accumulated in the obtained results (Bantscheff et al., 2012; Bantscheff et al., 2007b). However, label free quantification is worth considering for several reasons. In principle, there is no limit to the numbers of experiments that can be compared, whereas stable isotope labeling techniques are typically limited to 2–8 experiments that can be directly compared (Bantscheff et al., 2007b). Second, it also avoids additional labeling steps, which is more time and money consuming.

Aim of the thesis

Due to the incomplete understanding of a drug target spectrum at an early stage of drug discovery, small molecule kinase inhibitors are found to have many off-target effects. Chemical proteomics, notably the use of well-designed small molecule probes in combination with high-resolution mass spectrometry analysis exemplified by the Kinobeads technology, has emerged important tools for characterization of drug selectivity profiles under close to physiological conditions.

Although current Kinobeads probe set can enrich more than half of the human kinome, some kinases of great clinical relevant were still missing and improvements on higher kinome coverage of the Kinobeads is the consistent pursuit. The aim of this thesis was to develop and evaluate small molecules as affinity probes that would help achieve higher kinome coverage and the applications of these probes in chemical proteomics for drug selectivity profiling of clinical kinase inhibitors. One objective is to find new molecules which can provide general complementarity to the Kinobeads. For this purpose, pan kinase inhibitors are the ideal candidates. In Chapter II, the evaluation of a pan kinase inhibition probe VI16743 was described. This molecule was immobilized and its binding profile was characterized in a mixture of lysate from four cancer cell lines. On the other hand, some specific kinases were constantly out of reach by all the pan kinase inhibition probes of the Kinobeads, such as the angiogenesis related kinases VEGFRs and FGFRs, which have significant roles in cancers. These kinases have become very important anti-cancer targets with the corresponding drugs represent more than 1/3 of the all marketed kinase drugs. The second objective of this thesis was therefore to develop new probes to specifically enrich these missing kinases. For this purpose, guided by molecular modeling, 3 chemical probes were designed and synthesized for the enrichment of VEGFRs (Chapter III) and FGFRs (Chapter IV), respectively. Their binding profiles were evaluated in lysates of human placenta and different cancer cell lines. These probes were also combined with Kinobeads probes to identify the selectivity profiles of four clinical angiogenesis inhibitors, enabling the identification of several primary and off-targets.

Abbreviations

ABPP	activity-based protein profiling
ATP	adenosine-triphosphate
CID	collision induced dissociation
CML	chronic myelogenous leukemia
CRM	charge residue model
EMT	epithelial mesenchymal transition
ESI	electrospray ionization
FDR	false-discovery rate
FGF(R)	fibroblast growth factor (receptor)
FT-ICR	Fourier transform ion cyclotron mass spectrometer
GIST	gastrointestinal tumors
HCD	higher energy collision induced dissociation
HGFR	hepatocyte growth factor receptor
IEM	ion evaporation model
IMF	idiopathic myelofibrosis
LC	liquid chromatography
LC-MS/MS	liquid chromatography coupled to tandem mass spectrometry
LTQ	linear ion trap
mAb	monoclonal antibody
MALDI	matrix-assisted laser desorption/ ionization
MCL	mantle cell lymphoma
MS	mass spectrometry
MTC	medullary thyroid carcinoma
NSCLC	non small cell lung cancer
PI3K	phosphoinositide 3-kinase
PTM	post translational modification
RCC	renal cell carcinoma
SAR	structure activity relationship
TKI	tyrosine kinase inhibitor
TOF	time-of-flight
VEGF(R)	vascular endothelial growth factor (receptors)

References

- Aebersold, R., and Mann, M. (2003). Mass spectrometry-based proteomics. *Nature* *422*, 198-207.
- al-Tweigeri, T., Nabholz, J.M., and Mackey, J.R. (1996). Ocular toxicity and cancer chemotherapy. A review. *Cancer* *78*, 1359-1373.
- Anastassiadis, T., Deacon, S.W., Devarajan, K., Ma, H., and Peterson, J.R. (2011). Comprehensive assay of kinase catalytic activity reveals features of kinase inhibitor selectivity. *Nat Biotechnol* *29*, 1039-1045.
- Angel, T.E., Aryal, U.K., Hengel, S.M., Baker, E.S., Kelly, R.T., Robinson, E.W., and Smith, R.D. (2012). Mass spectrometry-based proteomics: existing capabilities and future directions. *Chem Soc Rev* *41*, 3912-3928.
- Apperley, J.F., Gardembas, M., Melo, J.V., Russell-Jones, R., Bain, B.J., Baxter, E.J., Chase, A., Chessells, J.M., Colombat, M., Dearden, C.E., *et al.* (2002). Response to imatinib mesylate in patients with chronic myeloproliferative diseases with rearrangements of the platelet-derived growth factor receptor beta. *The New England journal of medicine* *347*, 481-487.
- Bantscheff, M., and Drewes, G. (2012). Chemoproteomic approaches to drug target identification and drug profiling. *Bioorganic & medicinal chemistry* *20*, 1973-1978.
- Bantscheff, M., Eberhard, D., Abraham, Y., Bastuck, S., Boesche, M., Hobson, S., Mathieson, T., Perrin, J., Raida, M., Rau, C., *et al.* (2007a). Quantitative chemical proteomics reveals mechanisms of action of clinical ABL kinase inhibitors. *Nat Biotechnol* *25*, 1035-1044.
- Bantscheff, M., Hopf, C., Savitski, M.M., Dittmann, A., Grandi, P., Michon, A.-M., Schlegl, J., Abraham, Y., Becher, I., Bergamini, G., *et al.* (2011). Chemoproteomics profiling of HDAC inhibitors reveals selective targeting of HDAC complexes. *Nat Biotech* *29*, 255-265.
- Bantscheff, M., and Kuster, B. (2012). Quantitative mass spectrometry in proteomics. *Anal Bioanal Chem* *404*, 937-938.
- Bantscheff, M., Lemeer, S., Savitski, M.M., and Kuster, B. (2012). Quantitative mass spectrometry in proteomics: critical review update from 2007 to the present. *Anal Bioanal Chem* *404*, 939-965.
- Bantscheff, M., Schirle, M., Sweetman, G., Rick, J., and Kuster, B. (2007b). Quantitative mass spectrometry in proteomics: a critical review. *Anal Bioanal Chem* *389*, 1017-1031.
- Bantscheff, M., Scholten, A., and Heck, A.J. (2009). Revealing promiscuous drug-target interactions by chemical proteomics. *Drug Discov Today* *14*, 1021-1029.
- Baselga, J. (2001). The EGFR as a target for anticancer therapy--focus on cetuximab. *Eur J Cancer* *37 Suppl 4*, S16-22.
- Baselga, J. (2006). Targeting tyrosine kinases in cancer: the second wave. *Science* *312*, 1175-1178.

- Beck, M., Schmidt, A., Malmstroem, J., Claassen, M., Ori, A., Szymborska, A., Herzog, F., Rinner, O., Ellenberg, J., and Aebersold, R. (2011). The quantitative proteome of a human cell line. *Mol Syst Biol* 7, 549.
- Boisvert, F.M., Lam, Y.W., Lamont, D., and Lamond, A.I. (2010). A quantitative proteomics analysis of subcellular proteome localization and changes induced by DNA damage. *Mol Cell Proteomics* 9, 457-470.
- Bondarenko, P.V., Chelius, D., and Shaler, T.A. (2002). Identification and relative quantitation of protein mixtures by enzymatic digestion followed by capillary reversed-phase liquid chromatography-tandem mass spectrometry. *Analytical chemistry* 74, 4741-4749.
- Butowski, N., and Chang, S.M. (2005). Small molecule and monoclonal antibody therapies in neurooncology. *Cancer control : journal of the Moffitt Cancer Center* 12, 116-124.
- Bylund, D., Danielsson, R., Malmquist, G., and Markides, K.E. (2002). Chromatographic alignment by warping and dynamic programming as a pre-processing tool for PARAFAC modelling of liquid chromatography-mass spectrometry data. *Journal of chromatography A* 961, 237-244.
- Carroll, J., Protani, M., Walpole, E., and Martin, J.H. (2012). Effect of obesity on toxicity in women treated with adjuvant chemotherapy for early-stage breast cancer: a systematic review. *Breast cancer research and treatment* 136, 323-330.
- Carter, P. (2001). Improving the efficacy of antibody-based cancer therapies. *Nature reviews Cancer* 1, 118-129.
- Carter, P.J. (2006). Potent antibody therapeutics by design. *Nature reviews Immunology* 6, 343-357.
- Chan, D., Tyner, J.W., Chng, W.J., Bi, C., Okamoto, R., Said, J., Ngan, B.D., Braunstein, G.D., and Koeffler, H.P. (2012). Effect of dasatinib against thyroid cancer cell lines in vitro and a xenograft model in vivo. *Oncology letters* 3, 807-815.
- Chen, H.X., and Cleck, J.N. (2009). Adverse effects of anticancer agents that target the VEGF pathway. *Nature reviews Clinical oncology* 6, 465-477.
- Cohen, M.S., Hadjivassiliou, H., and Taunton, J. (2007). A clickable inhibitor reveals context-dependent autoactivation of p90 RSK. *Nat Chem Biol* 3, 156-160.
- Colvin, J.S., Bohne, B.A., Harding, G.W., McEwen, D.G., and Ornitz, D.M. (1996). Skeletal overgrowth and deafness in mice lacking fibroblast growth factor receptor 3. *Nature genetics* 12, 390-397.
- Comis, R.L. (2003). A brief history of the research and treatment of lung cancer from 1970 to 2003. *International journal of clinical oncology* 8, 230-233.
- Cravatt, B.F., Simon, G.M., and Yates, J.R., 3rd (2007). The biological impact of mass-spectrometry-based proteomics. *Nature* 450, 991-1000.
- Cravatt, B.F., Wright, A.T., and Kozarich, J.W. (2008). Activity-based protein profiling: from enzyme chemistry to proteomic chemistry. *Annu Rev Biochem* 77, 383-414.
- Croom, K.F., and Perry, C.M. (2003). Imatinib mesylate: in the treatment of gastrointestinal stromal tumours. *Drugs* 63, 513-522; discussion 523-514.

- Cross, M.J., and Claesson-Welsh, L. (2001). FGF and VEGF function in angiogenesis: signalling pathways, biological responses and therapeutic inhibition. *Trends in pharmacological sciences* 22, 201-207.
- Cross, M.J., Dixelius, J., Matsumoto, T., and Claesson-Welsh, L. (2003). VEGF-receptor signal transduction. *Trends in biochemical sciences* 28, 488-494.
- Dancey, J., and Sausville, E.A. (2003). Issues and progress with protein kinase inhibitors for cancer treatment. *Nature reviews Drug discovery* 2, 296-313.
- Daub, H., Olsen, J.V., Bairlein, M., Gnad, F., Oppermann, F.S., Korner, R., Greff, Z., Keri, G., Stemmann, O., and Mann, M. (2008). Kinase-selective enrichment enables quantitative phosphoproteomics of the kinome across the cell cycle. *Mol Cell* 31, 438-448.
- Deng, C.X., Wynshaw-Boris, A., Shen, M.M., Daugherty, C., Ornitz, D.M., and Leder, P. (1994). Murine FGFR-1 is required for early postimplantation growth and axial organization. *Genes & development* 8, 3045-3057.
- DeVita, V.T., Jr., and Chu, E. (2008). A history of cancer chemotherapy. *Cancer Res* 68, 8643-8653.
- Dotan, E., Cohen, S.J., Alpaugh, K.R., and Meropol, N.J. (2009). Circulating tumor cells: evolving evidence and future challenges. *The oncologist* 14, 1070-1082.
- Dreger, M. (2003). Subcellular proteomics. *Mass spectrometry reviews* 22, 27-56.
- Fedorov, O., Muller, S., and Knapp, S. (2010). The (un)targeted cancer kinome. *Nat Chem Biol* 6, 166-169.
- Fenn, J.B., Mann, M., Meng, C.K., Wong, S.F., and Whitehouse, C.M. (1989). Electrospray ionization for mass spectrometry of large biomolecules. *Science* 246, 64-71.
- Ferrara, N. (2004). Vascular endothelial growth factor as a target for anticancer therapy. *The oncologist* 9 *Suppl 1*, 2-10.
- Ferrara, N. (2005). VEGF as a therapeutic target in cancer. *Oncology* 69 *Suppl 3*, 11-16.
- Fishman, M.C., and Porter, J.A. (2005). Pharmaceuticals: a new grammar for drug discovery. *Nature* 437, 491-493.
- Fitzgibbon, M., Li, Q., and McIntosh, M. (2008). Modes of inference for evaluating the confidence of peptide identifications. *J Proteome Res* 7, 35-39.
- Folkman, J. (1971). Tumor angiogenesis: therapeutic implications. *The New England journal of medicine* 285, 1182-1186.
- Folkman, J., and Klagsbrun, M. (1987). Angiogenic factors. *Science* 235, 442-447.
- Galmarini, D., Galmarini, C.M., and Galmarini, F.C. (2012). Cancer chemotherapy: a critical analysis of its 60 years of history. *Critical reviews in oncology/hematology* 84, 181-199.
- Gashaw, I., Ellinghaus, P., Sommer, A., and Asadullah, K. (2011). What makes a good drug target? *Drug Discov Today* 16, 1037-1043.
- Gasparini, G., Longo, R., Toi, M., and Ferrara, N. (2005). Angiogenic inhibitors: a new therapeutic strategy in oncology. *Nature clinical practice Oncology* 2, 562-577.
- Gillet, L.C., Namoto, K., Ruchti, A., Hoving, S., Boesch, D., Inverardi, B., Mueller, D., Coulot, M., Schindler, P., Schweigler, P., *et al.* (2008). In-cell selectivity profiling of serine

- protease inhibitors by activity-based proteomics. *Mol Cell Proteomics* 7, 1241-1253.
- Goldberg, R.M. (2005). Cetuximab. *Nature reviews Drug discovery Suppl*, S10-11.
- Grant, S.K. (2009). Therapeutic protein kinase inhibitors. *Cell Mol Life Sci* 66, 1163-1177.
- Hait, W.N., and Hambley, T.W. (2009). Targeted cancer therapeutics. *Cancer Res* 69, 1263-1267; discussion 1267.
- Halin, C., and Neri, D. (2001). Antibody-Based targeting of angiogenesis. *Critical reviews in therapeutic drug carrier systems* 18, 299-339.
- Hall, S.E. (2006). Chemoproteomics-driven drug discovery: addressing high attrition rates. *Drug Discov Today* 11, 495-502.
- Halnan, K.E. (1999). Fifty years of the National Health Service 1948-1998: a personal history of progress in the treatment of cancer. *Clin Oncol (R Coll Radiol)* 11, 55-60.
- Han, X., Aslanian, A., and Yates, J.R., 3rd (2008). Mass spectrometry for proteomics. *Current opinion in chemical biology* 12, 483-490.
- Hanahan, D., and Weinberg, R.A. (2000). The hallmarks of cancer. *Cell* 100, 57-70.
- Hanahan, D., and Weinberg, R.A. (2011). Hallmarks of cancer: the next generation. *Cell* 144, 646-674.
- Heck, A.J., and Krijgsveld, J. (2004). Mass spectrometry-based quantitative proteomics. *Expert Rev Proteomics* 1, 317-326.
- Hennequin, L.F., Thomas, A.P., Johnstone, C., Stokes, E.S., Ple, P.A., Lohmann, J.J., Ogilvie, D.J., Dukes, M., Wedge, S.R., Curwen, J.O., *et al.* (1999). Design and structure-activity relationship of a new class of potent VEGF receptor tyrosine kinase inhibitors. *J Med Chem* 42, 5369-5389.
- Hicklin, D.J., Witte, L., Zhu, Z., Liao, F., Wu, Y., Li, Y., and Bohlen, P. (2001). Monoclonal antibody strategies to block angiogenesis. *Drug Discov Today* 6, 517-528.
- Hopkins, A.L., and Groom, C.R. (2002). The druggable genome. *Nature reviews Drug discovery* 1, 727-730.
- Huisgen, R. (2003). 1,3-Dipolar Cycloadditions. Past and Future. *Angew Chem Int Ed Engl* 2, 565-598.
- Imai, K., and Takaoka, A. (2006). Comparing antibody and small-molecule therapies for cancer. *Nature reviews Cancer* 6, 714-727.
- Iribarne, J.V., Thomson, B.A. (1976). On the evaporation of small ions from charged droplets. *Journal of Chemical Physics* 64, 2287-2294.
- Ivy, S.P., Wick, J.Y., and Kaufman, B.M. (2009). An overview of small-molecule inhibitors of VEGFR signaling. *Nature reviews Clinical oncology* 6, 569-579.
- Jaitly, N., Monroe, M.E., Petyuk, V.A., Clauss, T.R., Adkins, J.N., and Smith, R.D. (2006). Robust algorithm for alignment of liquid chromatography-mass spectrometry analyses in an accurate mass and time tag data analysis pipeline. *Analytical chemistry* 78, 7397-7409.

- Johnson, L.N., Lowe, E.D., Noble, M.E., and Owen, D.J. (1998). The Eleventh Datta Lecture. The structural basis for substrate recognition and control by protein kinases. *FEBS Lett* 430, 1-11.
- Johnson, R.S., Martin, S.A., Biemann, K., Stults, J.T., and Watson, J.T. (1987). Novel fragmentation process of peptides by collision-induced decomposition in a tandem mass spectrometer: differentiation of leucine and isoleucine. *Analytical chemistry* 59, 2621-2625.
- Karaman, M.W., Herrgard, S., Treiber, D.K., Gallant, P., Atteridge, C.E., Campbell, B.T., Chan, K.W., Ciceri, P., Davis, M.I., Edeen, P.T., *et al.* (2008). A quantitative analysis of kinase inhibitor selectivity. *Nat Biotechnol* 26, 127-132.
- Karas, M., and Hillenkamp, F. (1988). Laser desorption ionization of proteins with molecular masses exceeding 10,000 daltons. *Analytical chemistry* 60, 2299-2301.
- Kato, D., Boatright, K.M., Berger, A.B., Nazif, T., Blum, G., Ryan, C., Chehade, K.A., Salvesen, G.S., and Bogoy, M. (2005). Activity-based probes that target diverse cysteine protease families. *Nat Chem Biol* 1, 33-38.
- Katzel, J.A., Fanucchi, M.P., and Li, Z. (2009). Recent advances of novel targeted therapy in non-small cell lung cancer. *Journal of hematology & oncology* 2, 2.
- Kerbel, R., and Folkman, J. (2002). Clinical translation of angiogenesis inhibitors. *Nature reviews Cancer* 2, 727-739.
- Kidd, D., Liu, Y., and Cravatt, B.F. (2001). Profiling serine hydrolase activities in complex proteomes. *Biochemistry* 40, 4005-4015.
- Klint, P., and Claesson-Welsh, L. (1999). Signal transduction by fibroblast growth factor receptors. *Front Biosci* 4, D165-177.
- Kohler, G., and Milstein, C. (1975). Continuous cultures of fused cells secreting antibody of predefined specificity. *Nature* 256, 495-497.
- Kruse, U., Bantscheff, M., Drewes, G., and Hopf, C. (2008). Chemical and pathway proteomics: powerful tools for oncology drug discovery and personalized health care. *Mol Cell Proteomics* 7, 1887-1901.
- Kruse, U., Pallasch, C.P., Bantscheff, M., Eberhard, D., Frenzel, L., Ghidelli, S., Maier, S.K., Werner, T., Wendtner, C.M., and Drewes, G. (2011). Chemoproteomics-based kinome profiling and target deconvolution of clinical multi-kinase inhibitors in primary chronic lymphocytic leukemia cells. *Leukemia* 25, 89-100.
- Kumar, S., Zhou, B., Liang, F., Wang, W.Q., Huang, Z., and Zhang, Z.Y. (2004). Activity-based probes for protein tyrosine phosphatases. *Proc Natl Acad Sci U S A* 101, 7943-7948.
- Leiros, H.K., Brandsdal, B.O., Andersen, O.A., Os, V., Leiros, I., Helland, R., Otlewski, J., Willassen, N.P., and Smalas, A.O. (2004). Trypsin specificity as elucidated by LIE calculations, X-ray structures, and association constant measurements. *Protein science : a publication of the Protein Society* 13, 1056-1070.
- Lenz, T., Fischer, J.J., and Dreger, M. (2011). Probing small molecule-protein interactions: A new perspective for functional proteomics. *J Proteomics* 75, 100-115.

- Levitzki, A. (1999). Protein tyrosine kinase inhibitors as novel therapeutic agents. *Pharmacol Ther* 82, 231-239.
- Li, J., Rix, U., Fang, B., Bai, Y., Edwards, A., Colinge, J., Bennett, K.L., Gao, J., Song, L., Eschrich, S., *et al.* (2010). A chemical and phosphoproteomic characterization of dasatinib action in lung cancer. *Nat Chem Biol* 6, 291-299.
- Lieu, C., Heymach, J., Overman, M., Tran, H., and Kopetz, S. (2011). Beyond VEGF: inhibition of the fibroblast growth factor pathway and antiangiogenesis. *Clinical cancer research : an official journal of the American Association for Cancer Research* 17, 6130-6139.
- Liu, Y., and Gray, N.S. (2006). Rational design of inhibitors that bind to inactive kinase conformations. *Nat Chem Biol* 2, 358-364.
- Makarov, A. (2000). Electrostatic axially harmonic orbital trapping: a high-performance technique of mass analysis. *Analytical chemistry* 72, 1156-1162.
- Mallick, P., and Kuster, B. (2010). Proteomics: a pragmatic perspective. *Nat Biotechnol* 28, 695-709.
- Mann, M., and Jensen, O.N. (2003). Proteomic analysis of post-translational modifications. *Nat Biotechnol* 21, 255-261.
- Manning, G., Whyte, D.B., Martinez, R., Hunter, T., and Sudarsanam, S. (2002). The protein kinase complement of the human genome. *Science* 298, 1912-1934.
- Matthews, D.J., and Gerritsen, M.E. (2011). *Targeting Protein Kinases for Cancer Therapy* (Wiley).
- Moghaddas Gholami, A., Hahne, H., Wu, Z., Auer, F.J., Meng, C., Wilhelm, M., and Kuster, B. (2013). Global proteome analysis of the NCI-60 cell line panel. *Cell reports* 4, 609-620.
- Moreira, I.S., Fernandes, P.A., and Ramos, M.J. (2007). Vascular endothelial growth factor (VEGF) inhibition--a critical review. *Anti-cancer agents in medicinal chemistry* 7, 223-245.
- Nagaraj, N., Wisniewski, J.R., Geiger, T., Cox, J., Kircher, M., Kelso, J., Paabo, S., and Mann, M. (2011). Deep proteome and transcriptome mapping of a human cancer cell line. *Mol Syst Biol* 7, 548.
- Nesvizhskii, A.I., and Aebersold, R. (2005). Interpretation of shotgun proteomic data: the protein inference problem. *Mol Cell Proteomics* 4, 1419-1440.
- Nesvizhskii, A.I., Vitek, O., and Aebersold, R. (2007). Analysis and validation of proteomic data generated by tandem mass spectrometry. *Nature methods* 4, 787-797.
- Nguyen, S., and Fenn, J.B. (2007). Gas-phase ions of solute species from charged droplets of solutions. *Proc Natl Acad Sci U S A* 104, 1111-1117.
- Nomura, D.K., Dix, M.M., and Cravatt, B.F. (2010). Activity-based protein profiling for biochemical pathway discovery in cancer. *Nature reviews Cancer* 10, 630-638.
- Oda, Y., Owa, T., Sato, T., Boucher, B., Daniels, S., Yamanaka, H., Shinohara, Y., Yokoi, A., Kuromitsu, J., and Nagasu, T. (2003). Quantitative chemical proteomics for identifying candidate drug targets. *Analytical chemistry* 75, 2159-2165.

- Ong, S.E., Schenone, M., Margolin, A.A., Li, X., Do, K., Doud, M.K., Mani, D.R., Kuai, L., Wang, X., Wood, J.L., *et al.* (2009). Identifying the proteins to which small-molecule probes and drugs bind in cells. *Proc Natl Acad Sci U S A* *106*, 4617-4622.
- Pandey, A., and Mann, M. (2000). Proteomics to study genes and genomes. *Nature* *405*, 837-846.
- Parker, B.A., Vassos, A.B., Halpern, S.E., Miller, R.A., Hupf, H., Amox, D.G., Simoni, J.L., Starr, R.J., Green, M.R., and Royston, I. (1990). Radioimmunotherapy of human B-cell lymphoma with 90Y-conjugated antiidiotype monoclonal antibody. *Cancer Res* *50*, 1022s-1028s.
- Patricelli, M.P., Szardenings, A.K., Liyanage, M., Nomanbhoy, T.K., Wu, M., Weissig, H., Aban, A., Chun, D., Tanner, S., and Kozarich, J.W. (2007). Functional interrogation of the kinome using nucleotide acyl phosphates. *Biochemistry* *46*, 350-358.
- Pearson, M.A., and Fabbro, D. (2004). Targeting protein kinases in cancer therapy: a success? *Expert review of anticancer therapy* *4*, 1113-1124.
- Planchard, D. (2011). Bevacizumab in non-small-cell lung cancer: a review. *Expert review of anticancer therapy* *11*, 1163-1179.
- Rini, B.I. (2007). Vascular endothelial growth factor-targeted therapy in renal cell carcinoma: current status and future directions. *Clinical cancer research : an official journal of the American Association for Cancer Research* *13*, 1098-1106.
- Rix, U., Gridling, M., and Superti-Furga, G. (2012). Compound immobilization and drug-affinity chromatography. *Methods Mol Biol* *803*, 25-38.
- Rix, U., Hantschel, O., Durnberger, G., Remsing Rix, L.L., Planyavsky, M., Fernbach, N.V., Kaupe, I., Bennett, K.L., Valent, P., Colinge, J., *et al.* (2007). Chemical proteomic profiles of the BCR-ABL inhibitors imatinib, nilotinib, and dasatinib reveal novel kinase and nonkinase targets. *Blood* *110*, 4055-4063.
- Rix, U., and Superti-Furga, G. (2009). Target profiling of small molecules by chemical proteomics. *Nat Chem Biol* *5*, 616-624.
- Roepstorff, P., and Fohlman, J. (1984). Proposal for a common nomenclature for sequence ions in mass spectra of peptides. *Biomed Mass Spectrom* *11*, 601.
- Saghatelian, A., Jessani, N., Joseph, A., Humphrey, M., and Cravatt, B.F. (2004). Activity-based probes for the proteomic profiling of metalloproteases. *Proc Natl Acad Sci U S A* *101*, 10000-10005.
- Salisbury, C.M., and Cravatt, B.F. (2007). Activity-based probes for proteomic profiling of histone deacetylase complexes. *Proc Natl Acad Sci U S A* *104*, 1171-1176.
- Salisbury, C.M., and Cravatt, B.F. (2008). Optimization of activity-based probes for proteomic profiling of histone deacetylase complexes. *Journal of the American Chemical Society* *130*, 2184-2194.
- Savage, D.G., and Antman, K.H. (2002). Imatinib mesylate--a new oral targeted therapy. *The New England journal of medicine* *346*, 683-693.
- Savas, P., Hughes, B., and Solomon, B. (2013). Targeted therapy in lung cancer: IPASS and beyond, keeping abreast of the explosion of targeted therapies for lung cancer. *Journal of thoracic disease* *5*, S579-S592.

- Sawyers, C. (2004). Targeted cancer therapy. *Nature* 432, 294-297.
- Scagliotti, G., and Govindan, R. (2010). Targeting angiogenesis with multitargeted tyrosine kinase inhibitors in the treatment of non-small cell lung cancer. *The oncologist* 15, 436-446.
- Schirle, M., Bantscheff, M., and Kuster, B. (2012). Mass spectrometry-based proteomics in preclinical drug discovery. *Chem Biol* 19, 72-84.
- Sciabola, S., Stanton, R.V., Wittkopp, S., Wildman, S., Moshinsky, D., Potluri, S., and Xi, H. (2008). Predicting kinase selectivity profiles using Free-Wilson QSAR analysis. *Journal of chemical information and modeling* 48, 1851-1867.
- Scigelova, M., and Makarov, A. (2006). Orbitrap mass analyzer--overview and applications in proteomics. *Proteomics* 6 *Suppl* 2, 16-21.
- Senger, D.R., Galli, S.J., Dvorak, A.M., Perruzzi, C.A., Harvey, V.S., and Dvorak, H.F. (1983). Tumor cells secrete a vascular permeability factor that promotes accumulation of ascites fluid. *Science* 219, 983-985.
- Sharma, K., Weber, C., Bairlein, M., Greff, Z., Keri, G., Cox, J., Olsen, J.V., and Daub, H. (2009). Proteomics strategy for quantitative protein interaction profiling in cell extracts. *Nature methods* 6, 741-744.
- Sharpless, K.B., and Manetsch, R. (2006). In situ click chemistry: a powerful means for lead discovery. *Expert Opin Drug Discov* 1, 525-538.
- Shibuya, M., Ito, N., and Claesson-Welsh, L. (1999). Structure and function of vascular endothelial growth factor receptor-1 and -2. *Current topics in microbiology and immunology* 237, 59-83.
- Shing, Y., Folkman, J., Sullivan, R., Butterfield, C., Murray, J., and Klagsbrun, M. (1984). Heparin affinity: purification of a tumor-derived capillary endothelial cell growth factor. *Science* 223, 1296-1299.
- Siegel, R., Naishadham, D., and Jemal, A. (2013). Cancer statistics, 2013. *CA Cancer J Clin* 63, 11-30.
- Simon, G.M., and Cravatt, B.F. (2010). Activity-based proteomics of enzyme superfamilies: serine hydrolases as a case study. *The Journal of biological chemistry* 285, 11051-11055.
- Speers, A.E., and Cravatt, B.F. (2004). Profiling enzyme activities in vivo using click chemistry methods. *Chem Biol* 11, 535-546.
- Speers, A.E., and Cravatt, B.F. (2009). Activity-Based Protein Profiling (ABPP) and Click Chemistry (CC)-ABPP by MudPIT Mass Spectrometry. *Current protocols in chemical biology* 1, 29-41.
- Steen, H., and Mann, M. (2004). The ABC's (and XYZ's) of peptide sequencing. *Nature reviews Molecular cell biology* 5, 699-711.
- Sudhakar, A. (2009). History of Cancer, Ancient and Modern Treatment Methods. *Journal of cancer science & therapy* 1, 1-4.
- Taipale, J., Makinen, T., Arighi, E., Kukk, E., Karkkainen, M., and Alitalo, K. (1999). Vascular endothelial growth factor receptor-3. *Current topics in microbiology and immunology* 237, 85-96.

- Thakur, S.S., Geiger, T., Chatterjee, B., Bandilla, P., Frohlich, F., Cox, J., and Mann, M. (2011). Deep and highly sensitive proteome coverage by LC-MS/MS without prefractionation. *Mol Cell Proteomics* 10, M110 003699.
- Traxler, P., and Furet, P. (1999). Strategies toward the design of novel and selective protein tyrosine kinase inhibitors. *Pharmacol Ther* 82, 195-206.
- Trinkle-Mulcahy, L., Boulon, S., Lam, Y.W., Urcia, R., Boisvert, F.M., Vandermoere, F., Morrice, N.A., Swift, S., Rothbauer, U., Leonhardt, H., *et al.* (2008). Identifying specific protein interaction partners using quantitative mass spectrometry and bead proteomes. *The Journal of cell biology* 183, 223-239.
- Ubersax, J.A., and Ferrell, J.E., Jr. (2007). Mechanisms of specificity in protein phosphorylation. *Nature reviews Molecular cell biology* 8, 530-541.
- Verrill, M. (2009). Chemotherapy for early-stage breast cancer: a brief history. *British journal of cancer* 101 Suppl 1, S2-5.
- Wang, K., Yang, T., Wu, Q., Zhao, X., Nice, E.C., and Huang, C. (2012). Chemistry-based functional proteomics for drug target deconvolution. *Expert Rev Proteomics* 9, 293-310.
- WHO (2013). Latest world cancer statistics. Global cancer burden rises to 14.1 million new cases in 2012: Marked increase in breast cancers must be addressed. In World Health Organization Press Release (Lyon/Geneva).
- Wiener, M.C., Sachs, J.R., Deyanova, E.G., and Yates, N.A. (2004). Differential mass spectrometry: a label-free LC-MS method for finding significant differences in complex peptide and protein mixtures. *Analytical chemistry* 76, 6085-6096.
- Wilm, M. (2011). Principles of electrospray ionization. *Mol Cell Proteomics* 10, M111 009407.
- Wilm, M., Mann, M. (1994). Electrospray and Taylor-Cone theory, Dole's beam of macromolecules at last? *Int J Mass Spectrom Ion Process* 136 167-180.
- Xu, X., Weinstein, M., Li, C., Naski, M., Cohen, R.I., Ornitz, D.M., Leder, P., and Deng, C. (1998). Fibroblast growth factor receptor 2 (FGFR2)-mediated reciprocal regulation loop between FGF8 and FGF10 is essential for limb induction. *Development* 125, 753-765.
- Yates, J.R., Ruse, C.I., and Nakorchevsky, A. (2009). Proteomics by mass spectrometry: approaches, advances, and applications. *Annu Rev Biomed Eng* 11, 49-79.
- Zaia, J. (2004). Mass spectrometry of oligosaccharides. *Mass spectrometry reviews* 23, 161-227.
- Zhang, J., Yang, P.L., and Gray, N.S. (2009). Targeting cancer with small molecule kinase inhibitors. *Nature reviews Cancer* 9, 28-39.
- Zinn, N., Hopf, C., Drewes, G., and Bantscheff, M. (2012). Mass spectrometry approaches to monitor protein-drug interactions. *Methods* 57, 430-440.
- Zubarev, R.A., and Makarov, A. (2013). Orbitrap mass spectrometry. *Analytical chemistry* 85, 5288-5296.

Chapter II

Characterization of the binding profile of a small molecule pan-kinase inhibition probe VI16743

2.1 Introduction

Protein kinases play pivotal roles in the regulation of many signaling events that have great impact on diverse cellular processes. These proteins do not function independently but are tightly interconnected in cellular pathways and networks (see chapter I). Given this complexity, proteomics represents a powerful approach to study the cellular activities regulated by protein kinases. However, some of these key regulators still cannot be studied comprehensively, because of the relatively low cellular abundance. Small molecule probes have shown great capability for kinase enrichment in chemical proteomics under close to physiological conditions (see Chapter I). The probe set used in our lab (Kinobeads) is adapted from (Bantscheff et al., 2007) and is capable of enriching more than half of the human kinome. However, as our ultimate goal is to be able to cover the whole kinome, we keep on looking for better pan kinase inhibitors than we already have. In 2008, Daub et al. reported a capture molecule termed VI16832 with a high degree of nonselectivity in terms of kinase binding (Daub et al., 2008). Later, a systematic investigation on the binding profiles of 2 other analogs (VI16743 and VI16741) of VI16832 has also been published (Oppermann et al., 2009). Results show that each of the pyrido[2,3-d]pyrimidine-based affinity probes (VI-series compounds) alone was capable of enriching almost half of the expressed kinome in a given mammalian cell line. These molecules have greatly attracted our attention since on the one hand, they have rather broad kinome coverage, and on the other hand, some of the enriched kinases have not been tractable by our Kinobeads, such as the PI3K family members. Therefore, these molecules might provide potential complementarity to the Kinobeads and provide an improvement on the overall kinome coverage of the Kinobeads, which is our constant pursuit.

For this purpose, VI16743 was immobilized on sepharose beads and its binding profile was characterized by pulldown experiments using a lysate mixture of four cancer cell lines. The binding profile was compared to that of the Kinobeads. The VI16743 beads were further supplemented to Kinobeads, and the complementarity of VI16743 beads to the Kinobeads was evaluated by parallel pulldown experiments using the above-mentioned lysate mixture.

2.2 Materials and Methods

Cell Culture and Lysis

OVCAR8, K562, COLO205 and SKNBE2 cells were cultivated in humidified air supplemented with 10% CO₂ at 37 °C. K562 and COLO205 cells were cultured in Roswell Park Memorial Institute 1640 medium, OVCAR8 and SKNBE2 cells were cultured in Dulbecco's modified Eagle's medium (4.5 g/L glucose). All media were supplemented with 10%-20% fetal bovine serum (PAA, Pasching, Austria). For lysis, cells were washed with phosphate-buffered saline, then lysed in 50 mM Tris/HCl pH 7.5, 5% Glycerol, 0.8% Nonidet P-40 and freshly added protease (SIGMA-FAST, Sigma-Aldrich) and phosphatase inhibitors (Phosphatase Inhibitor Cocktail 3, Sigma-Aldrich, Munich, Germany). Homogenates were clarified by ultracentrifugation at 145,000 g at 4 °C for 30 min. Supernatants were collected and aliquots were stored at -80 °C until further use. Protein concentrations in lysates were determined by Bradford assay.

Compound Immobilization

Immobilization of the VI16743 (provided by Dr. Josef Wissing, Helmholtz Centre for Infection Research, Braunschweig, Germany) was accomplished by reaction of the primary amine of the probe with the NHS-activated sepharose beads (GE Healthcare, Freiburg, Germany) as described (Bantscheff et al., 2007; Ku et al., 2014; Pacht et al., 2013). Briefly, NHS-beads (1 ml settled beads) were suspended in isopropanol (1 ml) and washed with anhydrous dimethyl sulfoxide (3 x 10 ml). The beads were then re-suspended in anhydrous DMSO (1 ml) and a solution of the probe (20 µL, 100 mM in DMSO) was added to achieve a coupling density of 1,2 µmol of the probe per 1 ml settled beads, followed by addition of triethylamine (15 µL). The mixture was incubated in darkness for 16-20 h at room temperature on an end-over-end-shaker. Amino ethanol (50 µL) was then added to block the remaining binding sites of the NHS beads. The mixture was further incubated in the dark for 16-20 h at room temperature on an end-over-end-shaker. The functionalized beads were then washed once with anhydrous DMSO (10 ml) and ethanol (3x10 ml) and stored in ethanol (1 ml) at 4°C in the dark until use.

Affinity Purification

The pulldown assays were performed as described previously (Ku et al., 2014; Lemeer et al., 2013; Pachl et al., 2013; Wu et al., 2012). For each experiment, 5 mg of protein were used. Briefly, cell lysates were diluted with equal volumes of 1x compound pulldown (CP) buffer (50 mM Tris/HCl pH 7.5, 5% glycerol, 1.5 mM MgCl₂, 150 mM NaCl, 20 mM NaF, 1 mM sodium orthovanadate, 1 mM dithiothreitol, protease inhibitors (SIGMA-FAST, Sigma-Aldrich) and phosphatase inhibitors (Phosphatase Inhibitor Cocktail 3, Sigma-Aldrich, Munich, Germany). Lysates were further diluted if necessary to reach a final protein concentration of 5 mg/ml using 1x CP buffer supplemented with 0.4% Nonidet P-40. Lysates were incubated with the respective beads (100 µL settled amount) for another 0.5 h at 4 °C. The beads were then washed with CP buffer and collected by centrifugation. Bound proteins were eluted with 2x NuPAGE® LDS Sample Buffer (60 µL, Invitrogen, Darmstadt, Germany). Proteins in eluates were reduced by dithiothreitol (3 µL, 1M) and alkylated by iodoacetamide (6 µL, 200 mg/ml).

Aliquots of samples (30 µL) were then run into a 4–12% NuPAGE gel (Invitrogen, Darmstadt, Germany) for about 1 cm to concentrate the sample prior to in-gel tryptic digestion. In-gel trypsin digestion was performed according to standard procedures.

Liquid Chromatography Tandem Mass Spectrometry (LC-MS/MS)

Analysis

Peptides generated by in-gel trypsin digestion were dried in a vacuum concentrator and then dissolved in 20 µL 0.1% formic acid (FA) prior to LC-MS/MS analysis. LC-ESI-MS/MS was performed by coupling a nanoLC-Ultra (Eksigent, Dublin, CA) to a LTQ-Orbitrap Velos mass spectrometer (ThermoFisher Scientific). For each analysis, 10 µL of dissolved peptides was delivered to a trap column (ReproSil-pur C18-AQ, 5 µm, Dr. Maisch, Ammerbuch, Germany, 20 mm×75 µm, self-packed) at a flow rate of 5 µL/min in 100% solvent A (0.1% formic acid in HPLC grade water). After 10 min of loading and washing, peptides were transferred to an analytical column (ReproSil-gold C18-AQ, 3 µm, Dr. Maisch, Ammerbuch, Germany, 400 mm×75 µm, self-packed) and separated using a 210 min gradient from 7% to 35% of solvent B (0.1% formic acid in acetonitrile) at 300 nL/minute flow rate. The LTQ Orbitrap Velos was operated in data dependent mode, automatically switching between MS and MS/MS. Full scan MS spectra (300-1,300 m/z) were acquired in the Orbitrap at 30,000 resolution (at m/z 400) after

accumulation precursor ions to a target value of 1,000,000 for a maximum time of 100 ms. Internal lock mass calibration was performed using the ion signal $(\text{Si}(\text{CH}_3)_2\text{O})_6 \text{H}^+$ at m/z 445.120025 present in ambient laboratory air. Tandem mass spectra were generated for up to ten peptide precursors by higher energy collision induced dissociation (HCD, target value of 40,000, max 100 ms accumulation time) at a normalized collision energy of 40% and fragment ions were recorded at a resolution of 7,500 in the Orbitrap. To maximize the number of precursors targeted for analysis, dynamic exclusion was enabled with one repeat count in 10 s and 30 s exclusion time.

Peptide and Protein Identification and Quantification

For qualitative experiments, peak lists were generated from raw MS data files using Mascot Distiller v2.3.0 (Matrix Science, London) and were then searched against the human International Protein Index (IPI, version 3.68) using Mascot (version 2.3.0, Matrix Science, London). The search was performed considering carbamidomethylation of cysteine residues as fixed modification and methionine oxidation as variable modifications. Trypsin was specified as the proteolytic enzyme and up to two missed cleavages were allowed. The mass tolerances were set to 5 ppm for the precursor ions and 0.05 Da for the fragments. Further data interpretation was performed using Scaffold 3, v3.6.1. All proteins were filtered using a false discovery rate of 1%.

2.3 Results and discussion

After the compound VI16743 (Figure 1A) was immobilized (see method section), its protein binding profile was evaluated in pulldown experiments using a mixture of lysates from four human cancer cell lines (OVAR8, COLO203, SKNBE2 and K562), followed by tandem mass spectrometry analysis for protein identification. The analysis of triplicate experiments showed that VI16743 enabled the identification of 726 proteins, in which 179 are kinases (Figure 1). Although kinases accounted for just one fourth of all protein identifications, the comparison of the average intensities shows that the quantity of kinases represents 40% of the total identified proteins, indicating a high efficiency of VI16743 for kinase enrichment. VI16743 identified 50 more kinases in this experiment than it was reported (Oppermann et al., 2009), this is due to the use of a more diverse protein solution in this experiment. Visualization of the identified kinases on the phylogenetic kinome tree (Figure 2) revealed that the protein kinases enriched by VI16743 covered all major branches on the kinome tree, including AGC kinases as well as members of the CMGC, CAMK, TK, TKL, STE and CK1 kinase families.

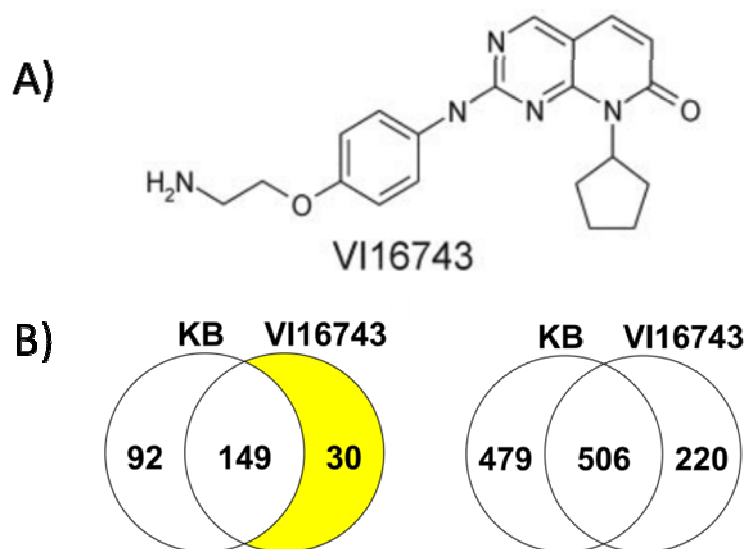


Figure 1 | The chemical structure of VI16743 and its binding profile compared to the Kinobeads (KB).

A) Chemical structure of VI16743. B) The binding profile of VI16743 compared to the Kinobeads (KB). The left Venn diagram showed numbers of enriched kinases and right Venn diagram represents the total proteins that were enriched by the Kinobeads and VI16743.

Compared to Kinobeads, VI16743 could enrich 30 extra kinases. It was reported in Daub's paper that the VI-series compounds can nicely enrich the phosphoinositide kinase family. This family is involved in many cellular activities such as cell growth, proliferation as well as intracellular trafficking, all of which are highly associated with cancer (Berdichevsky et al., 2013; Bhatt and Damania, 2012; Bitting and Armstrong, 2013). However, this family of kinases was previously out of reach by the Kinobeads. In the pulldown experiments of VI16743, 10 phosphoinositide kinases were successfully identified (Table 1), which confirmed that this probe was able to enrich this kinase family from a mixed cancer cell lysate. Importantly, members of the phosphoinositide 3 kinase family (PI3K) were also enriched in this experiment. PI3K family mediates one of the most important pathways in cells, the PI3K/AKT/mTOR pathway (Cidado and Park, 2012; Hemmings and Restuccia, 2012; Hennessy et al., 2005). This pathway has been reported to be overactive in many cancers. This hyperactivation has a number of downstream effects which either promote protein synthesis or inhibit protein breakdown and lead to the reduction of apoptosis and the increase of proliferation (Gonzalez-Angulo and Blumenschein, 2013; Heavey et al., 2014; Saini et al., 2013; Wolin, 2013). It is a very attractive target for kinase drug discovery, demonstrated by 142 ongoing clinical trials involving PI3K inhibitors in the US and 42 trials in Europe (EMA, 2014; NIH, 2014). It is a very important improvement to extend the coverage of our Kinobeads to this family, enabling the selectivity profiling of drugs against phosphoinositide kinase family members. Results also showed that more than half of the kinases (97/179) were enriched better in terms of quantity by VI16743 compared to the Kinobeads, when using the number of unique tandem mass spectra of identified proteins as semi-quantitative measure for protein abundance. It has to be noted that, due to the dilution effects, adding or mixing more probes usually results in a quick saturation of numbers of pulled kinases, in this regard, VI16743 may offer benefits as a single capture compound for kinase affinity purification and drug selectivity profiling because of the broad kinome coverage.

Table 1 | List of kinases that were exclusively enriched by VI16743 in triplicate.

Numbers in each replicate for the respective protein represent the identified numbers of unique spectra, which is a semi-quantitative parameter to assess the efficiency of the probe binding.

No	Accession Number	Molecular Weight	Gene Name	Replicates		
				1	2	3
1	IPI00008982	87 kDa	ALDH18A1	4	0	0
2	IPI00029162	158 kDa	CDC2L5	1	2	3
3	IPI00007811	34 kDa	CDK4	10	16	16
4	IPI00023529	37 kDa	CDK6	4	1	2
5	IPI00026791	53 kDa	CDK8	3	2	3
6	IPI00005104	85 kDa	CHUK	4	8	8
7	IPI00456641	107 kDa	ERN2	2	1	2
8	IPI00024709	87 kDa	IKBKB	5	2	2
9	IPI00168907	47 kDa	IPMK	9	12	10
10	IPI00216433	71 kDa	LIMK1	1	1	1
11	IPI00005741	42 kDa	MAPK13	1	0	0
12	IPI00008883	74 kDa	NUAK2	3	3	3
13	IPI00376955	60 kDa	PCTK2	7	5	8
14	IPI00465179	93 kDa	PFKM	1	0	0
15	IPI00020124	54 kDa	PI4K2A	1	4	3
16	IPI00291068	55 kDa	PI4K2B	1	5	4
17	IPI00070943	231 kDa	PI4KA	1	1	2
18	IPI00299755	102 kDa	PIK3C3	15	22	17
19	IPI00292690	126 kDa	PIK3CG	2	0	0
20	IPI00024006	153 kDa	PIK3R4	15	23	21
21	IPI00009688	46 kDa	PIP4K2A	3	8	6
22	IPI00216470	47 kDa	PIP4K2B	1	1	1
23	IPI00929676	45 kDa	PIP4K2C	1	1	1
24	IPI00479186	58 kDa	PKM2	5	2	2
25	IPI00219616	35 kDa	PRPS1	1	0	0
26	IPI00178899	48 kDa	SKP2	1	2	2
27	IPI00006064	68 kDa	TBKBP1	2	2	4
28	IPI00297452	89 kDa	TFG	1	1	1
29	IPI00299214	25 kDa	TK1	3	0	1
30	IPI00337659	85 kDa	TLK2	3	2	1

In addition to kinases, VI16743 also binds to a large number of other proteins. This is not surprising since this molecule is an ATP mimic and should bind the nucleotide binding proteins which are fairly abundant in mammalian cells. Gene ontology (GO)

analysis of the identified proteins reveals that all probes do bind a considerable number of these proteins.

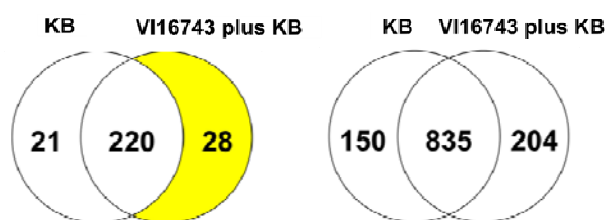


Figure 3 | Comparison of enriched protein numbers for Kinobeads (KB) and VI16743 plus Kinobeads.

The left Venn diagram showed numbers of enriched kinases and right Venn diagram represents the total number of enriched protein by the Kinobeads and KB plus VI16743.

Having established that VI16743 is an effective affinity tool for capturing kinases, the complementarity of this compound to the Kinobeads was evaluated. For this purpose, pulldown experiments using our Kinobeads (5 immobilized compounds, see Figure 6 in Chapter I for structures) in parallel with a mixture of Kinobeads supplemented with VI16743 beads (6 immobilized compounds, equal amount of each) were performed. In pulldowns using Kinobeads, 241 kinases (total of 985 proteins, Figure 3) were identified. For experiment using KB+VI16743, 248 kinases out of a total of 1039 proteins were identified. More than 90% (220 kinases) of the kinases were identified in both experiments. However, of all the 248 kinases identified by the KB+VI16743 beads, 60% (145 kinases) showed an improved in terms of quantification (judged by unique spectrum counts) over that of the Kinobeads (Figure 4). In addition, 28 kinases were exclusively found in the KB plus VI16743 experiment and members of the phosphoinositide kinase family were present in higher amounts on KB+VI16743 beads compared to Kinobeads. The 21 kinases exclusively identified on KB originate from many different areas of the kinome tree and these hits were mostly identified with few spectra, thus representing kinases with either low affinity to the Kinobeads or kinases of very low abundance in the sample.

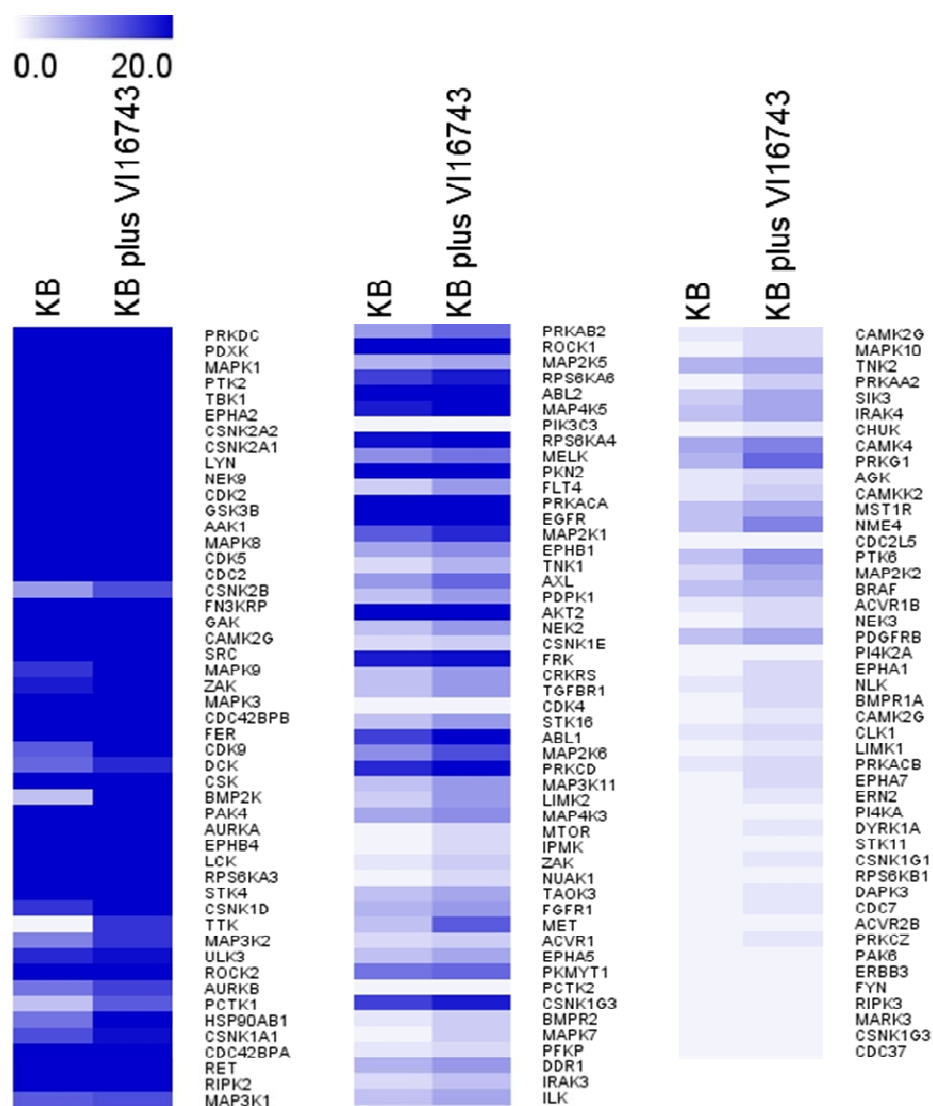


Figure 4 | Heatmap analysis of the abundance of identified kinases using the number of unique spectra as semi-quantitative measurement.

Results showed KB plus VI16743 showed an improvement on 60% (145 kinases) of all identified kinases in terms of quantification over that of the Kinobeads.

2.4 Conclusion

As shown, supplemented by the VI16743 beads, the new affinity matrix displayed an improvement both qualitatively and quantitatively over the original Kinobeads. Therefore VI16743 beads represent a good complementarity to the Kinobeads for kinase affinity purification. However, due to the great challenges in the synthesis of this compound, at this moment it is not considered to be supplemented to the Kinobeads for routine analysis.

In summary, the small molecule pan kinase inhibition probe VI16743 was immobilized and its target profile was characterized using mixtures of cancer cell lysates. Results show that it could enrich 179 kinases, in which 30 were previously out of reach by the Kinobeads, including kinases of great clinical relevance, such as PI3K family members. This demonstrates the capacity of VI16743 to pre-fractionate and detect almost nearly half of the expressed kinome, which makes it possible to serve as a “one-compound Kinobeads” for kinase affinity purification. On the other hand, when supplemented to the Kinobeads, VI16743 also demonstrated a good complementarity to the current Kinobeads. The new matrix achieved an improvement on protein quantities of 145 kinases (60% of the total identified proteins) including 28 newly identified kinases.

Acknowledgements

The compound VI16743 generously provided by Dr. Josef Wissing in Helmholtz Centre for Infection Research, Braunschweig, Germany.

Abbreviations

DMEM Dulbecco's modified Eagle's medium

FBS fetal bovine serum

GO gene ontology

HCD higher energy collision induced dissociation

IMDM Iscove's modified Dulbecco's medium

KB Kinobeads

LC-MS/MS liquid chromatography coupled to tandem mass spectrometry

PBS phosphate buffered saline

PI3K phosphoinositide 3 kinase family

RPMI1640 Roswell Park Memorial Institute 1640 medium

References

- Bantscheff, M., Eberhard, D., Abraham, Y., Bastuck, S., Boesche, M., Hobson, S., Mathieson, T., Perrin, J., Raida, M., Rau, C., *et al.* (2007). Quantitative chemical proteomics reveals mechanisms of action of clinical ABL kinase inhibitors. *Nat Biotechnol* 25, 1035-1044.
- Berdichevsky, Y., Dryer, A.M., Saponjian, Y., Mahoney, M.M., Pimentel, C.A., Lucini, C.A., Usenovic, M., and Staley, K.J. (2013). PI3K-Akt signaling activates mTOR-mediated epileptogenesis in organotypic hippocampal culture model of post-traumatic epilepsy. *The Journal of neuroscience : the official journal of the Society for Neuroscience* 33, 9056-9067.
- Bhatt, A.P., and Damania, B. (2012). AKTivation of PI3K/AKT/mTOR signaling pathway by KSHV. *Frontiers in immunology* 3, 401.
- Bitting, R.L., and Armstrong, A.J. (2013). Targeting the PI3K/Akt/mTOR pathway in castration-resistant prostate cancer. *Endocrine-related cancer* 20, R83-99.
- Cidado, J., and Park, B.H. (2012). Targeting the PI3K/Akt/mTOR pathway for breast cancer therapy. *J Mammary Gland Biol Neoplasia* 17, 205-216.
- Daub, H., Olsen, J.V., Bairlein, M., Gnad, F., Oppermann, F.S., Korner, R., Greff, Z., Keri, G., Stemmann, O., and Mann, M. (2008). Kinase-selective enrichment enables quantitative phosphoproteomics of the kinome across the cell cycle. *Mol Cell* 31, 438-448.
- EMA (2014). Clinical Trials for PI3K. In EU Clinical Trials Register.
- Gonzalez-Angulo, A.M., and Blumenschein, G.R., Jr. (2013). Defining biomarkers to predict sensitivity to PI3K/Akt/mTOR pathway inhibitors in breast cancer. *Cancer Treat Rev* 39, 313-320.
- Heavey, S., O'Byrne, K.J., and Gately, K. (2014). Strategies for co-targeting the PI3K/AKT/mTOR pathway in NSCLC. *Cancer Treat Rev* 40, 445-456.
- Hemmings, B.A., and Restuccia, D.F. (2012). PI3K-PKB/Akt pathway. *Cold Spring Harb Perspect Biol* 4, a011189.
- Hennessy, B.T., Smith, D.L., Ram, P.T., Lu, Y., and Mills, G.B. (2005). Exploiting the PI3K/AKT Pathway for Cancer Drug Discovery. *Nature reviews Drug discovery* 4, 988-1004.
- Ku, X., Heinzlmeir, S., Liu, X., Medard, G., and Kuster, B. (2014). A new chemical probe for quantitative proteomic profiling of fibroblast growth factor receptor and its inhibitors. *J Proteomics* 96, 44-55.
- Lemeer, S., Zorgiebel, C., Ruprecht, B., Kohl, K., and Kuster, B. (2013). Comparing immobilized kinase inhibitors and covalent ATP probes for proteomic profiling of kinase expression and drug selectivity. *J Proteome Res* 12, 1723-1731.
- NIH (2014). Studies found for: PI3K. In Clinical Trials of the US National Institutes of Health.

- Oppermann, F.S., Gnad, F., Olsen, J.V., Hornberger, R., Greff, Z., Keri, G., Mann, M., and Daub, H. (2009). Large-scale proteomics analysis of the human kinome. *Mol Cell Proteomics* 8, 1751-1764.
- Pachl, F., Plattner, P., Ruprecht, B., Medard, G., Sewald, N., and Kuster, B. (2013). Characterization of a chemical affinity probe targeting Akt kinases. *J Proteome Res* 12, 3792-3800.
- Saini, K.S., Loi, S., de Azambuja, E., Metzger-Filho, O., Saini, M.L., Ignatiadis, M., Dancey, J.E., and Piccart-Gebhart, M.J. (2013). Targeting the PI3K/AKT/mTOR and Raf/MEK/ERK pathways in the treatment of breast cancer. *Cancer Treat Rev* 39, 935-946.
- Wolin, E.M. (2013). PI3K/Akt/mTOR pathway inhibitors in the therapy of pancreatic neuroendocrine tumors. *Cancer letters* 335, 1-8.
- Wu, Z., Moghaddas Gholami, A., and Kuster, B. (2012). Systematic identification of the HSP90 candidate regulated proteome. *Mol Cell Proteomics* 11, M111 016675.

Chapter III

**A chemical probe for quantitative proteomic
profiling of fibroblast growth factor receptor
and its inhibitors**

3.1 Introduction

The completion of the human genome analysis has created great expectations (Lander et al., 2001; Reich et al., 2001). It has been believed that scientists could use the genome information to identify and validate a number of new drug targets and tailor specific therapeutics based on individual's genetic makeup (Cockett et al., 2000). However, this did not hold true. In spite of the discovery of tremendous proteins that have regulatory roles in cellular activities, the medical and pharmaceutical communities are still struggling to find new “druggable” targets. On the other hand, most clinical drugs are found to be more promiscuous than originally expected (Anastassiadis et al., 2011; Karaman et al., 2008). Kinobead, a comprehensive technology that is able to provide detailed drug target-interaction analysis is of great value (Bantscheff et al., 2007; Bantscheff and Kuster, 2012; Schirle et al., 2012). In addition to drug-centric target identification as exemplified by the characterization of the binding profile of VI16743 presented in Chapter II, Kinobeads also allow drug selectivity profiling when adapted into a competition binding assay (see Chapter I). However, as mentioned in previous chapters, a major challenge for Kinobeads approach is the incomplete coverage of the kinome. In spite of the presence of several pan kinase inhibition probes in the Kinobeads probe set, there were still some kinases which remained constantly out of reach or were enriched with rather low efficiency. Some of these kinases are of great clinical relevance, notably the angiogenesis related targets. Due to their significance in cancer research and drug discovery, specific probes that could enrich angiokinases for chemical proteomics approaches are of great value. Therefore, in this chapter, new chemical probes aiming of enriching Fibroblast Growth Factor Receptors (FGFRs), a crucial kinase family in the angiogenesis pathway, are described. In light of the previously successful case for the development of probes enriching AKT kinases (Pachl et al., 2013), chemical probes for FGFRs were designed applying the similar strategy. The designing strategy was to select a lead compound which has a broad selectivity and a high potency to the target kinases, followed by additions of carefully designed linkers to the parent compound based on the studies of the reported co-crystal structure and molecular docking. The designed FGFR probes were then synthesized and immobilized on sepharose beads. To evaluate the binding profiles of the probes, pulldown experiments using lysates of human placenta and cancer cell lines were performed and the better probe with better binding profile was selected. To realize the practical utility of the FGFR probe, the selected probe was

mixed with the Kinobeads (see Chapter I for Kinobeads probe structures). The new probe matrix was applied to the selectivity profiling of two angiogenesis drugs, Dovitinib and Orantinib. The selectivity profiles of the two drugs were acquired from label-free quantification data analyzed by LC-MS/MS.

3.2 Material and Methods

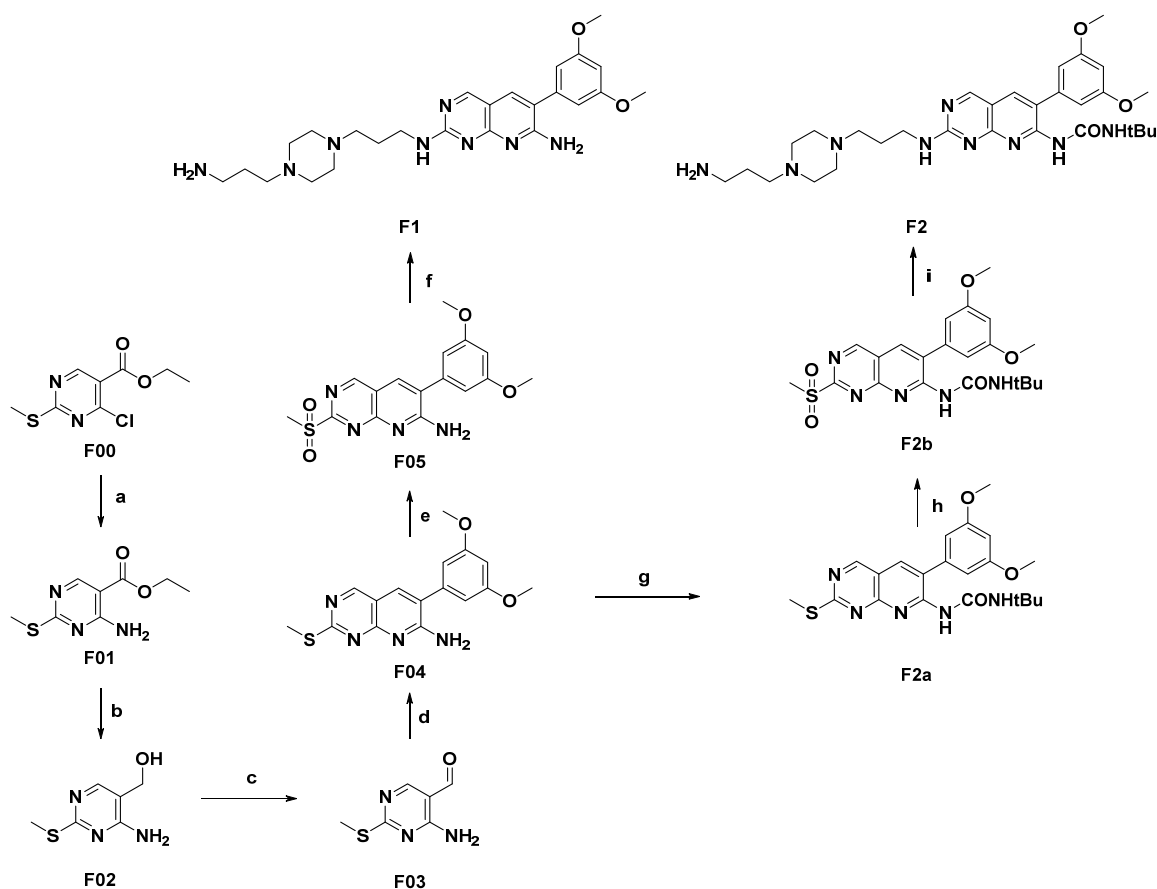
Molecular Docking

The binding pose of probe F2 in FGFR1's ATP-binding site was predicted by the software Glide (Schrödinger, Inc.). The crystal structure of FGFR1 in complex with PD173074 was retrieved from the Protein Data Bank (PDB code 2FGI) and prepared using the Protein Preparation Wizard in Maestro (Schrödinger, Inc.) to remove non amino acid molecules and add hydrogen atoms. The scoring grid was generated by enclosing the residues 14 Å around PD173074 in the binding site. The docking of F2 was performed in Glide SP mode and the top ranked binding pose was used for binding mode analysis.

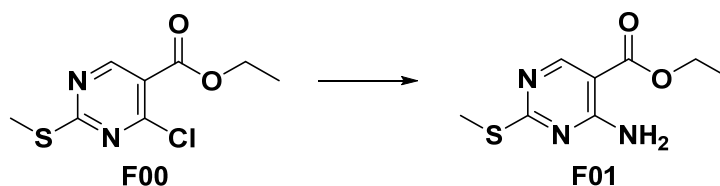
General Synthetic Methods

All chemicals and solvents were purchased from commercial suppliers (Sigma-Aldrich Co, VWR International, Carl Roth GmbH & Co.KG, Alfa Aesar, Fluorochem Ltd) and were used without further purification. All air- and moisture-sensitive reactions were carried out under an atmosphere of dry argon with heat-dried glassware and standard syringe techniques. Flash chromatography was performed on an Interchim puriFlash evo 430 system. Mass spectrometry (MS) analyses were conducted on an amazon speed ETD ion trap mass spectrometer in positive electrospray mode. The samples were separated by HPLC on an Agilent 1100 system prior to mass spectrometric analysis. Proton (^1H NMR) and carbon (^{13}C NMR) nuclear magnetic resonance spectra were obtained at 400 and 100 MHz, respectively unless otherwise noted. Chemical shifts were recorded in parts per million (ppm) and NMR signals were described as following: s (single), d (doublet), t (triplet), q (quadruplet), and m (multiplet). Reverse phase LC-MS was performed utilizing a TriArt C18 column and an 1100 series HPLC system, applying a 5-95% gradient of solvent B (0.1% TFA in acetonitrile) in solvent A (0.1% TFA in water) for 20 min, followed by a 20 min plateau of 95% solvent B. Chromatography signals were detected at λ : 254nm and 365 nm. Mass analysis was accomplished by an amazon speed ETD ion trap mass spectrometer.

Synthesis of Probe F1 and F2



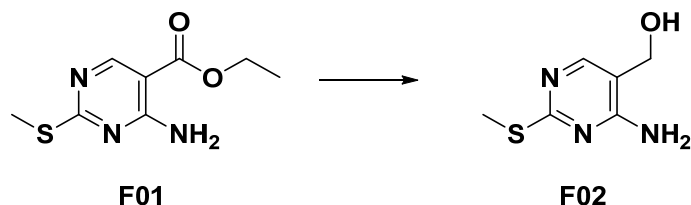
Ethyl 4-amino-2-(methylthio)pyrimidine-5-carboxylate (F01)



Ethyl 4-chloro-2-(methylthio)pyrimidine-5-carboxylate (F00) (5.05 g, 21.5 mmol) was dissolved in THF (69 ml). Triethylamine (9 ml, 64.5 mmol, 3 eq) and ammonium hydroxide solution (50% v/v, 6 ml, 86.0 mmol, 4 eq) were added and stirred at room temperature overnight. Consumption of starting material was verified by TLC (PE:EA = 2:1 [UV]). Reaction was quenched by addition of saturated aqueous NaHCO_3 and product was extracted with DCM. Compound F01 was obtained as white solid (4.17 g, 19.6 mmol) without further purification. LC-MS $[\text{M}+\text{H}^+]$: 213.91 (calculated mass: 213.06), ^1H NMR (400 MHz, DMSO-d_6) δ 8.53 (s, 1H), 7.79 (d, $J = 140.9$ Hz, 2H), 4.23 (q, $J = 7.1$ Hz, 2H), 2.43 (s, 3H),

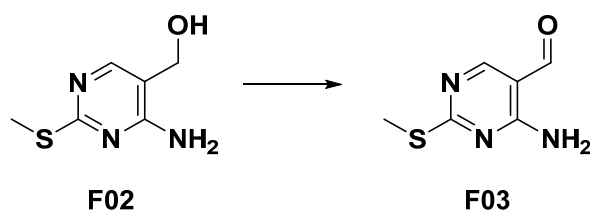
1.25 (t, $J = 7.1$ Hz, 4H).¹³C NMR (400 MHz, DMSO-d₆) δ 174.81 , 165.65 , 161.37 , 158.52 , 100.46 , 60.63 , 14.12 , 13.47 .

(4-amino-2-(methylthio)pyrimidin-5-yl)methanol (F02)



F01 (3.60 g, 16.9 mmol) was dissolved in anhydrous THF (53 ml) and a suspension of lithium aluminium hydride (2 eq, 1.28 g, 33.7 mmol) in anhydrous THF (36 ml) was added dropwise at room temperature. The reaction was monitored by TLC (PE:EA 1:1 [UV]) and finished after 30 min by addition of ddH₂O (2.7 ml). 15% aqueous NaOH (2.7 ml) dissolved the evolving gel and complete quenching was accomplished by further addition of ddH₂O (3.6 ml). The reaction mixture was stirred 20 min which lead to a color change from dark green to bright yellow. The white precipitate was filtrated with Celite and washed with EA. Product F02 was extracted from the filtrate between ddH₂O and EA. Compound F02 was obtained as yellow solid without further purification (2.44 g, 14.3 mmol). LC-MS [M+H⁺]: 171.87 (calculated mass: 171.05) ¹H NMR (400 MHz, DMSO-d₆) δ 7.84 (s, 1H), 6.64 (s, 2H), 5.02 (t, $J = 5.5$ Hz, 1H), 4.24 (d, $J = 5.3$ Hz, 2H), 2.34 (s, 3H).¹³C NMR (400 MHz, DMSO-d₆) δ 168.65 , 161.32 , 152.92 , 112.93 , 57.61 , 13.24 .

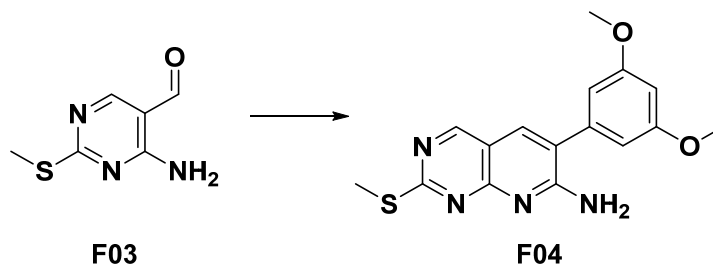
4-amino-2-(methylthio)pyrimidine-5-carbaldehyde (F03)



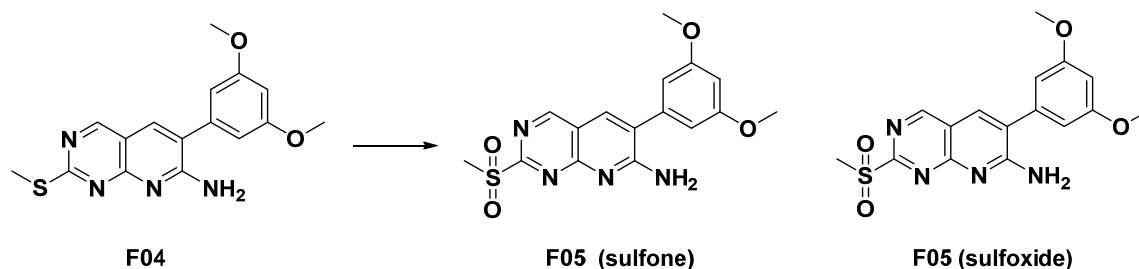
Compound F02 (1.88 g, 11.0 mmol) was dissolved in DCM (150 ml) and activated manganese (IV) oxide (10 eq, 9.54 g, 110.0 mmol) was added to the solution. Reaction mixture was stirred at room temperature and monitored by TLC (PE:EA 1:1, [UV]) until complete consumption of the starting material after 2 hours. The suspension was filtrated with Celite and washed with DCM. Crude product was obtained as pale yellow solid. After purification via flash chromatography (0-100% EtOAc in PE), the product F03 was obtained

as white powder (1.40 g, 8.3 mmol). Yield: 75.5% LC-MS [M+H⁺]: 169.88 (calculated mass: 169.03) ¹H NMR (400 MHz, DMSO-d₆) δ 9.71 (s, 1H), 8.52 (s, 1H), 8.09 (d, *J* = 97.4 Hz, 2H), 2.44 (s, 3H). ¹³C NMR (400 MHz, DMSO-d₆) δ 191.81 , 175.68 , 163.62 , 159.96 , 109.10 , 13.55.

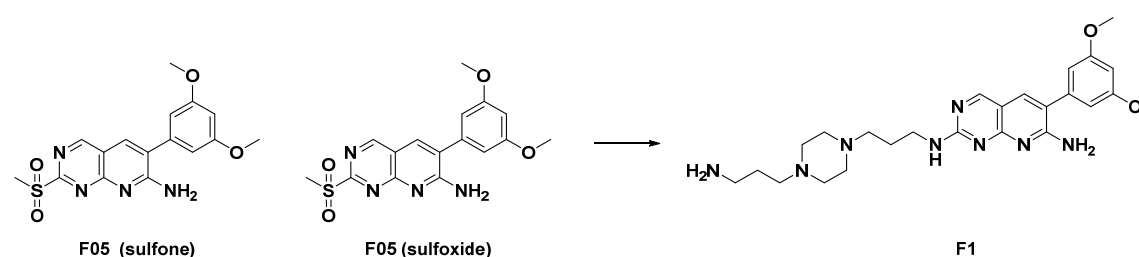
6-(3,5-dimethoxyphenyl)-2-(methylthio)pyrido[2,3-d]pyrimidin-7-amine (F04)



Sodium hydride (60%, 1 eq, 12.00 mg, 0.3 mmol) was mixed with anhydrous THF (1 ml). Then, (3,5-dimethoxyphenyl)-acetonitrile (1 eq, 53.16 mg, 0.3 mmol) was added to the suspension and the reaction mixture was stirred for 1.5 h at room temperature, before compound F03 (50.00 mg, 0.3 mmol) was added slowly. The reaction was performed overnight at room temperature and complete consumption of starting material F03 was verified by TLC (PE:EA 1:2 [UV]). Reaction mixture was partitioned between DCM and saturated aqueous NH₄Cl. Product F04 was obtained as yellow sticky solid (109.9 mg, 0.335 mmol) and was used for further steps without purification. LC-MS [M+H⁺]: 328.97 (calculated mass: 328.10) ¹H NMR (400 MHz, DMSO-d₆) δ 8.84 (s, 1H), 7.86 (s, 1H), 6.59 (d, *J* = 2.3 Hz, 2H), 6.53 (t, *J* = 2.2 Hz, 1H), 3.76 (s, 6H), 2.50 (s, 3H). ¹³C NMR (400 MHz, DMSO-d₆) δ 169.95 , 160.46 , 159.85 , 158.15 , 157.41 , 137.12 , 135.27 , 123.98 , 110.99 , 105.57 , 99.55 , 54.35 , 12.73.

6-(3,5-dimethoxyphenyl)-2-(methylsulfonyl)pyrido[2,3-d]pyrimidin-7-amine (F05)

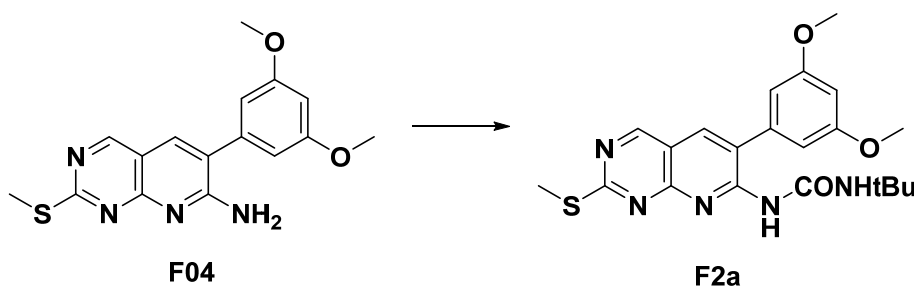
Compound F04 (0.61 mg, 1.8 mmol) and Oxone® (1.5 eq, 0.80 mg, 2.6 mmol) were dissolved in aqueous acetone solution (16.5 ml ddH₂O : 10 ml acetone) and pH: 7.5 – 8.0 was adjusted by addition of NaHCO₃. Oxidation potency was checked via iod starch paper and reaction mixture was stirred 48 h at room temperature. Since the reaction was not finished, further Oxone® (1.5 eq, 291.3 mg, 0.95 mmol) was added and pH was adjusted again by addition of NaHCO₃. Progress of the reaction was monitored by TLC (10% MeOH in DCM [UV]). After 1.5 h stirring at room temperature, Oxone® was neutralized by addition of aqueous saturated Na₂S₂O₃ solution and product F05 was extracted with EA. The product mixture F05 (0,60 mg, 1.7 mmol) was obtained as orange solid and contained sulfoxide as well as sulfone species, which react both in the next reaction. Therefore, further separation was not performed. LC-MS [M+H⁺]: sulfone 361.00 (calculated mass: 360.09), sulfoxide 345.00 (calculated mass: 344.09) ¹H NMR (400 MHz, DMSO-d₆) δ 9.24 (s, 1H), 8.09 (s, 1H), 6.66 (d, *J* = 2.3 Hz, 2H), 6.60 (t, *J* = 2.3 Hz, 1H), 3.80 (s, 6H), 3.40 (s, 3H). ¹³C NMR (400 MHz, DMSO-d₆) δ 164.68 , 162.48 , 160.92 , 159.58 , 158.92 , 137.30 , 135.80 , 128.83 , 116.55 , 106.54 , 101.01 , 55.38 .

N2-(3-(4-(3-aminopropyl)piperazin-1-yl)propyl)-6-(3,5-dimethoxyphenyl)pyrido[2,3-d]pyrimidine-2,7-diamine (F1)

Product mixture F05 (87.00 mg, 0.253 mmol) was dissolved in dry isopropanol (3 ml) at 50°C. After cooling down to RT, +Camphor-10-sulfonic acid (1 eq, 58.70 mg, 0.25 mmol) and 1,4-Bis(3-aminopropyl)piperazine (1 eq, 56.2 µl, 0.25 mmol) were added. Reaction mixture

was stirred overnight at RT and monitored by TLC (2M ammonia in MeOH [UV, Ninhydrin]). Quenching of the reaction was performed by addition of ddH₂O and extraction of starting material or side products was accomplished three times with EA, whereas the product stayed in the aqueous layer. Product F1 was further purified via flash chromatography using a C18 column (25 g) and applying a gradient of 0-100 % MeOH in ddH₂O. Afterwards, ion exchange chromatography (SCX) was performed in order to desalt the product F1. SCX column was conditioned applying 2x 3 ml MeOH and 2x 3 ml ddH₂O. After sample loading (0.25 meq per 0.5 g column), column was washed with 2x 3 ml washing solution 1 (acetic acid : ddH₂O 5:95) and 2x 3 ml washing solution 2 (MeOH : ddH₂O 20:80). Product F1 was eluted by 2x 2 ml elution solution (MeOH : acetone 50 : 50 + 5% NH₃). Solvent was removed and gave F1 as sticky yellow solid (31.7 mg, 0.066 mmol). LC-MS [M+H⁺]: 241.03 and 481.23 (calculated mass: 480.30), double charged 241.03. ¹H NMR (400 MHz, CDCl₃) δ 8.61 (s, 1H), 7.56 (s, 1H), 6.57 (d, *J* = 2.2 Hz, 2H), 6.50 (t, *J* = 2.2 Hz, 1H), 6.09 (s, 1H), 5.40 (s, 2H), 3.83 (s, 6H), 3.64 (d, *J* = 6.3 Hz, 2H), 2.77 (t, *J* = 6.8 Hz, 2H), 2.57 – 2.39 (m, 12H), 1.86 – 1.81 (m, 2H), 1.66 (dt, *J* = 14.1, 6.9 Hz, 2H). ¹³C NMR (400 MHz, CDCl₃) δ 162.61, 161.59, 160.67, 160.33, 136.56, 109.52, 106.99, 100.28, 55.64, 55.64, 40.91, 29.83, 26.19.

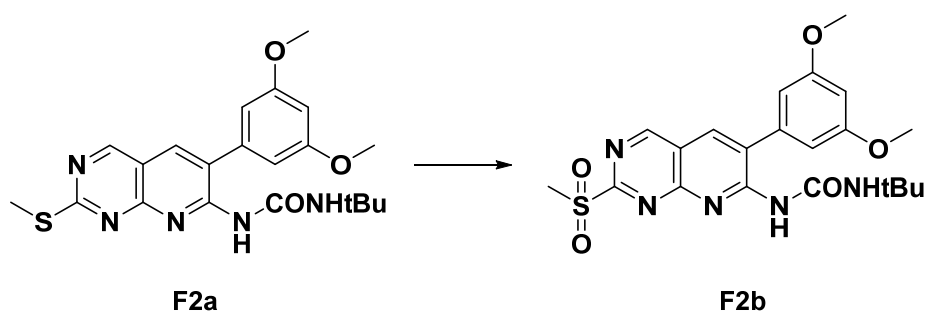
1-(tert-butyl)-3-(6-(3,5-dimethoxyphenyl)-2-(methylthio)pyrido[2,3-d]pyrimidin-7-yl)urea (F2a)



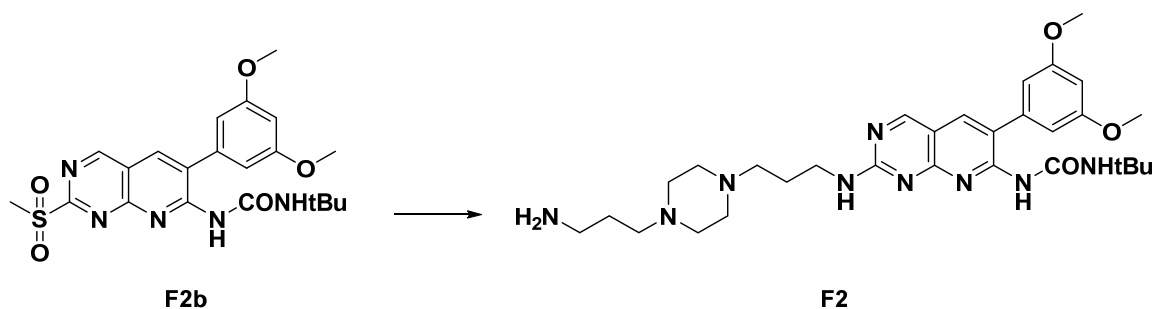
Compound F04 (350.00 mg, 1.06 mmol) was dissolved in dry DMF. At 40 °C, NaH (60%, 1.1 eq, 51.00 mg, 1.18 mmol) was added and reaction mixture was stirred for 1h (argon atmosphere). After cooling down to 0°C, tert-butyl-isocyanate (1.4 eq, 163.8 µl, 1.47 mmol) was added dropwise and reaction mixture was stirred over night while it slowly changed to room temperature. Consumption of starting material was monitored by TLC (EA [UV]). Product was extracted with EA and organic layer was washed ten times with ddH₂O. Compound F2a was obtained as yellow needles (258.00 mg, 0.60 mmol). NMR analysis revealed that the product formed a complex with DMF (258.00 mg, 0.52 mmol). LC-MS

[M+H⁺]: 428.13 (calculated mass 427.17) ¹H NMR (400 MHz, DMSO-d₆) δ 10.11 (s, 1H), 9.19 (s, 1H), 8.25 (s, 1H), 7.39 (s, 1H), 6.68 (d, *J* = 2.0 Hz, 3H), 6.67 (d, *J* = 1.9 Hz, 2H), 3.80 (s, 5H), 2.61 (s, 3H), 1.40 (s, 9H). ¹³C NMR (101 MHz, DMSO-d₆) δ 172.44, 162.32, 161.28, 160.09, 156.08, 155.35, 138.02, 136.26, 126.02, 112.82, 107.09, 100.85, 55.54, 50.29, 28.61, 13.68.

1-(tert-butyl)-3-(6-(3,5-dimethoxyphenyl)-2-(methylsulfonyl)pyrido[2,3-d]pyrimidin-7-yl)urea (F2b)



Compound F2a (150.00 mg, 0.30 mmol) and ammonium molybdate tetrahydrate (0.027 eq, 10 mg, 0.008 mmol) were dissolved in 2-methoxy-ethanol (20 ml) containing sulfuric acid (0.06 eq, 1 μ l, 0.019 mmol). Reaction mixture was stirred 2h at room temperature before H₂O₂ (30%, 15 eq, 356 μ l, 4.55 mmol) was added dropwise. Reaction was monitored by TLC (10% MeOH in DCM, [UV]) stirred at room temperature overnight. Product was extracted with EA and organic layer was washed seven times with ddH₂O to remove the solvent. Product was crashed out from MeOH with ether. The obtained product mixture contained sulfoxide as well as sulfone species, which react both in the next reaction. Therefore, further separation was not performed (38.4 mg, 0.085 mmol). LC-MS [M+H⁺]: sulfone 460.08 (calculated mass: 459.16), sulfoxide 444.08 (calculated mass: 443.16)

1-(tert-butyl)-3-(6-(3,5-dimethoxyphenyl)-2-(methylsulfonyl)pyrido[2,3-d]pyrimidin-7-yl)urea (F2)

Product mixture F2b (196.00 mg, 0.43 mmol) was resuspended in dry isopropanol (5 ml) and +Camphor-10-sulfonic acid (1.1 eq, 111 mg, 0.48 mmol) and 1,4-Bis(3-aminopropyl)piperazine (1 eq, 88.5 μ l, 0.43 mmol) were added. The reaction was performed under argon atmosphere overnight and consumption of starting material was verified by TLC (2M ammonia in MeOH [UV, Ninhydrin]). Reaction was quenched with ddH₂O and acidified to pH:3 by addition of HCl. Starting material and side products were extracted with EA. Then, NaOH was added to pH=9 in order to extract the basic product with EA. Product F2 was obtained as brown sticky solid (13.10 mg, 0.023 mmol). MS: 580.26 (calculated mass: 579.36), double charged 290.56 ¹H NMR (400 MHz, CDCl₃) δ 8.70 (s, 1H), 7.65 (s, 1H), 6.51 (t, J = 2.2 Hz, 1H), 6.47 (d, J = 2.2 Hz, 2H), 3.82 (s, 6H), 3.67 – 3.59 (m, 2H), 2.81 (dd, J = 16.6, 10.1 Hz, 2H), 2.68 – 2.33 (m, 12H), 1.88 – 1.82 (m, 2H), 1.74 – 1.64 (m, 2H), 1.49 (s, 9H), 1.31 (s, 1H). ¹³C NMR (101 MHz, CDCl₃) δ 161.83 , 158.80 , 137.22 , 107.47 , 100.89 , 57.06 (d, J = 29.3 Hz), 55.70 , 53.42 , 50.95 , 41.10 , 29.85 , 29.12.

Sample Preparation

Placenta Lysis. Post-delivery human placenta tissue (obtained from Freising hospital following informed consent by the donor) was thoroughly washed with cold phosphate buffered saline (PBS) and homogenized in lysis buffer (50 mM Tris/HCl pH 7.5, 5% Glycerol, 1.5 mM MgCl₂, 150 mM NaCl, 0.8% NP-40, 1 mM dithiothreitol and 25 mM NaF with freshly added protease inhibitors (SIGMA-FAST, Sigma-Aldrich) and phosphatase inhibitors (Phosphatase Inhibitor Cocktail 3, Sigma-Aldrich, Munich, Germany)) using a tissue grinder. Lysates were incubated for 30 min at 4 °C and protein extracts were clarified by ultracentrifugation for 1 h at 145,000 x g at 4 °C. Protein concentrations were determined by Bradford assay.

Cell Culture and Lysis. Five cancer cell lines derived from different human tissues were cultivated in humidified air supplemented with 10% CO₂ at 37 °C. K562 and COLO205 cells were cultured in Roswell Park Memorial Institute 1640 medium, OVCAR8 and SKNBE2 cells were cultured in Dulbecco's modified Eagle's medium (4.5 g/l glucose) and MDAMB453 cells were cultured in Iscove's Modified Dulbecco's Medium. All media were supplemented with 10%-20% fetal bovine serum (PAA, Pasching, Austria). For lysis, cells were washed with phosphate-buffered saline, then lysed in 50 mM Tris/HCl pH 7.5, 5% Glycerol, 0.8% Nonidet P-40 and freshly added protease (SIGMA-FAST, Sigma-Aldrich) and phosphatase inhibitors (Sigma-Aldrich, Munich, Germany). Homogenates were clarified by ultracentrifugation at 145,000 g at 4 °C for 30 min. Supernatants were collected and aliquots were stored at 80 °C until further use. Protein concentration in lysates was determined by the Bradford assay.

Compound Immobilization

Immobilization of the synthesized compounds was accomplished by a coupling reaction between the primary amine of the linkable inhibitor and NHS-activated sepharose beads as described (Bantscheff et al., 2007; Pachl et al., 2013). Briefly, beads were suspended in iPrOH (1 ml settled beads) and washed three times with 10 ml anhydrous DMSO. The beads were then re-suspended in 1 ml anhydrous DMSO and 20 µL compound stock solution (100 mM in DMSO) as well as triethylamine (15 µL) was added. The mixture was incubated in darkness for 16-20 h at room temperature on an end-over-end-shaker. Amino ethanol (50 µL) was then added to block the remaining binding sites of the NHS beads. The mixture was further incubated in the dark for 16-20 h at room temperature on an end-over-end-shaker. The functionalized beads were then washed once with anhydrous DMSO (10 ml) and ethanol (3X10 ml) and stored in ethanol (1 ml/ml beads) at 4°C in the dark.

Kinobeads Drug Competition Assay

Kinobead pulldowns were performed as described previously (Lemeer et al., 2013a; Wu et al., 2011; Wu et al., 2012). Protein concentration was determined by a standard Bradford Assay. Briefly, tissue lysates were diluted with equal volumes of 1× compound pulldown buffer (50 mM Tris/HCl pH 7.5, 5% glycerol, 1.5 mM MgCl₂, 150 mM NaCl, 20 mM NaF, 1 mM sodium orthovanadate, 1 mM dithiothreitol, 5 mM calyculin A, protease and phosphatase inhibitors). Lysates were further diluted if necessary to reach a final protein concentration of 5 mg/ml using 1× compound pulldown buffer supplemented with 0.4% Nonidet P-40.

These lysates were incubated with the respective drug in 6 concentrations (DMSO, 2.5 nM, 25 nM, 250 nM, 2.5 μ M, 25 μ M) for 0.5 h at 4 °C. Afterwards, the treated lysates were incubated with Kinobeads for another 0.5 h at 4 °C. Subsequently, beads were washed with compound pulldown buffer and collected by centrifugation. Bound proteins were eluted with 2 \times NuPAGE® LDS Sample Buffer (Invitrogen, Darmstadt, Germany) and eluates were reduced by 10 mM dithiothreitol and alkylated by 55 mM iodoacetamide. Samples were then run into a 4–12% NuPAGE gel (Invitrogen, Darmstadt, Germany) for about 1 cm to concentrate the sample prior to in-gel tryptic digestion. In-gel trypsin digestion was performed according to standard procedures.

Liquid Chromatography Tandem Mass Spectrometry (LC-MS/MS)

Analysis

Peptides generated by in-gel trypsin digestion were dried in a vacuum concentrator and then dissolved in 20 μ L 0.1% formic acid (FA) prior to LC-MS/MS analysis. LC-ESI-MS/MS was performed by coupling a nanoLC-Ultra (Eksigent, Dublin, CA) to a LTQ-Orbitrap Velos mass spectrometer (ThermoFisher Scientific). For each analysis, 10 μ L of dissolved peptides was delivered to a trap column (ReproSil-pur C18-AQ, 5 μ m, Dr. Maisch, Ammerbuch, Germany, 20 mm \times 75 μ m, self-packed) at a flow rate of 5 μ L/min in 100% solvent A (0.1% formic acid in HPLC grade water). After 10 min of loading and washing, peptides were transferred to an analytical column (ReproSil-gold C18-AQ, 3 μ m, Dr. Maisch, Ammerbuch, Germany, 400 mm \times 75 μ m, self-packed,) and separated using a 210 min gradient from 2% to 35% of solvent B (0.1% formic acid in acetonitrile) at 300 nL/minute flow rate. The LTQ Orbitrap Velos was operated in data dependent mode, automatically switching between MS and MS/MS. Full scan MS spectra were acquired in the Orbitrap at 30,000 resolution. Tandem mass spectra were generated by beam type collision induced dissociation (HCD) for up to ten peptide precursors and fragment ions were analyzed in the orbitrap.

Peptide and Protein Identification and Quantification

For qualitative experiments, peak lists were generated from raw MS data files using Mascot Distiller v2.3.02 (Matrix Science, UK) and were then searched against the IPI human database (version 3.68). Search parameters: Carbamidomethylation of cysteine residues as fixed modification and acetyl (Protein N-term) as variable modification. Trypsin was specified as the proteolytic enzyme and up to two missed cleavages were allowed. The mass tolerance of the precursor ion was set to 5 ppm and for fragmentations to 0.02 Da. Further data interpretation was performed using Scaffold 3, v3.6.1. All proteins were filtered using a false discovery rate of 0.1%. Label free quantification was achieved by integration of the precursor ion peak volumes over the whole MS run using Progenesis LC-MS v4.0 (Nonlinear Dynamics Limited, UK). The raw intensities given by Progenesis were normalized based on the sum of the 20 most abundant but not inhibited kinases. Proteins which displayed a dose-dependent inhibition were selected and analyzed in GraphPad Prism. Half maximal inhibition of binding concentrations (IC_{50}) of proteins was calculated by non-linear regression with variable slope and the constraint of the DMSO control value to be equal to 1.

Data Analysis

Proteins which displayed a dose-dependent inhibition were selected and analyzed in GraphPad Prism. Half maximal inhibition of binding concentrations (IC_{50}) of proteins was calculated by non-linear regression with variable slope and the constraint of the DMSO control value to be equal to 1. K_d values were calculated using a depletion factor as described (Ku et al., 2014a; Lemeer et al., 2013b; Sharma et al., 2009). Briefly, the depletion factor 'r' for each protein was defined as a ratio and calculated using protein intensities observed for the DMSO pulldown (denominator), and for the pulldown of the supernatant of the latter (pulldown of pulldown, numerator). The dissociation constants were then calculated following the equation $K_d = r \times IC_{50}$. Molecular function and cellular pathway annotations of drug affected proteins were manually assigned according to the gene ontology information provided in the Uniprot database and by reading the relevant literature.

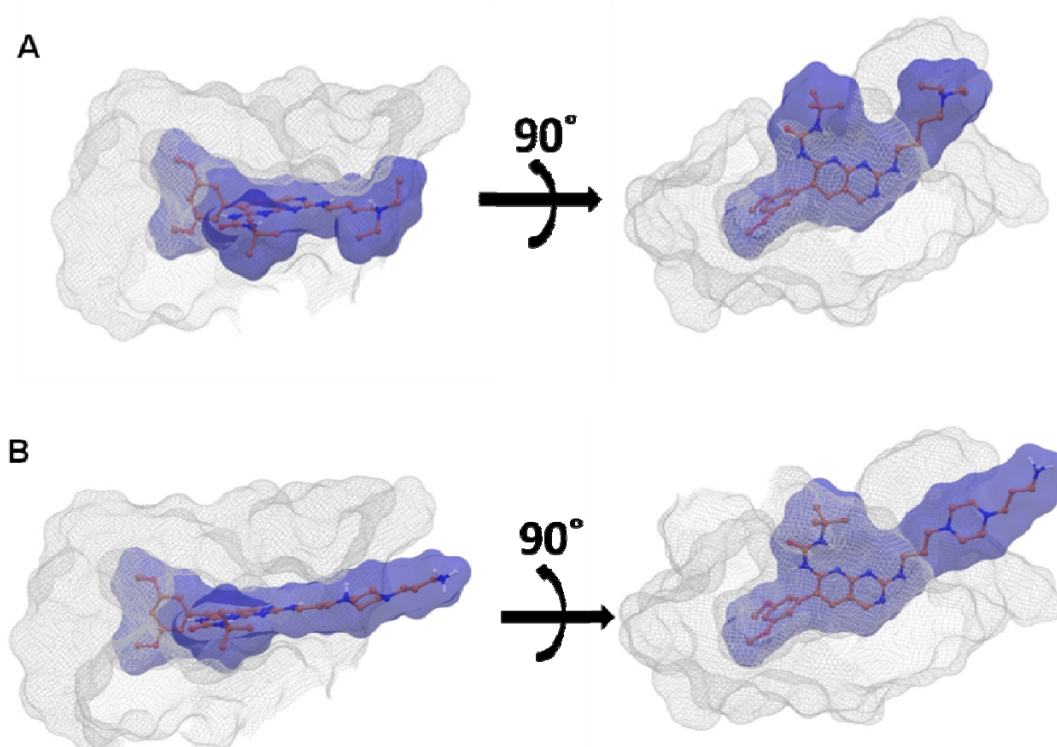


Figure 2 | Three-dimensional binding pose of PD173074 and probe F2.

(A) 3D binding pose of PD173074 (dark blue surface) in the FGFR1 ATP binding pocket (grey mesh). (B) The same as (A) but for probe F2, showing that the introduced linker extends into the solvent as required for subsequent immobilization of the probe to beads.

The pyrido[2,3-d]pyrimidine core is located in the center of the ATP-binding site and forms two pivotal hydrogen bonds with the Ala564 backbone at the hinge region. The dimethoxyphenyl-substituent is deeply buried inside the binding pocket and contributes to the overall binding affinity by forming an extra hydrogen bond between one methoxyl oxygen atom and Asp641, which is part of the DFG motif. Importantly, PD173074 contains a tertiary amine which forms a salt bridge with the carboxyl group of Glu571. The two ethyl moieties in the compound are, however, solvent exposed, strongly suggesting that derivatisation of this position with an appropriate linker would not negatively affect binding to FGFR. On the basis of this hypothesis, compounds F1 and F2 were designed (Figure 1B and 1C) both containing an elongated piperazine linker that would presumably maintain the salt bridge to Glu571 but would also protrude into solvent space to create clearance between the probe and the beads. This should thus avoid steric hindrance during coupling to NHS-activated sepharose beads via the primary amine moiety. Molecular docking analysis of compound F2 confirmed that it binds in the same way as PD173704 in the FGFR ATP-

binding site with all the key interaction features preserved. The docking data also shows that the linker moiety extends well into solvent space as desired for subsequent bead coupling (Figure 1 and 2).

Together, the molecular docking data identified the site on PD173074 where a suitable linker for the generation of an affinity probe can be placed. Probes F1 and F2 differ in structure at position 7; while F2 features the *tert*-butyl urea group also present in the parent compound, F1 contains an amino group at this position. This *tert*-butyl urea group is reported to contribute to the binding affinity via van der Waals contacts with the hydrophobic sub pocket formed by Gly485, Glu486, and Phe489 near the P-loop of FGFR1 and the conformation of which is one of the important factors for kinase inhibitor selectivity. Therefore, probe F1 was designed without this *tert*-butyl urea group, with the hope that at least one molecule which would have a similarly broad or even broader kinase binding profile than the parental compound PD173074, following the same strategy before for the generation of affinity probes targeting VEGFR and further kinases (Ku et al., 2014b). Probes F1 and F2 were then synthesized and immobilized separately on sepharose beads (see method section) for subsequent evaluation.

3.3.2 Protein binding properties of probes F1 and F2 in lysates of cancer cells and human tissue

After F1 and F2 were synthesized, their suitability as affinity tools for the enrichment of FGFR and other kinases from cancer cell lines and human tissue was evaluated. The functionalized beads were incubated separately with three different complex protein mixtures: (1) lysates of the breast cancer cell line MDAMB453, (2) mixed lysates of the cancer cell lines K562, COLO205, OVCAR8, and SKNBE2 (hereinafter referred to as cell mix), and (3) a lysate of human placenta tissue. Each of the lysates provides a different set of expressed proteins and thus, increases the breadth of protein target profiles.

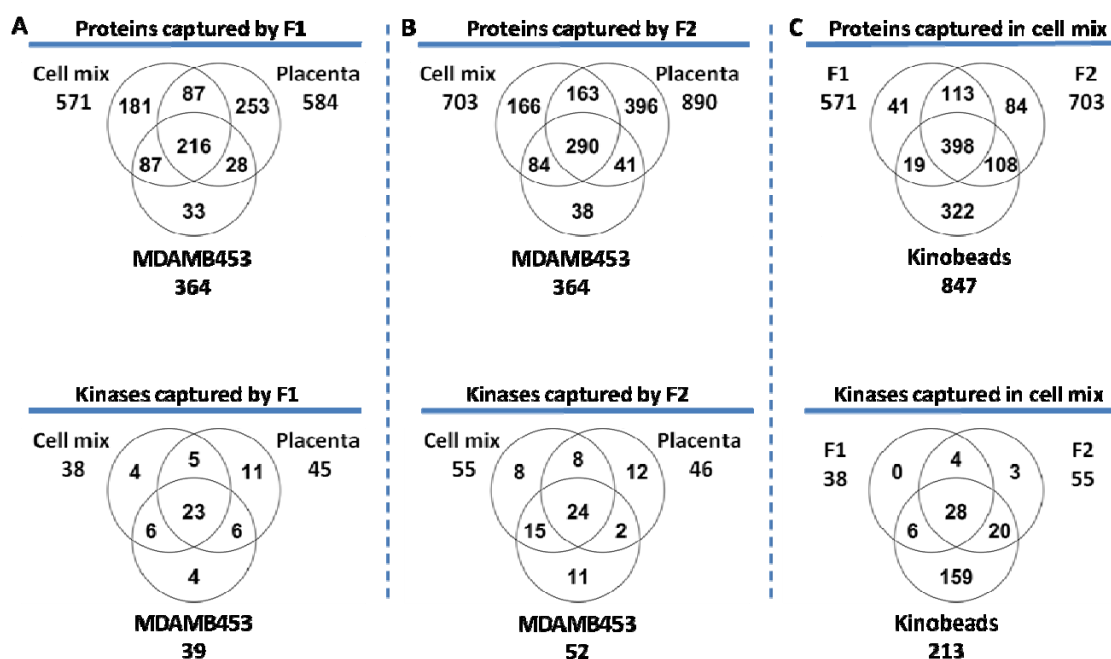


Figure 3 | Comparison of the number of enriched proteins and kinases of probes F1, F2 and Kinobeads from three different biological sources, placenta tissue, a mixed lysate of four human cancer cell lines (cell mix) and MDAMB453 cell line.

(A) Number of proteins and kinases captured by probe F1. (B) Same as panel (A) but for probe F2. (C) Comparison of proteins and kinases numbers captured by probe F1, F2 and Kinobeads from cell mix.

Mass spectrometric analysis of pulldown experiments using immobilized Probe F1 identified a total of 885 proteins including 59 kinases from the different lysates (Figure 3A). The respective figures for Probe F2 are 1,178 proteins including 80 kinases (Figure 3B). Using the cell mix, the binding profiles of F1 and F2 to that of the published Kinobeads (see Figure 5 in Chapter I for probe structures) were also compared and found that they captured seven kinases not represented on Kinobeads (Figure 3C, namely FGFR1, FGFR3, TK1, EIF2AK2, ADPGK, PFKP and HKDC1).

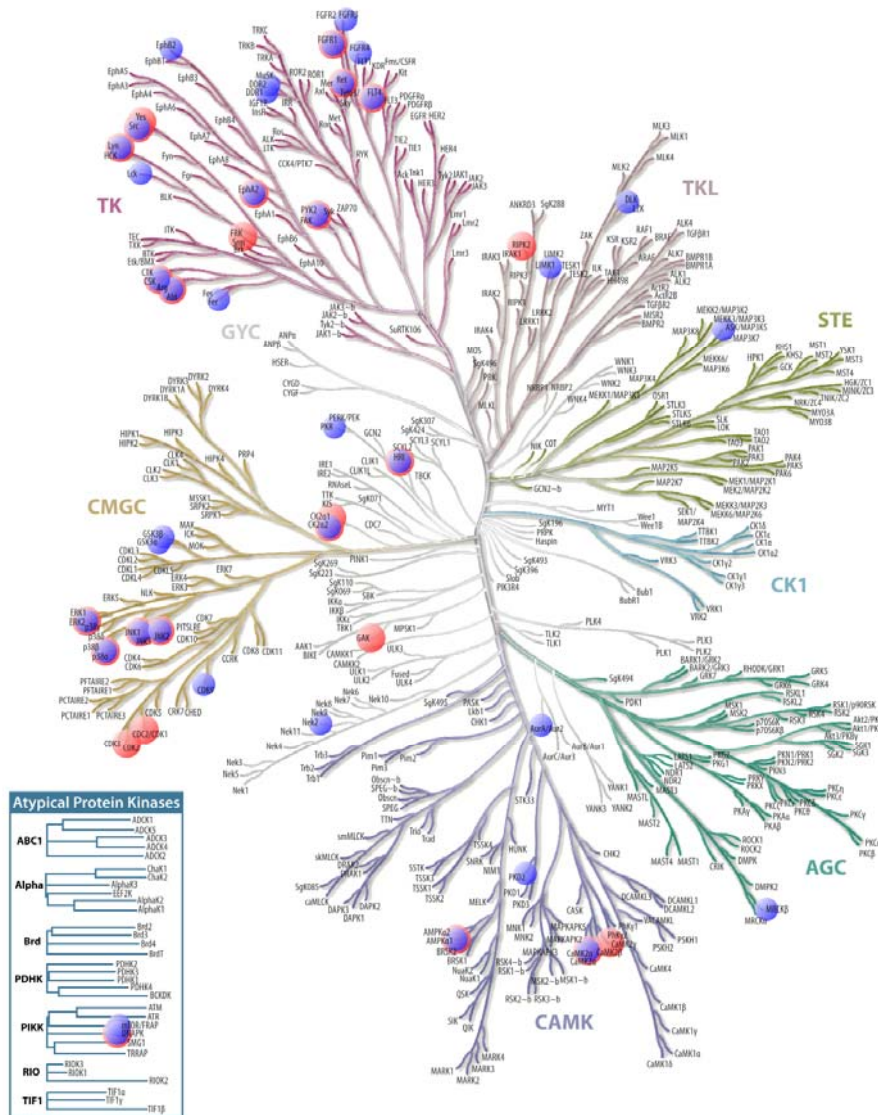


Figure 4 | Characterization of the kinase binding profiles of probes F1 and F2 in cell mix.

(A) Mapping of all identified kinases onto the phylogenetic kinome tree (kinases captured by F1 in red and those captured by F2 in blue; kinome tree illustration reproduced courtesy of Cell Signaling Technology, Inc., www.cellsignal.com).

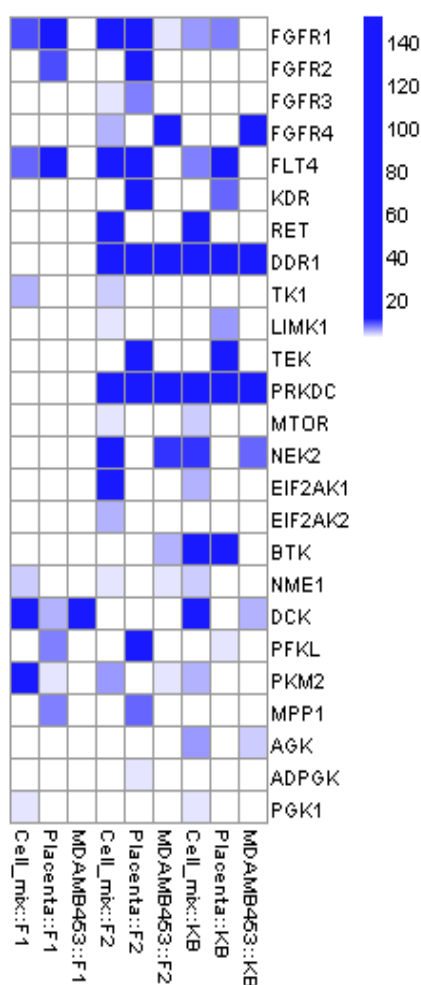


Figure 5 | Heat map analysis of binding profile of probes F1, F2 and Kinobeads from lysates of cell mix, MDAMB453 cells and human placenta tissue.

The number of unique spectra obtained by LC-MS/MS for a given protein is used as a semi-quantitative measure for the efficiency with which said protein is purified. It is evident that the new probes allow for a more efficient purification of the FGF receptors.

When plotting, the protein kinases enriched by F1 and F2 from the cell mix onto the phylogenetic tree of kinases (Figure 4), it is apparent, that most of the captured kinases belong to the tyrosine kinase family where the main targets of the lead compound PD173074 (notably FGFR1, VEGFR2, PDGFR and SRC) are also located (Pardo et al., 2009). In terms of kinome coverage, probe F2 displays a more extensive target spectrum than F1 which is also in line with our expectation noted earlier that the *tert*-butyl moiety contacts the P-loops of different kinases and thus contributes to the overall binding energy. While probe F1 was capable of capturing FGFR1, FGFR2, VEGFR3, and SRC as intended by the underlying probe design, probe F2, purified, among others, all four FGF receptors, VEGFR2,

VEGFR3 as well as TEK and TGF- β 1, which are also involved in angiogenesis. The semi-quantitative heat map shown in Figure 5 illustrates the improvement that probe F2 provides over Kinobeads for the capture of FGFRs thus meeting a primary objective of this study. In addition, F2 also improved the detection of a range of kinases including VEGFR2/KDR, VEGFR3/FLT4, EIF2AK1 and 2 as well as NEK2 thus extending the range of kinases that can be addressed. Probe F1 also improved the detection of some kinases over Kinobeads and F2. However, these were mainly metabolic kinases such as PKM2, PFK1 and DCK which are of lesser interest in the context of profiling kinase inhibitor selectivity. Given that fact that F2 performed better than F1 (more relevant kinases), F2 beads were chosen as an addition to Kinobeads for further subsequent experiments.

3.3.3 Selectivity profiling of Dovitinib and Orantinib

To illustrate the practical utility of the synthesized affinity probe, F2 was applied in conjunction with Kinobeads to the selectivity profiling of the clinical FGFR inhibitors Dovitinib and Orantinib (Figure 6). Dovitinib is currently tested in about two dozen clinical trials including one phase IV trial for the treatment of gastrointestinal stromal tumors and one Phase III for metastatic renal cell carcinoma. Orantinib is currently evaluated in a phase III trial for the treatment of unresectable hepatocellular carcinoma. The lysates of the cell mix were chosen as the source of proteins for the selectivity profiling in order to expose the drug molecules to a wide range of expressed kinases and other proteins. It is acknowledged that cell mix is not an ideal protein source for FGFRs and VEGFRs, the well described targets of these molecules. However, it is believed that this is permissible here as the objective of the experiment was to identify the general kinase profile including perhaps off-targets of these molecules for which broad kinome coverage is more important than coverage of already known targets.

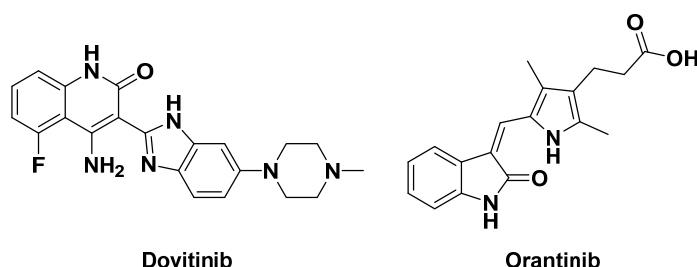


Figure 6 | Chemical structures of Dovitinib and Orantinib.

Briefly, lysates are incubated with increasing doses of a drug. Immobilized probes are then added to the lysate to bind the fraction of a protein (or proteins) that is not in complex with the inhibitor in solution. The higher the drug dose, the lower the amount of a target that can be captured by the beads. In the next step, bead bound proteins are eluted, digested with trypsin and subjected to LC-MS/MS analysis. The tandem mass spectra are used for protein identification and the mass spectral intensity of the peptides is used as a measure for the quantity of a protein bound to the beads relative to the DMSO vehicle control. As a result, dose response curves are generated from the MS data allowing the calculation of the half maximal inhibitory concentration (IC_{50}) of bead binding. IC_{50} values derived in this fashion can be converted into disassociation constant (K_d) values as described (Lemeer et al., 2013b; Pachl et al., 2013; Sharma et al., 2009).

Table 1 and Figure 6 summarized the selectivity profiles obtained. In general, for Dovitinib, about 20 proteins show sub micromolar inhibition of binding including the known primary targets like FGFR1, FLT4 and PDGFR β . In addition, a number of kinases, previously reported as off-targets of Dovitinib by large-scale in vitro recombinant kinase assays also showed potent binding inhibition in our study, notably RET (K_d 29 nM), NUA1 (K_d 100 nM) and AURKA (K_d 117 nM). The AURKA finding is notable because the literature reports conflicting data on this target. While one report showed 60% residual kinase activity at 500 nM Dovitinib and 10 μ M ATP (Anastassiadis et al., 2011), no inhibition of AURKA even at 10 μ M of the drug was found in other in vitro assay (Karaman et al., 2008). Interestingly, the Adaptor-associated protein kinase 1 (AAK1) exhibits a K_d of about 100 nM as well as four other members of the AP-2 complex (AP2A1, AP2B1, AP2M1 and AP2S1). A similar observation was made for TBK1 which co-purifies its interaction partner TBKBP1 confirming the ability of chemical affinity probes to purify kinases as part of protein complexes under close to physiological conditions.

Table 1 | Comparison between previously reported inhibition values or interaction constants of Dovitinib and Orantinib targets and those determined in this study (KB).

Drug treatment	Protein	Recomb. kinase assay IC₅₀ [nM]	KB assay IC₅₀ [nM]	KB K_d [nM]
Dovitinib	FGFR1	8	1429	347
	FLT4	8	381	85
	PDGFR β	27	70	38
	FGFR3	9	>10000	>10000
	FLT3	1	>10000	>10000
	CSF-1R	60	>10000	>10000
	VEGFR1	10	>10000	>10000
	VEGFR2	13	>10000	>10000
	c-KIT	2	>10000	>10000
	RET	71(K _d)	113	29
	NUAK1	240(K _d)	272	100
	AURKA	~600	656	117
	AURKB	280(K _d)	2570	668
AURKC	1100(K _d)	>10000	>10000	
Orantinib	AURKA	850	4782	1065
	AURKB	35	324	148
	AURKC	210	>10000	>10000
	TBK1	1400	948	552
	PDGFRB	8	34	30
	FLT4	10	36	14
	RET	562	345	146

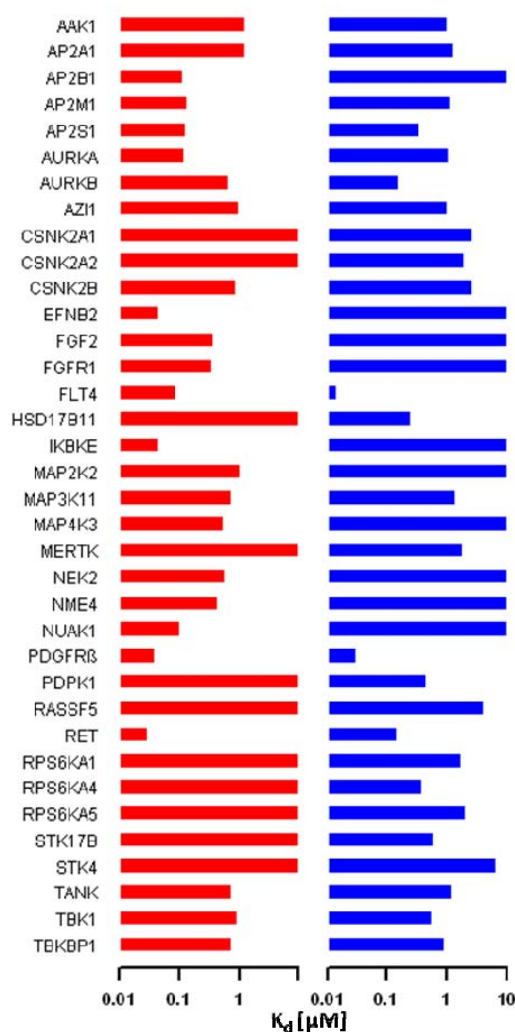


Figure 7 | Comparison of potencies (K_d value) of all major targets identified for Axitinib and Pazopanib in the dose dependant competition assay.

The selectivity profile of Orantinib (Figure 7) highlights potent interaction of the compound with PDGFR β (K_d 30 nM), VEGFR3/FLT4 (K_d 14 nM), AURKB (K_d 148 nM) (Godl et al., 2005; Sun et al., 1999) and RET (K_d 146 nM), all of which are known targets of this compound (Ahmed et al., 2004; Kim et al., 2006). Among the other sub-micromolar interactors are members of the AP-2 and TBK1 complexes as noted above although Orantinib appears to have lower affinity towards these proteins than Dovitinib. Further Orantinib interactions include members of the ribosomal S6 kinases and casein kinases as well as kinases and proteins with binding inhibition potencies in the order of 1-5 M that are likely clinically less relevant.

To generate a more systematic view, all the identified primary and off-targets for the two drugs are divided into several groups in terms of function and pathway involved (Figure 9 and 10), including angiogenesis, proto-oncogenes, and NF- κ B signaling, implying that the cellular mode of action of FGFR-targeted drugs in the cells may be more complex than originally anticipated.

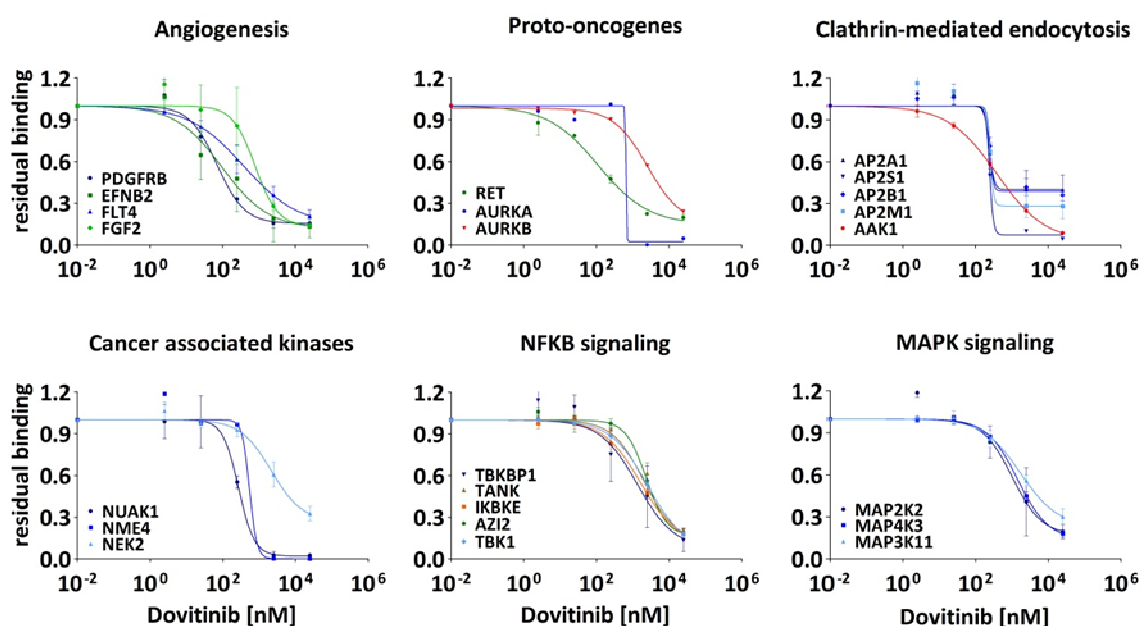


Figure 8 | Summary of obtained selectivity profiles for Dovitinib.

Besides the strong interaction of Dovitinib with PDGFR β (K_d 38 nM) and VEGFR3/FLT4 (K_d 85 nM), the angiogenic signaling factors Ephrin B2 (K_d 45 nM) and FGF2 (K_d 369 nM) also displayed dose-dependent binding inhibition curves (Figure 8). This is noteworthy because the cell surface transmembrane ligand Ephrin B2 as well as the extracellular matrix factor FGF2 are not capable of binding ATP implying that they are co-purified along with their corresponding receptors and/or interaction partners. For FGF2, this is most likely FGFR1 because their IC_{50} values are quite similar in the same assay (\sim 800 nM and 1,400 nM respectively). Recent work has shown that Ephrin B2 controls the internalization and signaling of VEGF receptors (Sawamiphak et al., 2010; Wang et al., 2010). VEGFR3 as well as Ephrin B2 binding inhibition is observed with an IC_{50} of 381 nM and 97 nM respectively in response to Dovitinib treatment. It is therefore tempting to speculate that Ephrin B2 indeed co-purifies with several VEGFRs on Kinobeads and that this interaction is disrupted by Dovitinib and contributes to the anti-angiogenic effect of the drug. It is further interesting to note in this context that members of the endocytosis machinery (particularly the AP-2

complex) (Collins et al., 2002; Kelly et al., 2008) are also strongly inhibited by Dovitinib strengthening the link between Ephrin B2 controlled VEGFR internalization and signaling. Still, there are discrepancies in IC_{50} values for FGF2/FGFR1 and Ephrin B2/VEGFR3 which may be explained by a number of factors. First, the ligands may bind to more than one receptor but not all of the receptors were detected in the Kinobead experiment so that the apparent discrepancy may be explained by the sequestering of e.g. Ephrin B2 between all three VEGFRs. Second, the ligand may only be bound to the active conformation of the receptor but Kinobeads bind both the active and inactive forms of the receptor resulting in too high apparent IC_{50} values of e.g. FGFR1 in the drug assay (i.e. Dovitinib only inhibiting the binding of active FGFR1 to Kinobeads).

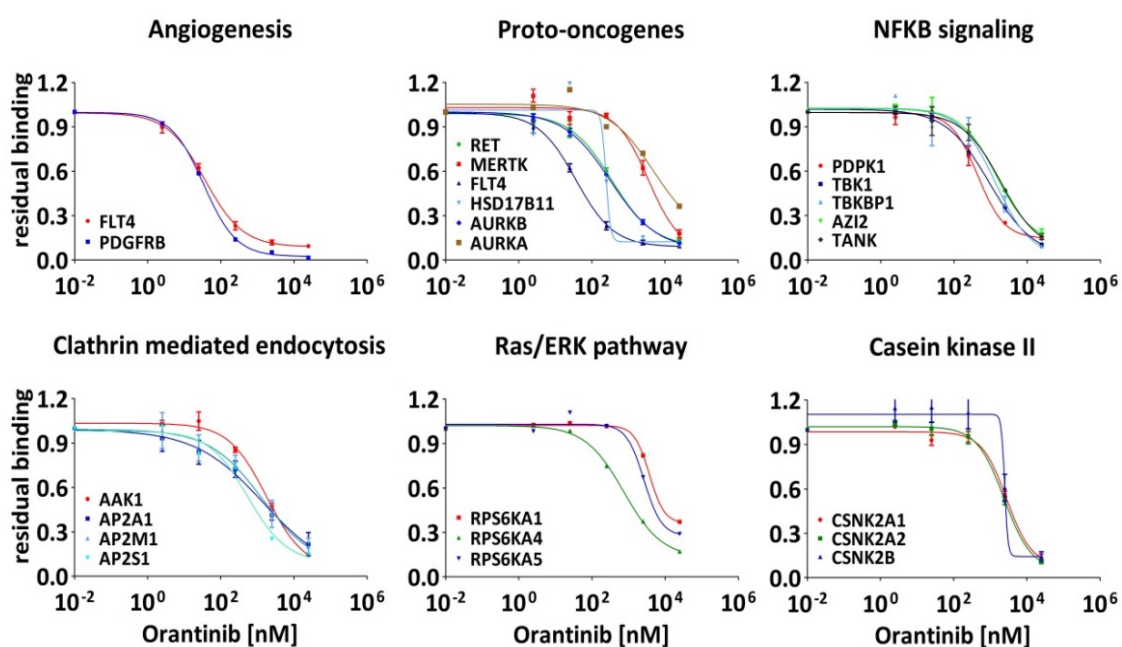


Figure 9 | Summary of obtained selectivity profiles for Orantinib.

Several further kinases previously reported to be inhibited by both Dovitinib and Orantinib were also found affected in our test (Figure 8 and 9), including proto-oncogenes like RET and Aurora kinase family members. Both Dovitinib and Orantinib were previously confirmed to inhibit RET kinase using recombinant kinase assays (Table 1) (Ahmed et al., 2004; Kim et al., 2006). In our study, RET binding to Kinobeads was inhibited with an IC_{50} of 113 nM (K_d 29 nM) using Dovitinib and 345 nM (K_d 146 nM) by Orantinib, which are close to the reported inhibitory activities. Meanwhile, Dovitinib and Orantinib were reported to exhibit slightly different selectivities across the 3 Aurora kinases (see Table 1). In our study,

AURKB was hit by both Orantinib (IC_{50} 324 nM; K_d 148 nM) and Dovitinib (IC_{50} 2570 nM; K_d 668 nM), in line with previous chemical proteomic experiments and in vitro kinase assays (Godl et al., 2005; Karaman et al., 2008). Interestingly, AURKA was identified as a target of Dovitinib (IC_{50} 656 nM; K_d 117 nM), which was, however, not detected in large-scale in vitro kinase activity profiling campaigns using recombinant proteins (Karaman et al., 2008). Besides, both Orantinib and Dovitinib are reported to inhibit AURKC at submicromolar to micromolar concentration; however, this kinase could not be detected in either our experiments which is probably attributable to insufficient protein expression levels within the component cell lines of the cell mix.

Albeit not very strongly, both inhibitors also affect members of the NF κ B signaling pathway (with multiple implications in modulating immune responses as well as oncogenic signaling) including TBKBP1 (IC_{50} : 1344 nM), IKBKE (IC_{50} : 1667 nM), TANK (IC_{50} : 2018 nM), and TBK1 (IC_{50} : 2633 nM). TBKBP1 and TANK are both adapter proteins for IKBKE and TBK1 and do not possess ATP binding pockets (Chariot et al., 2002; Goncalves et al., 2011). Therefore, it can be concluded that these proteins are co-enriched with their kinase binding partners IKBKE and TBK1. Whether or not Dovitinib or Orantinib have sufficient potency against these targets in order to elicit a functional effect in cells or therapeutic/toxic effect in human remains to be investigated (Czabanka et al., 2008; Guan et al., 2010; Guo et al., 2009; Hildebrandt et al., 2012). Similarly, measurable but fairly weak inhibitory effects (1-3 μ M range) were observed for members of the RAS/ERK/MAPK pathway and a couple of other cancer associated kinases and tumor suppressors. A noteworthy exception to this is the kinase NUA1 (Inazuka et al., 2012; Sun et al., 2013), which is involved in many biological processes including cell adhesion, regulation of cell ploidy, DNA damage repair and tumor progression and the kinase is inhibited by Dovitinib with a potency of 100 nM (K_d). Inhibition of NUA1 may be an interesting avenue to follow and our data suggests that Dovitinib might be a suitable starting point for the development of more selective chemical probes for this kinase.

3.5 Conclusion

Two small molecular FGFR binding probes were designed and synthesized which extend the range of kinases that can be addressed by chemical affinity proteomics and application of the tools to the selectivity profiling of Dovitinib and Orantinib, confirmed most of the known primary and off-targets of these molecules. The work also identified members of protein complexes and receptor ligands affected by the drugs, a feature that is intractable by biochemical kinase assays and highlights the usefulness of a proteomic approach to kinase inhibitor MoA studies in cells. In light of the above, it can be anticipated that chemical proteomics will become more and more widely used particularly in drug discovery and that the field will continue to improve the repertoire of chemical tools required for a full understanding of how a drug molecule exerts its action on the molecular as well as systems level.

Acknowledgements

I am indebted to Stephanie Heinzlmeir who performed the kinase inhibitor profiling and part of the synthesis during her MSc thesis under my supervision. I also want to thank Dr. Sabine Schweizer and Dr. Xiaofeng Liu for assistance with docking studies.

Abbreviations

DMEM Dulbecco's modified Eagle's medium

FBS fetal bovine serum

GO gene ontology

HCD higher energy collision induced dissociation

IC₅₀ half maximal inhibitory concentration

IMDM Iscove's modified Dulbecco's medium

K_d dissociation constant

KB Kinobeads

KI kinase inhibitor

LC-MS/MS liquid chromatography coupled to tandem mass spectrometry

PBS phosphate buffered saline

RPMI1640 Roswell Park Memorial Institute 1640 medium

SAR structure activity relationship

References

- Ahmed, S.I., Thomas, A.L., and Steward, W.P. (2004). Vascular endothelial growth factor (VEGF) inhibition by small molecules. *J Chemother* 16 *Suppl* 4, 59-63.
- Anastassiadis, T., Deacon, S.W., Devarajan, K., Ma, H., and Peterson, J.R. (2011). Comprehensive assay of kinase catalytic activity reveals features of kinase inhibitor selectivity. *Nat Biotechnol* 29, 1039-1045.
- Bantscheff, M., Eberhard, D., Abraham, Y., Bastuck, S., Boesche, M., Hobson, S., Mathieson, T., Perrin, J., Raida, M., Rau, C., *et al.* (2007). Quantitative chemical proteomics reveals mechanisms of action of clinical ABL kinase inhibitors. *Nat Biotechnol* 25, 1035-1044.
- Bantscheff, M., and Kuster, B. (2012). Quantitative mass spectrometry in proteomics. *Anal Bioanal Chem* 404, 937-938.
- Chariot, A., Leonardi, A., Muller, J., Bonif, M., Brown, K., and Siebenlist, U. (2002). Association of the adaptor TANK with the I kappa B kinase (IKK) regulator NEMO connects IKK complexes with IKK epsilon and TBK1 kinases. *The Journal of biological chemistry* 277, 37029-37036.
- Cockett, M., Dracopoli, N., and Sigal, E. (2000). Applied genomics: integration of the technology within pharmaceutical research and development. *Current opinion in biotechnology* 11, 602-609.
- Collins, B.M., McCoy, A.J., Kent, H.M., Evans, P.R., and Owen, D.J. (2002). Molecular architecture and functional model of the endocytic AP2 complex. *Cell* 109, 523-535.
- Czabanka, M., Korherr, C., Brinkmann, U., and Vajkoczy, P. (2008). Influence of TBK-1 on tumor angiogenesis and microvascular inflammation. *Front Biosci* 13, 7243-7249.
- Godl, K., Gruss, O.J., Eickhoff, J., Wissing, J., Blencke, S., Weber, M., Degen, H., Brehmer, D., Orfi, L., Horvath, Z., *et al.* (2005). Proteomic characterization of the angiogenesis inhibitor SU6668 reveals multiple impacts on cellular kinase signaling. *Cancer Res* 65, 6919-6926.
- Goncalves, A., Burckstummer, T., Dixit, E., Scheicher, R., Gorna, M.W., Karayel, E., Sugar, C., Stukalov, A., Berg, T., Kralovics, R., *et al.* (2011). Functional dissection of the TBK1 molecular network. *PloS one* 6, e23971.
- Guan, H., Zhang, H., Cai, J., Wu, J., Yuan, J., Li, J., Huang, Z., and Li, M. (2010). IKBKE is over-expressed in glioma and contributes to resistance of glioma cells to apoptosis via activating NF-kappaB. *The Journal of pathology* 223, 436-445.
- Guo, J.P., Shu, S.K., He, L., Lee, Y.C., Kruk, P.A., Grenman, S., Nicosia, S.V., Mor, G., Schell, M.J., Coppola, D., *et al.* (2009). Deregulation of IKBKE is associated with tumor progression, poor prognosis, and cisplatin resistance in ovarian cancer. *The American journal of pathology* 175, 324-333.
- Hildebrandt, M.A., Tan, W., Tamboli, P., Huang, M., Ye, Y., Lin, J., Lee, J.S., Wood, C.G., and Wu, X. (2012). Kinome expression profiling identifies IKBKE as a predictor of overall survival in clear cell renal cell carcinoma patients. *Carcinogenesis* 33, 799-803.

- Inazuka, F., Sugiyama, N., Tomita, M., Abe, T., Shioi, G., and Esumi, H. (2012). Muscle-specific knock-out of NUA family SNF1-like kinase 1 (NUAK1) prevents high fat diet-induced glucose intolerance. *The Journal of biological chemistry* 287, 16379-16389.
- Karaman, M.W., Herrgard, S., Treiber, D.K., Gallant, P., Atteridge, C.E., Campbell, B.T., Chan, K.W., Ciceri, P., Davis, M.I., Edeen, P.T., *et al.* (2008). A quantitative analysis of kinase inhibitor selectivity. *Nat Biotechnol* 26, 127-132.
- Kelly, B.T., McCoy, A.J., Spate, K., Miller, S.E., Evans, P.R., Honing, S., and Owen, D.J. (2008). A structural explanation for the binding of endocytic dileucine motifs by the AP2 complex. *Nature* 456, 976-979.
- Kim, D.W., Jo, Y.S., Jung, H.S., Chung, H.K., Song, J.H., Park, K.C., Park, S.H., Hwang, J.H., Rha, S.Y., Kweon, G.R., *et al.* (2006). An orally administered multitarget tyrosine kinase inhibitor, SU11248, is a novel potent inhibitor of thyroid oncogenic RET/papillary thyroid cancer kinases. *The Journal of clinical endocrinology and metabolism* 91, 4070-4076.
- Ku, X., Heinzlmeir, S., Liu, X., Medard, G., and Kuster, B. (2014a). A new chemical probe for quantitative proteomic profiling of fibroblast growth factor receptor and its inhibitors. *J Proteomics* 96, 44-55.
- Ku, X., Heinzlmeir, S., Liu, X., Medard, G., and Kuster, B. (2014b). A new chemical probe for quantitative proteomic profiling of fibroblast growth factor receptor and its inhibitors. *J Proteomics* 96, 44-55.
- Lander, E.S., Linton, L.M., Birren, B., Nusbaum, C., Zody, M.C., Baldwin, J., Devon, K., Dewar, K., Doyle, M., FitzHugh, W., *et al.* (2001). Initial sequencing and analysis of the human genome. *Nature* 409, 860-921.
- Lemeer, S., Zorgiebel, C., Ruprecht, B., Kohl, K., and Kuster, B. (2013a). Comparing Immobilized Kinase Inhibitors and Covalent ATP Probes for Proteomic Profiling of Kinase Expression and Drug Selectivity. *J Proteome Res.*
- Lemeer, S., Zorgiebel, C., Ruprecht, B., Kohl, K., and Kuster, B. (2013b). Comparing Immobilized Kinase Inhibitors and Covalent ATP Probes for Proteomic Profiling of Kinase Expression and Drug Selectivity. *Journal of proteome research* 12, 1723-1731.
- Mohammadi, M., Froum, S., Hamby, J.M., Schroeder, M.C., Panek, R.L., Lu, G.H., Eliseenkova, A.V., Green, D., Schlessinger, J., and Hubbard, S.R. (1998). Crystal structure of an angiogenesis inhibitor bound to the FGF receptor tyrosine kinase domain. *The EMBO journal* 17, 5896-5904.
- Pachl, F., Plattner, P., Ruprecht, B., Medard, G., Sewald, N., and Kuster, B. (2013). Characterization of a chemical affinity probe targeting Akt kinases. *J Proteome Res* 12, 3792-3800.
- Pardo, O.E., Latigo, J., Jeffery, R.E., Nye, E., Poulosom, R., Spencer-Dene, B., Lemoine, N.R., Stamp, G.W., Aboagye, E.O., and Seckl, M.J. (2009). The fibroblast growth factor receptor inhibitor PD173074 blocks small cell lung cancer growth in vitro and in vivo. *Cancer Res* 69, 8645-8651.

- Reich, D.E., Cargill, M., Bolk, S., Ireland, J., Sabeti, P.C., Richter, D.J., Lavery, T., Kouyoumjian, R., Farhadian, S.F., Ward, R., *et al.* (2001). Linkage disequilibrium in the human genome. *Nature* *411*, 199-204.
- Sawamiphak, S., Seidel, S., Essmann, C.L., Wilkinson, G.A., Pitulescu, M.E., Acker, T., and Acker-Palmer, A. (2010). Ephrin-B2 regulates VEGFR2 function in developmental and tumour angiogenesis. *Nature* *465*, 487-491.
- Schirle, M., Bantscheff, M., and Kuster, B. (2012). Mass spectrometry-based proteomics in preclinical drug discovery. *Chem Biol* *19*, 72-84.
- Sharma, K., Weber, C., Bairlein, M., Greff, Z., Keri, G., Cox, J., Olsen, J.V., and Daub, H. (2009). Proteomics strategy for quantitative protein interaction profiling in cell extracts. *Nat Methods* *6*, 741-744.
- Sharpe, R., Pearson, A., Herrera-Abreu, M.T., Johnson, D., Mackay, A., Welti, J.C., Natrajan, R., Reynolds, A.R., Reis-Filho, J.S., Ashworth, A., *et al.* (2011). FGFR signaling promotes the growth of triple-negative and basal-like breast cancer cell lines both in vitro and in vivo. *Clinical cancer research : an official journal of the American Association for Cancer Research* *17*, 5275-5286.
- Sun, L., Tran, N., Liang, C., Tang, F., Rice, A., Schreck, R., Waltz, K., Shawver, L.K., McMahon, G., and Tang, C. (1999). Design, synthesis, and evaluations of substituted 3-[(3- or 4-carboxyethylpyrrol-2-yl)methylidene]indolin-2-ones as inhibitors of VEGF, FGF, and PDGF receptor tyrosine kinases. *J Med Chem* *42*, 5120-5130.
- Sun, X., Gao, L., Chien, H.Y., Li, W.C., and Zhao, J. (2013). The regulation and function of the NUAK family. *J Mol Endocrinol* *51*, R15-22.
- Wang, Y., Nakayama, M., Pitulescu, M.E., Schmidt, T.S., Bochenek, M.L., Sakakibara, A., Adams, S., Davy, A., Deutsch, U., Luthi, U., *et al.* (2010). Ephrin-B2 controls VEGF-induced angiogenesis and lymphangiogenesis. *Nature* *465*, 483-486.
- Wu, Z., Doondeea, J.B., Gholami, A.M., Janning, M.C., Lemeer, S., Kramer, K., Eccles, S.A., Gollin, S.M., Grenman, R., Walch, A., *et al.* (2011). Quantitative chemical proteomics reveals new potential drug targets in head and neck cancer. *Mol Cell Proteomics* *10*, M111 011635.
- Wu, Z., Moghaddas Gholami, A., and Kuster, B. (2012). Systematic identification of the HSP90 candidate regulated proteome. *Mol Cell Proteomics* *11*, M111 016675.

Chapter IV

**An affinity probe targeting VEGF receptors
for kinase inhibitor selectivity profiling by
chemical proteomics**

4.1 Introduction

As mentioned in previous chapters, selectivity profiling of kinase drugs using chemical proteomics approach has become a very good complementarity to the recombinant assays since it assesses the binding in the presence of cellular factors in a relevant biological context. However, the kinome coverage in these approaches (e.g. Kinobeads) is limited by the binding profile of the immobilized probes. In the Chapter II and III, the characterization of binding profiles of chemical probes with broad selectivity (VI16743) and with special focus on the enrichment of FGFRs (F1 and F2) were presented. These probes successfully extend the range of kinases that can be addressed by the Kinobeads. Given that the Vascular Endothelial Growth Factor Receptors (VEGFRs) were still out of reach, which also play important roles in tumor angiogenesis (see Chapter I), in this chapter, continuing with the successful strategy, the development of a new affinity probe targeting VEGFRs is described. This probe was derived from a potent and multi-angiokinase inhibitor named BIBF1120 (Nintedanib, Boehringer Ingelheim) (Hilberg et al., 2008). Guided by studies of the reported co-crystal structure and molecular docking, a carefully designed linker was added to the lead compound, with the hope that this modification will not undermine the binding of BIBF1120 to VEGFRs and other kinases. The probe was synthesized and immobilized on sepharose beads. To access the binding profile, the new probe was applied in pulldown experiments using lysates of human placenta and cancer cell lines. The new probe was also supplemented to the Kinobeads and applied to the selectivity profiling of two angiogenesis drugs, Dovitinib and Orantinib, leading to the identification of several primary and off-targets.

4.2 Materials and Methods

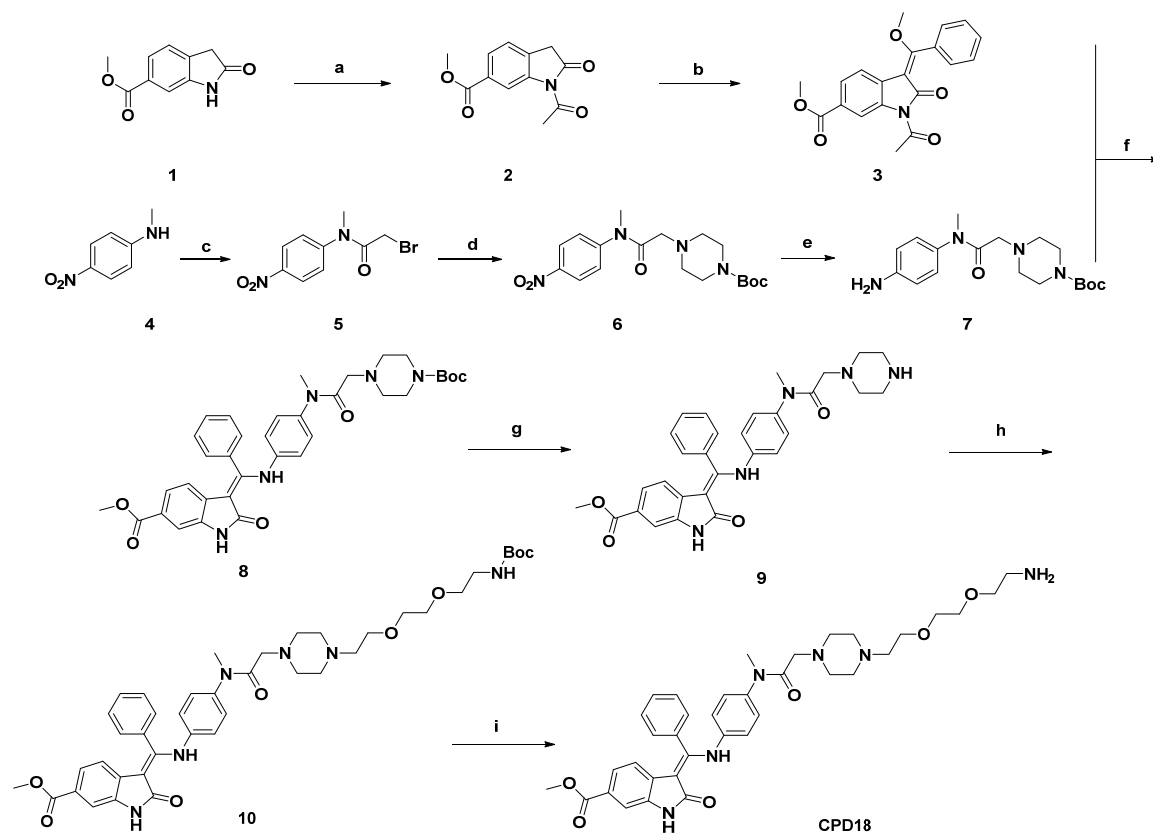
Molecular Docking

The binding pose of the VEGFR probe in the ATP-binding site of VEGFR2 was predicted by the software Glide (Schrödinger, Inc.). The crystal structure of VEGFR2 in complex with BIB1120 was retrieved from the Protein Data Bank (PDB code 3C7Q) and prepared using the Protein Preparation Wizard in Maestro (Schrödinger, Inc.) to remove non amino acid molecules, add hydrogen atoms, and assign the protonation states for the polar residues. The scoring grid was generated by enclosing the residues 14 Å around BIB1120 in the binding site. The docking of the probe was performed in Glide SP mode. Among the top 20 ranked binding poses, the best pose featuring a salt bridge between the 4-nitrogen atom of the N-methyl piperazinyl moiety and the carboxylate oxygen of Glu850 was used for binding mode analysis, for its similarity to the co-crystal structure.

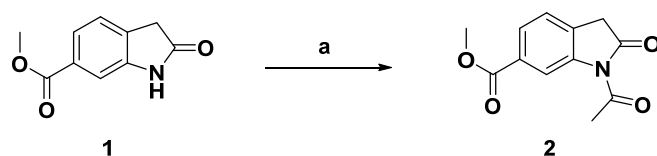
General Synthetic Methods

All chemicals and solvents were purchased from commercial suppliers (Sigma-Aldrich Co, VWR International, Carl Roth GmbH & Co.KG, Alfa Aesar, Santa Cruz, Fluorochem Ltd) and were used without further purification. All air- and moisture-sensitive reactions were carried out under an atmosphere of dry argon with heat-dried glassware and standard syringe techniques. Flash chromatography was performed on an Interchim puriFlash evo 430 system. Proton (¹H NMR) nuclear magnetic resonance spectra were obtained at 400 MHz, respectively unless otherwise noted. Chemical shifts were recorded in parts per million (ppm) and NMR signals were described as following: s (single), d (doublet), t (triplet), q (quadruplet), and m (multiplet). Mass spectrometry (MS) analyses were conducted on an amazon speed ETD ion trap mass spectrometer in positive electrospray mode. The samples were separated by HPLC on an Agilent 1100 system prior to mass spectrometric analysis utilizing a TriArt C18 column and an 1100 series HPLC system, applying a 5-95% gradient of solvent B (0.1% TFA in acetonitrile) in solvent A (0.1% TFA in water) for 25 min, followed by plateau of 95% solvent B for 5 min. Chromatography signals were detected using DAD detector at λ: 254 nm and 365 nm.

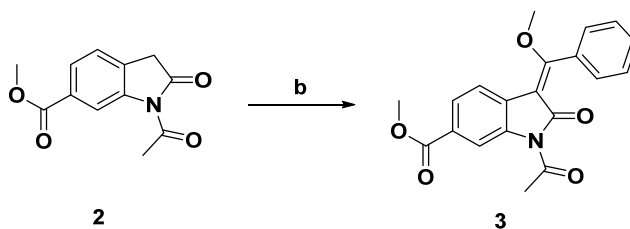
Synthesis of Compounds



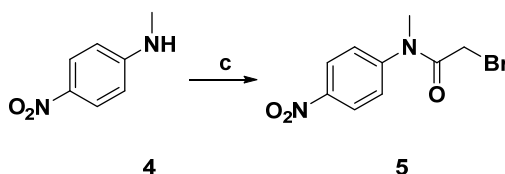
6-Acetyl-2-oxo-2,3-dihydro-1H-indole-6-carboxylic acid methyl ester (2)



2-Oxo-2,3-dihydro-1H-indole-6-carboxylic acid methyl ester (**1**) (1.15 g, 6.02 mmol) was suspended in acetic anhydride (10 ml) and refluxed at 130 °C for 6 h. After that time, the mixture was cooled down and the precipitate was filtered off and washed with petroleum ether. This precipitate were further purified by flash chromatography (0-100% ethyl acetate in petroleum ether) to give 0.5 g of 6-acetyl-2-oxo-2,3-dihydro-1H-indole-6-carboxylic acid methyl ester (**2**). LC/MS: 233.898 [M+H⁺] ¹H NMR: (400 MHz, DMSO-d₆) δ 8.68 (s, 1H), 7.84 (d, *J* = 8 Hz, 1H), 7.50 (d, *J* = 8 Hz, 1H), 3.92 (s, 3H), 3.88 (s, 3H), 2.58 (s, 2H).

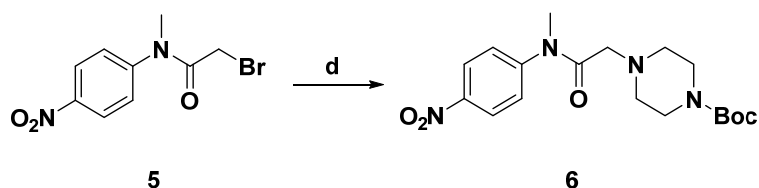
(E)-1-acetyl-6-chloro-3-(ethoxy-phenyl-methylene)-indolin-2-one (3)

6-Acetyl-2-oxo-2,3-dihydro-1H-indole-6-carboxylic acid methyl ester (**2**) (0.419 g, 2 mmol) was dissolved in acetic anhydride (5 ml), and ortho-benzoic acid triethyl ester (1.36 ml, 6 mmol) was added. The mixture was stirred at 120 °C for 2 h. After that, the solvent was removed by evaporation. The residue was triturated with petroleum ether (100 ml), filtered off, and dried to give 0.2 g of (E)-1-acetyl-6-chloro-3-(ethoxy-phenyl-methylene)-indolin-2-one (**3**). LC/MS: 351.935 [M+H⁺] ¹H NMR (400 MHz, CDCl₃) δ 8.94 (s, 1H), 8.04 (d, *J* = 8 Hz, 1H), 7.98 (d, *J* = 8 Hz, 1H), 7.60-7.62 (m, 3H), 7.40-7.43 (m, 2H), 3.60 (s, 3H), 3.79 (s, 3H), 2.60 (s, 3H).

2-bromo-N-methyl-N-(4-nitrophenyl)acetamide (5)

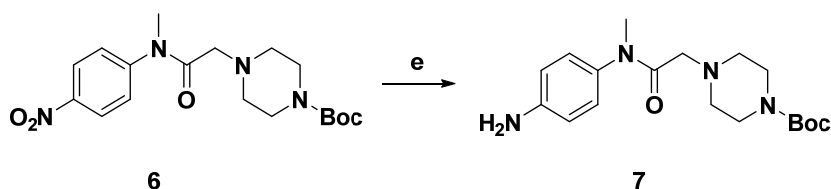
N-Methyl-4-nitroaniline (**4**) (1.52g, 1 mmol) and potassium carbonate (1.66g, 1.2 mmol) were dissolved in anhydrous THF. Furthermore, 2-bromoacetyl bromide (1.05 ml, 1.2 mmol) was dissolved in a small amount of anhydrous tetrahydrofuran (THF) and was added dropwise to the reaction mixture at 0°C. Reaction was stirred at room temperature and monitored by TLC. H₂O was added after the reaction was complete and the mixture was extracted with 3×20 ml ethyl acetate. The organic phases were combined and dried with magnesium sulfate. The solvent was then evaporated and the crude product was purified by flash chromatography using a solvent gradient of 0-100 % ethyl acetate in petroleum ether to give 1.8 g of the target molecule (**5**) LC/MS: 273.018 [M+H⁺] ¹H NMR (400 MHz, DMSO-d₆) δ 4.12 (s, 2H), δ 7.69(d, 2H, *J* = 8Hz), δ 8.30 (d, 2H, *J* = 8Hz)

Tert-butyl 4-(2-(methyl(4-nitrophenyl)amino)-2-oxoethyl)piperazine-1-carboxylate (6)



1-Boc-piperazine (0.97 g, 5.2 mmol) and potassium hydroxide (0.42 g, 7.5 mmol) were dissolved in anhydrous THF. Then, 2-bromo-N-methyl-N-(4-nitrophenyl)acetamide (1.04 g, 3.8 mmol) was added and the reaction mixture was stirred at room temperature and monitored by TLC. H₂O was added after the reaction was complete and the mixture was extracted with 3×20 ml ethyl acetate. The organic phases was combined and dried with magnesium sulfate. The solvent was then evaporated and the crude product was purified by flash chromatography using a solvent gradient of 0-100 % ethyl acetate in petroleum ether to give 1.8 g of the target molecule (6). LC/MS: 272.946 [M+H⁺] ¹H NMR (400 MHz, DMSO-d₆) δ 1.36 (s, 9H), δ 2.29 (s, 4H), δ 3.16 (s, 6H), δ 3.27 (s, 3H), δ 7.63 (d, 2H, J = 8Hz), δ 8.24 (d, 2H, J = 8Hz).

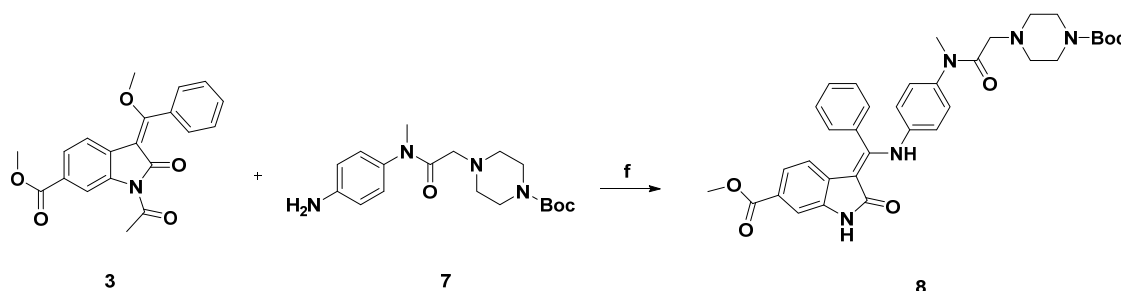
Tert-butyl 4-(2-((4-aminophenyl)(methyl)amino)-2-oxoethyl)piperazine-1-carboxylate (7)



Tert-butyl 4-(2-((4-nitrophenyl)(methyl)amino)-2-oxoethyl)piperazine-1-carboxylate (6) (0.4 g, 1.05 mmol) was dissolved in 10 ml EtOH / NH₄Cl saturated solution (v/v = 1/1). After addition of iron (300 mg, 5.3 mmol), the reaction mixture was stirred at 110°C for 1h. The reaction mixture was cooled down and filtered. 100 ml H₂O was added and extraction was performed 5 times with 20 ml ethyl acetate. Organic layers were combined and dried with MgSO₄. The solvent was removed by the vacuum evaporator and crude product was obtained. Recrystallization was performed in order to give the target molecule (7). LC/MS: 349.080 [M+H⁺] ¹H NMR (400 MHz, DMSO-d₆) δ 1.38 (s, 9H),

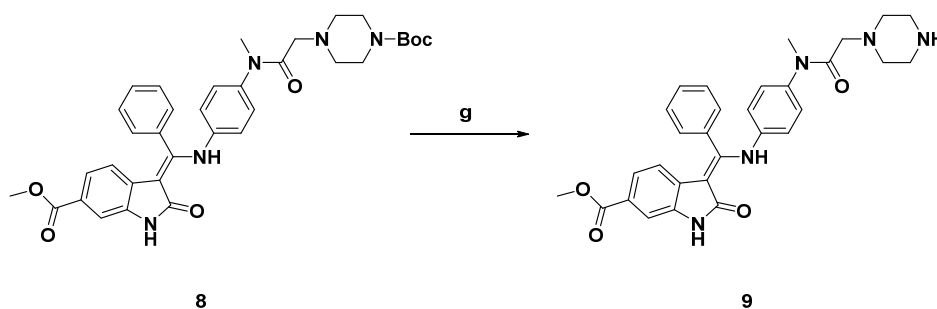
δ 2.30 (s, 4H), δ 2.85 (s, 2H), δ 3.05 (s, 3H), δ 3.24 (s, 4H), δ 5.23 (s, 2H), δ 6.57 (d, J = 8Hz, 2H), δ 6.91 (d, J = 8Hz, 2H).

Methyl (Z)-3-(((4-(2-(4-(tert-butoxycarbonyl)piperazin-1-yl)-N-methylacetamido)phenyl)amino)(phenyl)methylene)-2-oxoindoline-6-carboxylate (8)



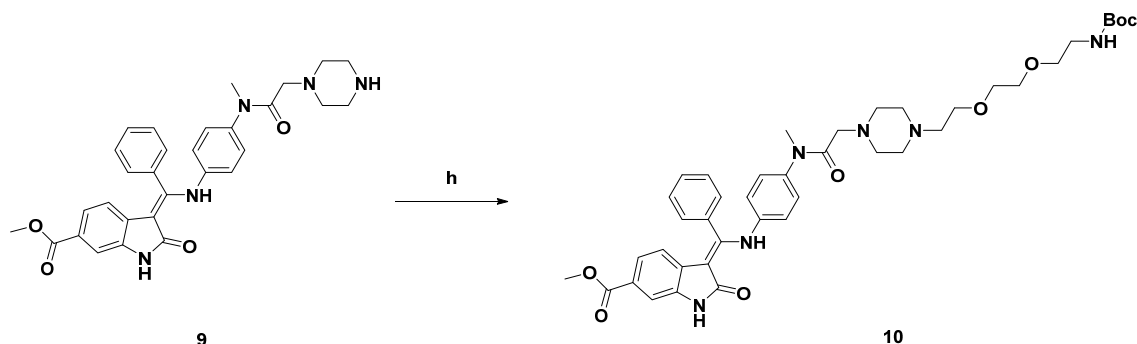
Methyl (E)-1-acetyl-3-(methoxy(phenyl)methylene)-2-oxoindoline-6-carboxylate (**3**) (0.18 g, 0.5 mmol) and tert-butyl 4-(2-((4-aminophenyl)(methyl)amino)-2-oxoethyl)piperazine-1-carboxylate (**7**) (0.19g, 0.55 mmol) were dissolved in 10 ml DMF and was heated at 80 °C for 1h, then piperidine (1.1 ml) was added and the reaction was kept at room temperature for 3 h. After that, water was added and the mixture was extracted using 3×20 ml ethyl acetate. The organic phases were combined and concentrated to give the crude product. The crude product was then purified by flash chromatography using a solvent gradient of 0-100 % ethyl acetate in petroleum ether to give 0.18 g of the target molecule (**8**) LC/MS: 626.312 [M+H⁺]; ¹H NMR (400 MHz, DMSO-d₆) δ 12.23 (s, 1H), 10.98 (s, 1H), δ 7.58 (m, 4H), 7.52 (d, J = 7.3, 2H), 7.43 (s, 1H), 7.20 (dd, J = 8.2, 1.6 Hz, 1H), 7.16 (d, J = 8.2 Hz, 2H), 6.91 (d, J = 8.1 Hz, 2H), 3.78 (s, 3H), 3.16 (s, 4H), 3.07 (s, 3H), 2.17 (s, 4H), 1.40 (s, 9H).

Methyl (Z)-3-(((4-(N-methyl-2-(piperazin-1-yl)acetamido)phenyl)amino)(phenyl)methylene)-2-oxoindoline-6-carboxylate (9)



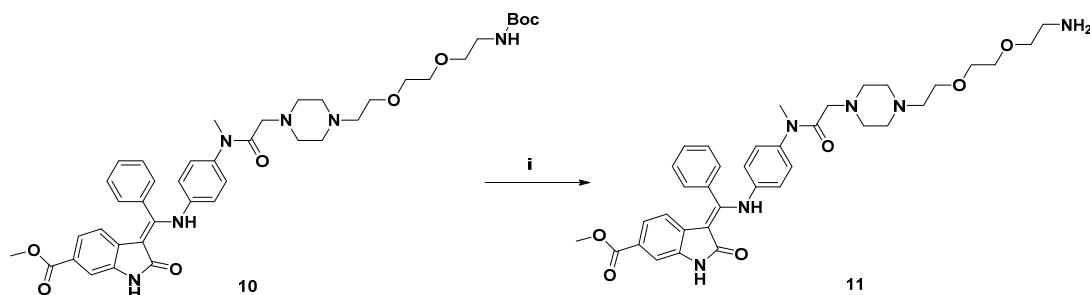
Methyl (Z)-3-(((4-(2-(4-(tert-butoxycarbonyl)piperazin-1-yl)-N-methylacetamido)phenyl) amino) (phenyl)methylene)-2-oxoindoline-6-carboxylate (**8**) (0.1 g, 0.16 mmol) was dissolved in 5 ml CH₂Cl₂/CF₃COOH (v/v=1/1) solution. The reaction finished in 1 h. The solvent was then evaporated and the crude product was used without further purification. LC/MS: 526.240 [M+H⁺].

Methyl (Z)-3-(((4-(2-(4-(2,2-dimethyl-4-oxo-3,8,11-trioxa-5-azatridecane-13-yl)piperazin-1-yl)-N-methylacetamido)phenyl)amino)(phenyl)methylene)-2-oxoindoline-6-carboxylate (10)



Methyl (Z)-3-(((4-(N-methyl-2-(piperazin-1-yl)acetamido)phenyl)amino)(phenyl)methylene)-2-oxoindoline-6-carboxylate (**9**) (70 mg, 0.133 mmol) and tert-butyl (2-(2-(2-bromoethoxy)ethoxy)ethyl)carbamate (45 mg, 0.15 mmol) were dissolved in DMF and Cs₂CO₃ (60 mg, 0.17 mmol) was added. The mixture was stirred at room temperature overnight. After completion, water was added and the mixture was extracted 3×20 ml with ethyl acetate. The organic phases were combined and concentrated to give the crude product. The crude product was then purified by flash chromatography using a solvent gradient of 0-100 % ethyl acetate in petroleum ether to give 60.5 mg of the target molecule (**10**) LC/MS: 757.432 [M+H⁺], ¹H NMR (400 MHz, CDCl₃) δ 12.20 (s, 1H), 8.11 (s, 1H), 7.72 – 7.52 (m, 4H), 7.50 – 7.35 (m, 3H), 6.99 (d, *J* = 8.3 Hz, 2H), 6.81 (d, *J* = 8.3 Hz, 2H), 6.01 (d, *J* = 8.3 Hz, 1H), 5.10 (s, 1H), 3.88 (s, 3H), 3.64-3.54 (m, 8H), 3.33 (d, *J* = 5.4 Hz, 2H), 3.19 (s, 3H), 2.81 (s, 2H), 2.63 – 2.45 (m, 8H), 1.46 (s, 9H).

Methyl (Z)-3-(((4-(2-(4-(2-(2-(2-aminoethoxy)ethoxy)ethyl)piperazin-1-yl)-N-methylacetamido)phenyl)amino)(phenyl)methylene)-2-oxoindoline-6-carboxylate (11)



Methyl (Z)-3-(((4-(2-(4-(2,2-dimethyl-4-oxo-3,8,11-trioxa-5-azatriodecan-13-yl)piperazin-1-yl)-N-methylacetamido)phenyl)amino)(phenyl)methylene)-2-oxoindoline-6-carboxylate (**10**) (30 mg, 0.04 mmol) was dissolved in 5 ml $\text{CH}_2\text{Cl}_2/\text{CF}_3\text{COOH}$ (v/v:1/1) solution. The reaction finished in 1 h. The solvent was then evaporated. The crude product was transferred on top of a SCX column, washed 2 times with methanol and eluted with ammonia in methanol (2M), resulted in compound **11** with 7 mg. LC/MS: 657.336 $[\text{M}+\text{H}^+]$. LC/MS: 657.432 $[\text{M}+\text{H}^+]$, ^1H NMR (400 MHz, Methanol- d_4) δ 7.63 (dt, $J = 14.1, 6.9$ Hz, 4H), 7.59 – 7.55 (m, 1H), 7.51 (d, $J = 6.9$ Hz, 2H), 7.30 (d, $J = 8.3$ Hz, 1H), 7.15 (d, $J = 8.1$ Hz, 2H), 6.96 (d, $J = 8.2$ Hz, 2H), 5.98 (d, $J = 8.2$ Hz, 1H), 3.85 (d, $J = 6.0$ Hz, 5H), 3.72 (d, $J = 5.5$ Hz, 6H), 3.63 (q, $J = 7.0$ Hz, 5H), 3.19 – 3.12 (m, 4H), 2.85 (s, 3H), 2.72 (s, 2H), 2.06 (s, 3H).

Cell Culture/Lysis, Placenta Lysis, Compound Immobilization, Affinity Purification, Drug Competition Assay, LC-MS/MS Analysis and Data Analysis

All the mentioned material and experimental procedures were the same as described in Chapter III (3.2 Material and Method)

Peptide and Protein Identification and Quantification

All raw MS spectra were processed by MaxQuant software (version 1.4.0.5) for peak detection and quantification. MS/MS spectra was searched against the IPI human database human (version 3.68, 87,061 sequences) by Andromeda search engine enabling contaminants and the reversed versions of all sequences with the following

Chapter IV | Development and application of a VEGFR probe

search parameters: Carbamidomethylation of cysteine residues as fixed modification and Acetyl (Protein N-term), Oxidation (M) as variable modifications. Trypsin was specified as the proteolytic enzyme with up to 2 miss cleavages were allowed. For identification 0.01 peptide and protein FDRs were used. Feature matching between raw files was enabled, using a match time window of 2 min.

4.3 Results and Discussion

4.3.1 Probe design and synthesis

In keeping with the idea that immobilized inhibitors should be potent but unselective to the target class, after a deep mining of the literature, 9 VEGFR inhibitors representing 8 different scaffolds were selected (Figure 1) as a starting point for probe design to enrich the VEGFRs. These 9 molecules are all potent multi-angiokinase inhibitors (Borzilleri et al., 2005; Gingrich et al., 2003; Harris et al., 2008; Hu-Lowe et al., 2008; Matsui et al., 2008; Polverino et al., 2006; Renhowe et al., 2009; Roth et al., 2009; Wedge et al., 2005). The availability of co-crystal structures and detailed structure activity relationships (SARs) lead to the prioritization of BIBF1120, a 6-methoxycarbonyl-substituted indolinone derivative (Figure 1), reported to have high inhibitory activity against multiple angiokinases (IC_{50} : VEGFR1/2/3: 104/5/5 nM, PDGFR α : 18 nM, Phase III) (Roth et al., 2009).

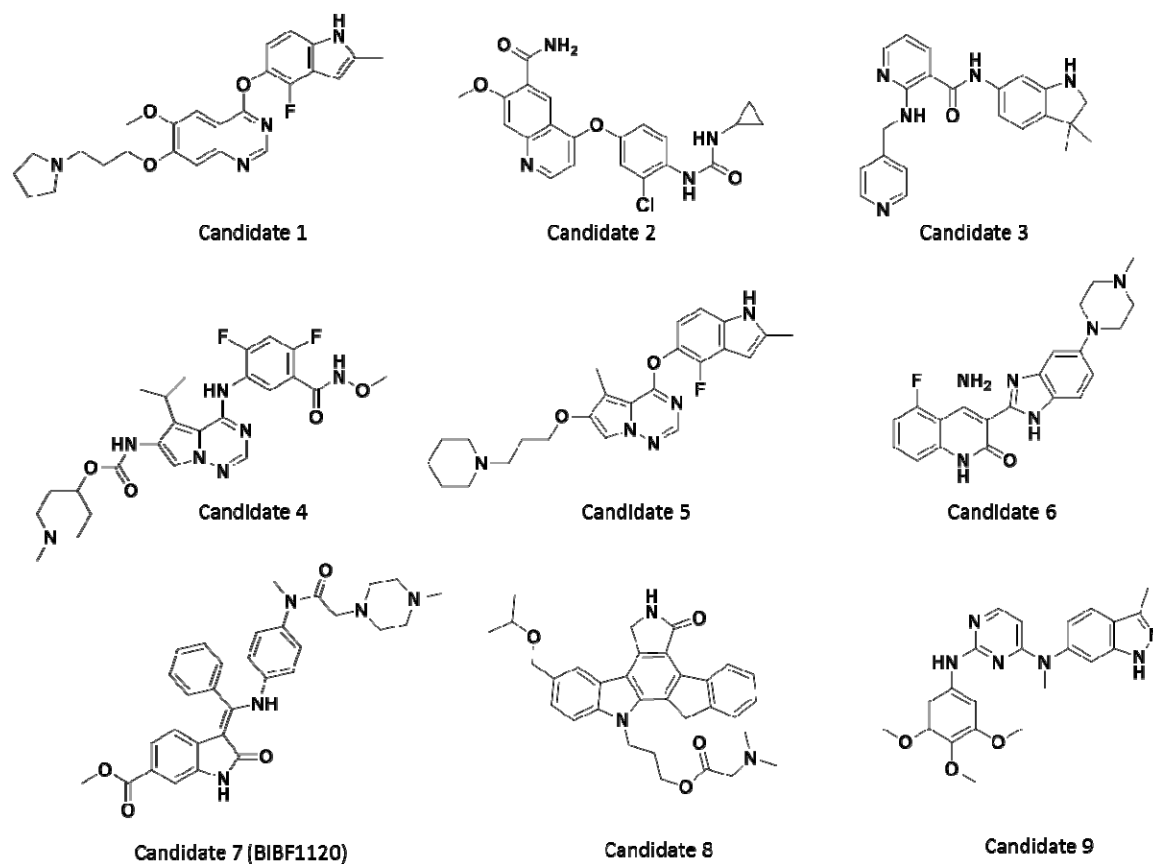


Figure 1 | Chemical structures of selected VEGFR kinase inhibitors from the literature considered as potential starting points to design VEGFR affinity probe.

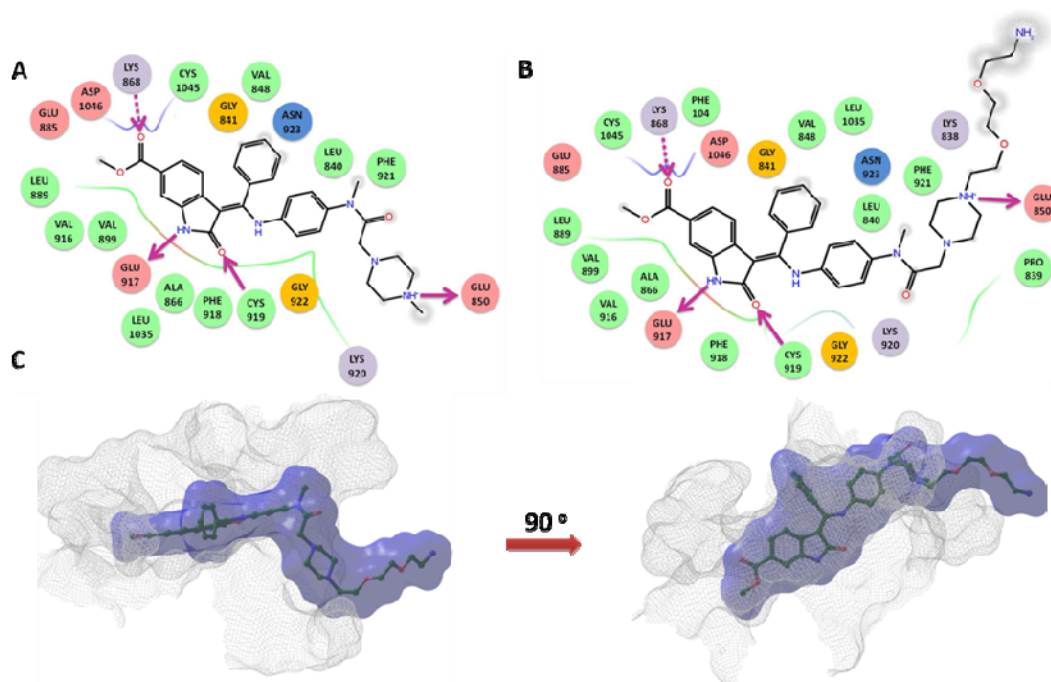


Figure 2 | Co-crystal structure and molecular docking study of parent compound BIBF1120 and the designed probe Compound 18, based on VEGFR2 crystal structure (PDB 3C7Q).

(A) Two-dimensional interaction map of BIBF1120 in the ATP binding pocket of VEGFR2. (B) Binding pose of Compound 18 in the ATP binding pocket of VEGFR2. (C) 3D binding poses of Compound 18 (dark blue surface) in the VEGFR2 binding pocket (grey mesh), showing that the introduced linker extends into the solvent as required for subsequent immobilization of the probe.

The co-crystal structure of BIBF1120 bound to the intracellular kinase domain of VEGFR2 (Figure 2A) reveals the binding mode of the inhibitor at the atomic level (Hilberg et al., 2008) and provides a rationale for the placement of the linker for later immobilization. BIBF1120 forms two hydrogen bonds with the enzyme backbone on Cys919 and Glu917 in the hinge region. The only solvent exposed part is the methyl piperazinyl group with the 4-nitrogen atom of the N-methyl piperazinyl moiety tethered by a bidentate ionic interaction with the carboxylate oxygens of Glu850. The fixed orientation of the methyl piperazinyl group towards the solvent strongly suggests that this position would accommodate a linker for immobilization without impairing target binding. Multiple sequence alignments (Figure 3) show that this Glu residue is

conserved in VEGFR3, PDGFR alpha and beta as well as c-KIT, indicating that linkage at this position would be tolerable for binding other angiokinases too. On the basis of this hypothesis, a probe was designed that would maintain the salt bridge to Glu850 and carrying a primary amine terminated PEG linker for immobilization to beads (designated as Compound 18, Figure 1B). Molecular docking analysis confirmed that the designed probe binds in the same way to VEGFR2 as does BIBF1120 with all the key interactions preserved (Figure 1B). The docking data also suggested that, as expected, the linker moiety reaches into solvent space without interrupting the binding pose of BIBF1120 (Figure 1C). Compound 18 was prepared following the synthetic scheme described by Roth et al (Roth et al., 2009), replacing methylpiperazine by Boc-piperazine as the solvent pointing moiety. The linker was then attached to the deprotected piperazine to obtain the probe in a total of 9 steps (see method section).

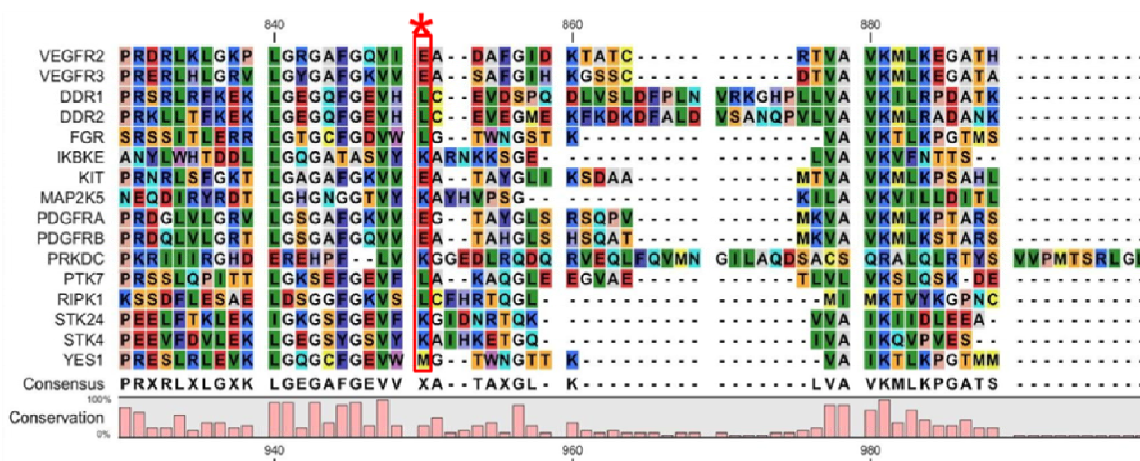


Figure 4 | Sequence alignment of 16 kinases that were preferentially enriched by Compound 18.

The alignment shows that Glu850 (marked by an asterisk) of VEGFR2 is conserved in some but not all kinases.

4.3.2 Characterization of the VEGFR probe binding profiles in cell and tissue lysates

Having the probe in hand, the practical utility of Compound 18 as a Kinobead compound for the selectivity profiling of kinase inhibitors was evaluated. In order to determine the protein binding profile, duplicate pulldown experiments were performed using the immobilized probe in conjunction with mass spectrometric analysis for protein identification in mixed lysates of four cancer cell lines (K562,

COLO205, OVCAR8, and SKNBE2, hereinafter referred to as cell mix) and human placenta tissue lysate. As these lysates provide complementary sets of expressed proteins, they allow painting a more complete picture of the protein binding potential of the probe.

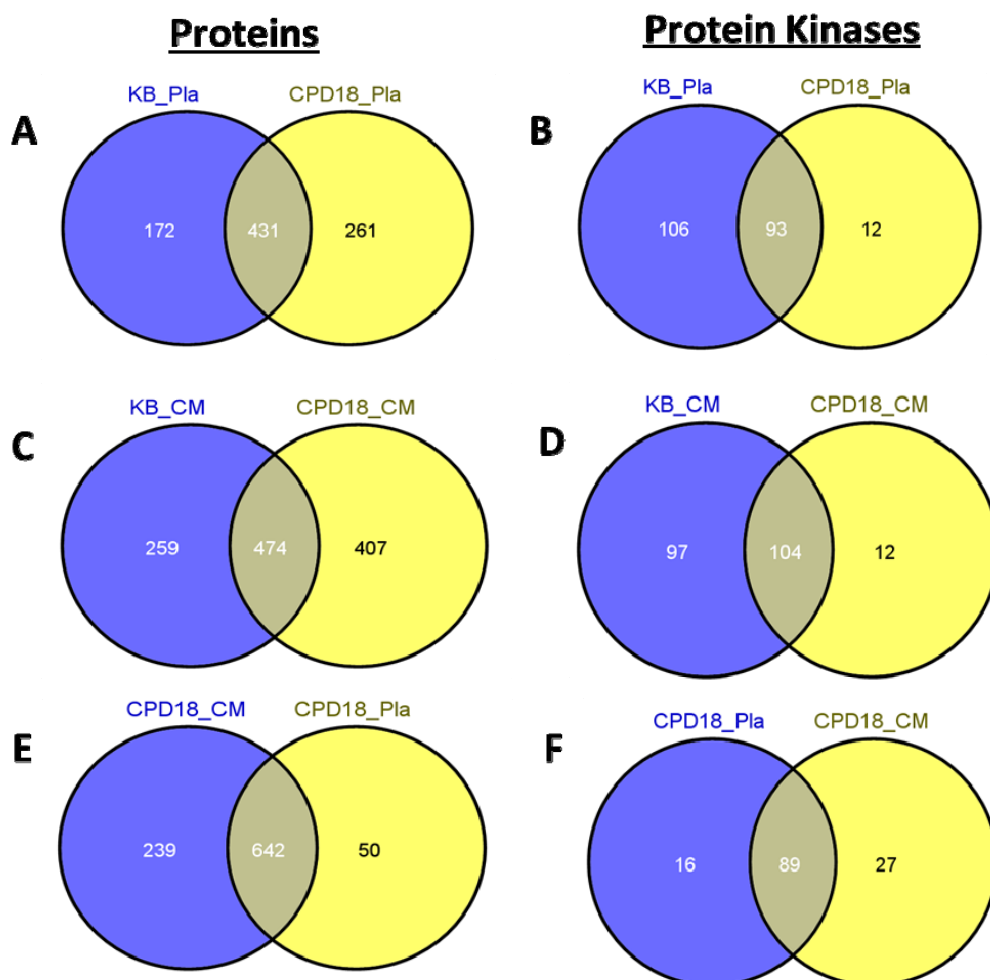


Figure 4 | Comparison of proteins and kinases captured by Compound 18 (CPD18) and Kinobeads (KB) in a mixed lysate of four human cancer cell lines (CM) and in placenta lysate (Pla). The reported numbers (nonredundant) refer to the sum of the duplicates. The Venn diagrams A-D show the comparison between Kinobeads and Compound 18, whereas E and F show the comparison of the numbers of proteins/kinases identified by Compound 18 in two different lysates.

In total, the pulldown experiments identified 931 proteins including 132 protein kinases making Compound 18 one of most promiscuous kinase affinity probes described to date (Figure 4). Although the number of kinases only account for 14% of the total number of captured proteins, they account for 40% of the protein amount present on the beads

(judged by the mass spectrometric signal intensity). Gene ontology (GO) analysis showed that 33% of the identified proteins were classified as nucleotide binding proteins in placenta and cell mix which is not surprising given that BIBF1120 as the molecule underlying the probe design is an ATP competitive drug. Compound 18 captured 105 protein kinases from human placenta lysate and 116 protein kinases from the cell mix (Figure 4). Among these are VEGFRs, PDGFRs and KIT, the main targets of the lead compound BIBF1120, which meets a primary objective of the study. In addition, Visualization of the identified kinases from cell mix on the phylogenetic kinase tree (Figure 5) revealed that the Compound 18 captured not only targets in the tyrosine kinase branch, but also displays affinity for kinases across all major kinase groups, including AGC, CMGC, CAMK as well as STE kinase families. This broad kinase binding profile achieved an important objective of the probe design which was to be rather unselective within the target class. Besides kinases, the probe also binds a considerable number of other proteins. Gene ontology (GO) analysis showed that 30% of all identified proteins were classified as nucleotide binding proteins in placenta and cell mix. This is not surprising, since the probe mimicks the ATP structure and has the potential to bind a huge amount of these nucleotide binding proteins.

Next, the kinase binding profile of Compound 18 to that of Kinobeads was compared. Out of the 105 protein kinases enriched by the probe from placenta lysate, 12 were more efficiently captured by Compound 18 compared to Kinobeads (using a 2-fold higher average MS intensity as a criterion). Similarly, Compound 18 also led to an improvement over Kinobeads for 12 kinases using the cell mix (Figure 4D). Importantly, VEGFRs, PDGFRs and KIT were captured 10 to >100-fold more efficient with Compound 18 than using Kinobeads depending on whether placenta or cell mix lysates were used. This difference is likely due to strong abundance differences of these targets in the respective lysates and the comparatively weak affinity of Kinobeads towards these proteins. In addition, PTK7, RIPK1 and STK24 were exclusively captured by Compound 18 demonstrating the overall success of the probe design. Multiple sequence alignment of the 16 kinases preferentially enriched by Compound 18 show that VEGFR2/3, PDGFR α/β , Kit all contain the conserved Glu residue mentioned above providing a rational why they are so efficiently captured. The other 11 kinases do not contain this sequence feature suggesting that the presence of the Glu residue is advantageous but not essential for probe binding (Figure 4).

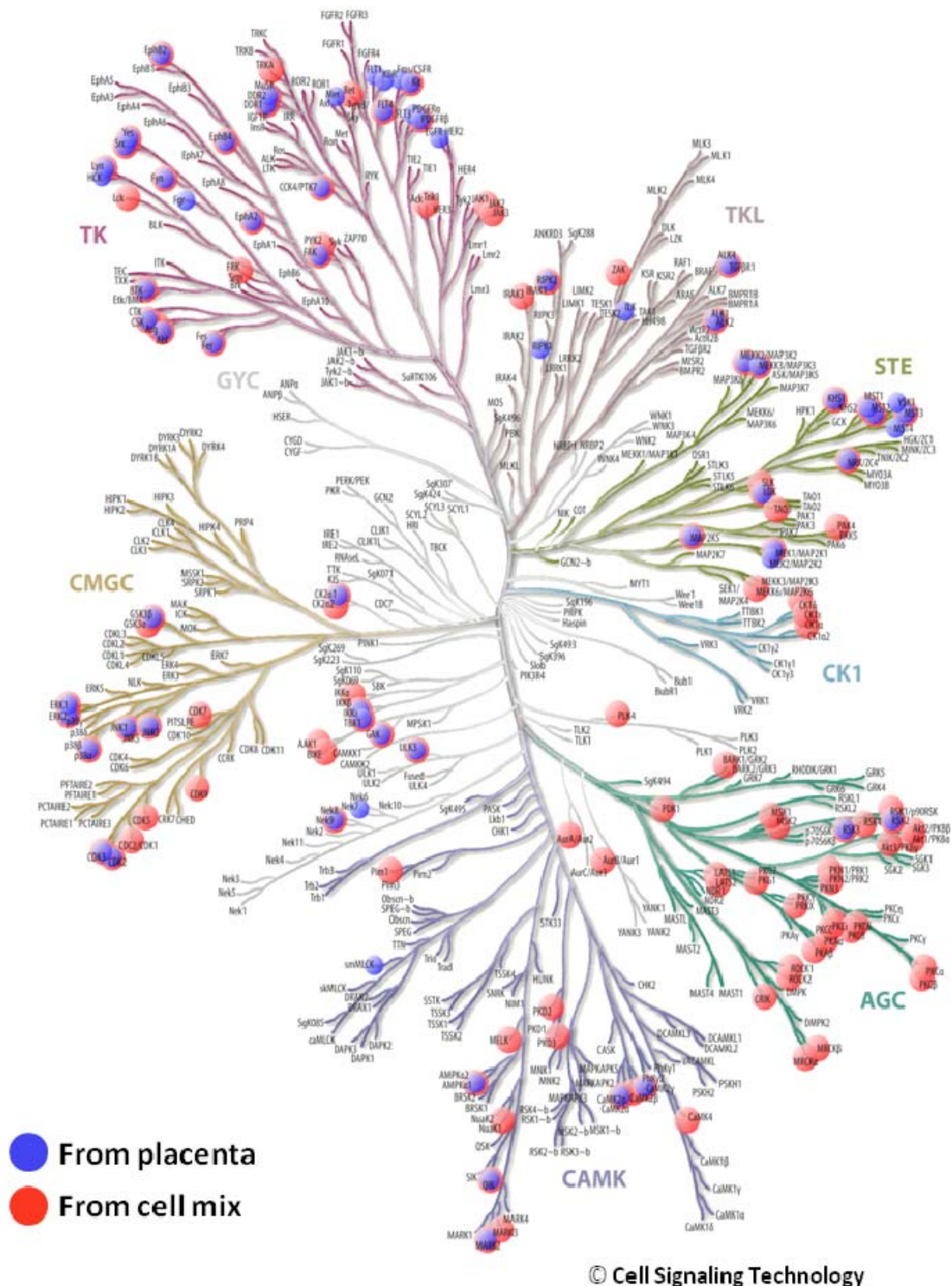


Figure 5 | Visualization of all identified kinases onto the phylogenetic kinase tree.

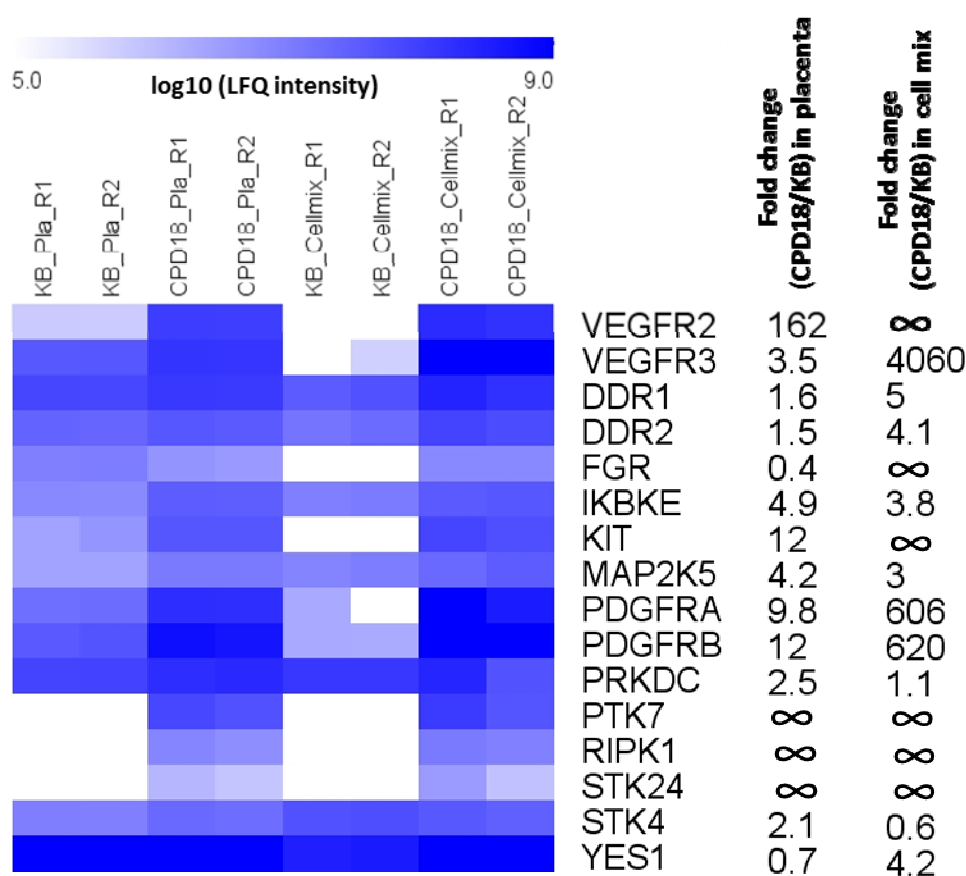


Figure 6 | Comparison of duplicates of Compound 18 (CPD18) and Kinobeads (KB) pulldowns for the enrichment of kinases from lysates of a 4 cell line mix (CM) and human placenta (Pla). The heat map coloring uses the \log_{10} transformed label-free quantification (LFQ) values from the MaxQuant for protein quantification.

4.3.3 Selectivity profiling of Axitinib and Pazopanib

After the binding profile of Compound 18 was identified, this probe was applied in conjunction with the established set of affinity probes used in the Kinobeads approach to establish the selectivity profiles of the two clinical VEGFR inhibitors Axitinib and Pazopanib (Figure 7). Pazopanib (Votrient®, GlaxoSmithKline) has been approved in 2009 for the treatment of soft tissue sarcoma as well as renal cell carcinoma. Axitinib (Inlyta®, Pfizer) has been approved by the FDA in early 2012 for the treatment of advanced renal cell carcinoma. Axitinib (Hu-Lowe et al., 2008) is a pan-VEGFR inhibitor and Pazopanib (Deeks, 2012) a multi-target kinase inhibitor affecting many angiokinases.

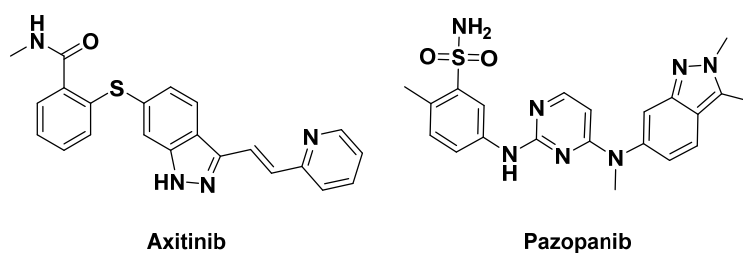


Figure 7 | Chemical structures of Axitinib and Pazopanib.

The cell mix (see above) was chosen for this experiment, since the drugs would be exposed to a broad range of natively expressed kinases and other nucleotide binding proteins, although it is not the ideal protein source of VEGFRs and other angiogenesis related proteins. Pulldowns using Compound 18 plus Kinobeads were performed in a competition set-up using lysates pre-incubated with 6 different concentrations (0, 2.5 nM, 25 nM, 250 nM, 2,500 nM, and 25,000 nM) of Pazopanib or Axitinib respectively (see Chapter 1, Figure 5 for a schematic workflow). In this assay, targets of any one drug exhibit a dose dependent reduction of bead binding while the protein amounts of non-targets remain unaffected. Binding (or loss) can be quantified by label free LC-MS/MS analysis and half maximal inhibitory concentration (IC_{50}) of bead binding as well as binding constants (K_d) values were derived from the dose response curves as described (Ku et al., 2014; Lemeer et al., 2013; Sharma et al., 2009).

Table 1 | Inhibitory concentrations and binding constants of Pazopanib and Axitinib for protein targets as determined in this study (KB assay) compared to potency values determined by recombinant kinase assays reported in the literature (Davis et al., 2011).

Target	Pazopanib			Axitinib		
	KB assay IC ₅₀	KB assay K _d	Recomb. Assay, K _d	KB assay IC ₅₀	KB assay K _d	Recomb. Assay, K _d
ABL1	2.78	1.61	0.62	2.61	1.07	0.084
ABL2	>10	>10	3	2.51	0.53	0.07
AURKA	2.97	0.65	7.1/0.17*	2.34	0.37	0.072
AURKB	>10	>10	—	1.25	0.83	0.011
DDR1	0.26	0.14	0.057	3.30	1.42	0.34
DDR2	0.32	0.23	0.098	>10	>10	5.3
LIMK1	1.42	0.70	0.72	2.32	0.49	—
MAP4K2	2.84	1.16	2.7	3.08	1.45	1.3
PDGFRβ	0.67	0.63	0.002	0.62	0.59	0.006
RET	0.26	0.11	0.31	0.25	0.08	0.12
RIPK2	2.61	0.78	0.58	>10	>10	9.9
TNIK	1.38	1.38	0.31	3.38	2.40	0.18
VEGFR3	0.02	0.01	0.027	0.007	0.003	0.17

* IC₅₀ value obtained by *in vitro* kinase activity assay using recombinant full length AURKA (Isham et al., 2013).

Comparison of Axitinib and Pazopanib showed clear similarities as well as differences in their respective selectivity profile. As expected, both drugs show potent inhibition of the primary target VEGFR3/FLT4 which is in good agreement with the published data using recombinant kinase assays (Table 1) (Anastassiadis et al., 2011; Karaman et al., 2008; Sonpavde et al., 2008). Kinobeads enrichment of PDGFRβ was also diminished by Pazopanib and Axitinib in a dose dependent manner, but with lower potency than expected from the recombinant assay data (Anastassiadis et al., 2011; Karaman et al., 2008; Sonpavde et al., 2008). This observation is not surprising and may be rationalized by a number of factors including: i) PDGFRβ is generally autoinhibited in cells in order to keep the receptor inactive in the absence of ligand (Chiara et al., 2004). As a result,

Pazopanib and Axitinib may not bind this conformation very effectively (while the immobilized compounds can); ii) in vitro kinase assays utilize isolated recombinant kinase (or even just the kinase domain) and thus lack auxiliary proteins or other cofactors and naturally occurring post-translational modifications that impact on drug-protein interactions.

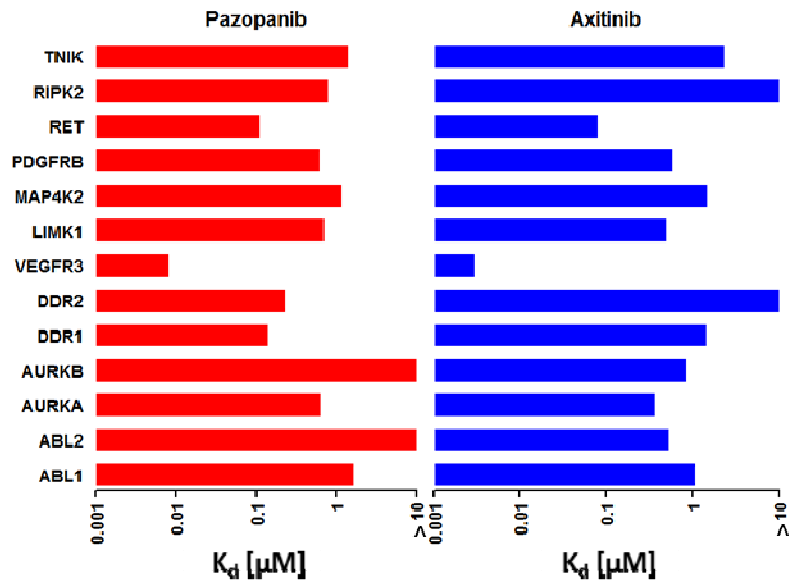


Figure 8 | Comparison of potencies (K_d value) of all major kinase targets identified for Axitinib and Pazopanib in the dose dependent competition assay.

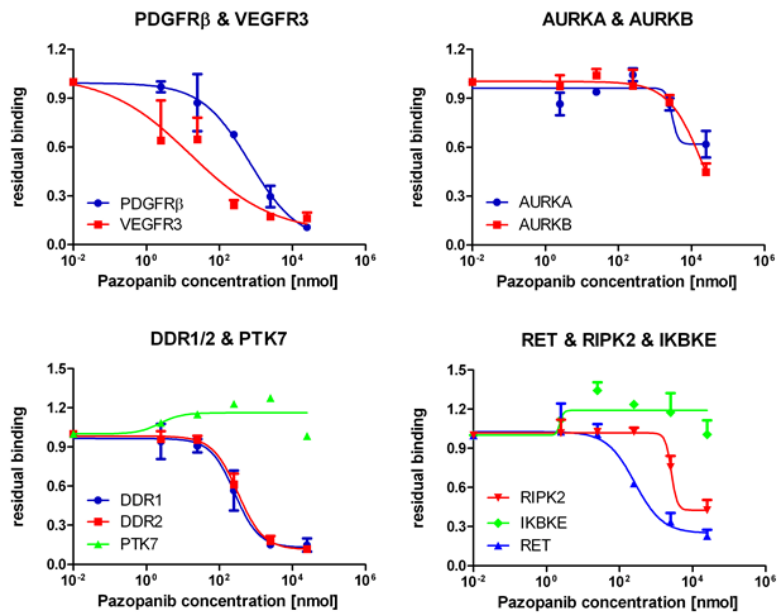
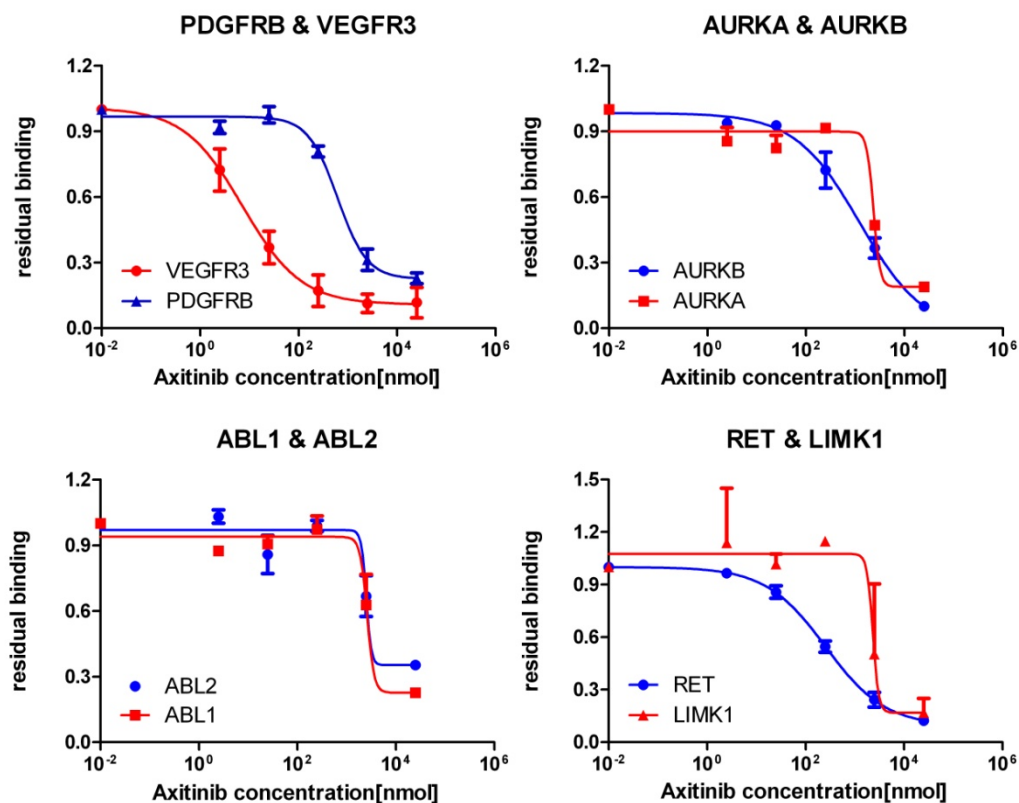


Figure 9 | Overview of targets identified in the dose dependent competition assay for Pazopanib.

Besides the primary targets, both two drugs show medium to high interaction potency to several other kinases (Figures 3 and Table 1). Pazopanib showed sub-micromolar affinity to 6 further kinases in Kinobeads assay: AURKA (~80-fold window over VEGFR3), DDR1/2 (~20-fold window), LIMK1 (~80-fold window), RET (~10-fold window) and RIPK2 (~100-fold window). For Axitinib, 5 such cases were identified: ABL2 (~180-fold window), AURKA&B (~10-fold window, LIMK1 (~160-fold window) and RET (~25-fold window). Depending on the pharmacokinetic and pharmacodynamic properties of the inhibitors, the above potencies may be of physiological relevance.

**Figure 10 | Overview of all major kinase targets identified in the dose dependent competition assay for Axitinib.**

The AURKA/B and RET oncogenes are often overexpressed in tumor cells (Borrello et al., 2013; Fu et al., 2007; Marumoto et al., 2005; Mehra et al., 2013; Takaya et al., 1996), both are reported targets of Axitinib *in vitro* (Anastassiadis et al., 2011; Karaman et al.,

2008; Sonpavde et al., 2008) and, according to the Kinobeads assay data, the drug also appears to be active against these targets in cell lysates. In recombinant kinase assays, Axitinib showed no binding affinity to LIMK1 at a concentration of 10 μM (Davis et al., 2011). It was, however, detected in this assay with a K_d of 490 nM suggesting that this interaction may have been missed in previous studies. LIMK1 is a critical regulator of actin dynamics (Khurana et al., 2002) and has been shown to play a regulatory role in tumor cell invasion (Yoshioka et al., 2003) and is also involved in tumor cell-induced angiogenesis (Vlecken and Bagowski, 2009). Therefore, simultaneously targeting AURKA/B, RET and LIMK1 may provide additional therapeutic benefit for the treatment of cancer using Axitinib. Reported off-targets of Pazopanib include ABL1, RET, DDR1, DDR2, LIMK1, RIPK2, as well as TNIK (Anastassiadis et al., 2011; Karaman et al., 2008; Sonpavde et al., 2008) and these targets were broadly recapitulated in this assay (Table 1).

Interestingly, a strong discrepancy in the data for AURKA was initially observed; while the reported *in vitro* kinase assay data using kinase domain for Pazopanib determined a K_d of 7.1 μM , Kinobeads assay data showed a K_d of 650 nM. The latter is more in line with a recent study by Isham *et al* (Isham et al., 2013), who reported an inhibitory concentration of 167 nM when using the full length protein. The same authors also showed that Pazopanib synergizes with paclitaxel in anaplastic thyroid cancer lines, providing strong evidence that the drug also inhibits AURKA *in vivo*. However, the observed discrepancy between the chemical proteomic and *in vitro* kinase assay data for AURKA is only an individual case rather than a general feature of all AURKA inhibitors (work done by the other people).

3.4 Conclusion

In summary, a small molecule probe Compound 18 was designed and synthesized which has enabled the affinity enrichment of more than 130 other kinases from human cancer cell lines and human placenta. More importantly, the probe binds kinases such as VEGF receptors that were not detected using other broad-spectrum kinase inhibitors before. The probe can be added to the chemical proteomics arsenal or be used alone for e. g. profiling the expression of kinases in human cells or the determination of the selectivity of kinase inhibitors. Compound 18 exemplifies the ongoing efforts to make all human kinases accessible to chemical proteomic experiments and the results obtained validate the structure based design approach for the development of broadly selective affinity tools.

Acknowledgements

I want to thank Dr. Sabine Schweizer and Dr. Xiaofeng Liu for assistance with docking studies.

Abbreviations

DMEM Dulbecco's modified Eagle's medium

FBS fetal bovine serum

GO gene ontology

HCD higher energy collision induced dissociation

IC₅₀ half maximal inhibitory concentration

IMDM Iscove's modified Dulbecco's medium

K_d dissociation constant

KB Kinobeads

KI kinase inhibitor

LC-MS/MS liquid chromatography coupled to tandem mass spectrometry

MoA mode of action

PBS phosphate buffered saline

PTM post translational modification

RPMI1640 Roswell Park Memorial Institute 1640 medium

SAR structure activity relationships

References

- Anastassiadis, T., Deacon, S.W., Devarajan, K., Ma, H., and Peterson, J.R. (2011). Comprehensive assay of kinase catalytic activity reveals features of kinase inhibitor selectivity. *Nat Biotechnol* 29, 1039-1045.
- Borrello, M.G., Ardini, E., Locati, L.D., Greco, A., Licitra, L., and Pierotti, M.A. (2013). RET inhibition: implications in cancer therapy. *Expert opinion on therapeutic targets* 17, 403-419.
- Borzilleri, R.M., Zheng, X., Qian, L., Ellis, C., Cai, Z.W., Wautlet, B.S., Mortillo, S., Jeyaseelan, R., Sr., Kukral, D.W., Fura, A., *et al.* (2005). Design, synthesis, and evaluation of orally active 4-(2,4-difluoro-5-(methoxycarbamoyl)phenylamino)pyrrolo[2,1-f][1,2,4]triazines as dual vascular endothelial growth factor receptor-2 and fibroblast growth factor receptor-1 inhibitors. *J Med Chem* 48, 3991-4008.
- Chiara, F., Bishayee, S., Heldin, C.H., and Demoulin, J.B. (2004). Autoinhibition of the platelet-derived growth factor beta-receptor tyrosine kinase by its C-terminal tail. *The Journal of biological chemistry* 279, 19732-19738.
- Davis, M.I., Hunt, J.P., Herrgard, S., Ciceri, P., Wodicka, L.M., Pallares, G., Hocker, M., Treiber, D.K., and Zarrinkar, P.P. (2011). Comprehensive analysis of kinase inhibitor selectivity. *Nat Biotechnol* 29, 1046-1051.
- Deeks, E.D. (2012). Pazopanib: in advanced soft tissue sarcoma. *Drugs* 72, 2129-2140.
- Fu, J., Bian, M., Jiang, Q., and Zhang, C. (2007). Roles of Aurora kinases in mitosis and tumorigenesis. *Molecular cancer research : MCR* 5, 1-10.
- Gingrich, D.E., Reddy, D.R., Iqbal, M.A., Singh, J., Aimone, L.D., Angeles, T.S., Albom, M., Yang, S., Ator, M.A., Meyer, S.L., *et al.* (2003). A new class of potent vascular endothelial growth factor receptor tyrosine kinase inhibitors: structure-activity relationships for a series of 9-alkoxymethyl-12-(3-hydroxypropyl)indeno[2,1-a]pyrrolo[3,4-c]carbazole-5-ones and the identification of CEP-5214 and its dimethylglycine ester prodrug clinical candidate CEP-7055. *J Med Chem* 46, 5375-5388.
- Harris, P.A., Bloor, A., Cheung, M., Kumar, R., Crosby, R.M., Davis-Ward, R.G., Epperly, A.H., Hinkle, K.W., Hunter, R.N., 3rd, Johnson, J.H., *et al.* (2008). Discovery of 5-[[4-[(2,3-dimethyl-2H-indazol-6-yl)methylamino]-2-pyrimidinyl]amino]-2-methyl-benzenesulfonamide (Pazopanib), a novel and potent vascular endothelial growth factor receptor inhibitor. *J Med Chem* 51, 4632-4640.
- Hilberg, F., Roth, G.J., Krssak, M., Kautschitsch, S., Sommergruber, W., Tontsch-Grunt, U., Garin-Chesa, P., Bader, G., Zoephel, A., Quant, J., *et al.* (2008). BIBF 1120: triple angiokinase inhibitor with sustained receptor blockade and good antitumor efficacy. *Cancer Res* 68, 4774-4782.
- Hu-Lowe, D.D., Zou, H.Y., Grazzini, M.L., Hallin, M.E., Wickman, G.R., Amundson, K., Chen, J.H., Rewolinski, D.A., Yamazaki, S., Wu, E.Y., *et al.* (2008). Nonclinical antiangiogenesis and antitumor activities of axitinib (AG-013736), an oral, potent, and selective inhibitor of vascular endothelial growth factor receptor

- tyrosine kinases 1, 2, 3. *Clinical cancer research : an official journal of the American Association for Cancer Research* 14, 7272-7283.
- Isham, C.R., Bossou, A.R., Negron, V., Fisher, K.E., Kumar, R., Marlow, L., Lingle, W.L., Smallridge, R.C., Sherman, E.J., Suman, V.J., *et al.* (2013). Pazopanib enhances paclitaxel-induced mitotic catastrophe in anaplastic thyroid cancer. *Sci Transl Med* 5, 166ra163.
- Karaman, M.W., Herrgard, S., Treiber, D.K., Gallant, P., Atteridge, C.E., Campbell, B.T., Chan, K.W., Ciceri, P., Davis, M.I., Edeen, P.T., *et al.* (2008). A quantitative analysis of kinase inhibitor selectivity. *Nature biotechnology* 26, 127-132.
- Khurana, T., Khurana, B., and Noegel, A.A. (2002). LIM proteins: association with the actin cytoskeleton. *Protoplasma* 219, 1-12.
- Ku, X., Heinzlmeir, S., Liu, X., Medard, G., and Kuster, B. (2014). A new chemical probe for quantitative proteomic profiling of fibroblast growth factor receptor and its inhibitors. *J Proteomics* 96, 44-55.
- Lemeer, S., Zorgiebel, C., Ruprecht, B., Kohl, K., and Kuster, B. (2013). Comparing Immobilized Kinase Inhibitors and Covalent ATP Probes for Proteomic Profiling of Kinase Expression and Drug Selectivity. *J Proteome Res* 12, 1723-1731.
- Marumoto, T., Zhang, D., and Saya, H. (2005). Aurora-A - a guardian of poles. *Nature reviews Cancer* 5, 42-50.
- Matsui, J., Yamamoto, Y., Funahashi, Y., Tsuruoka, A., Watanabe, T., Wakabayashi, T., Uenaka, T., and Asada, M. (2008). E7080, a novel inhibitor that targets multiple kinases, has potent antitumor activities against stem cell factor producing human small cell lung cancer H146, based on angiogenesis inhibition. *Int J Cancer* 122, 664-671.
- Mehra, R., Serebriiskii, I.G., Burtness, B., Astsaturov, I., and Golemis, E.A. (2013). Aurora kinases in head and neck cancer. *The lancet oncology* 14, e425-435.
- Polverino, A., Coxon, A., Starnes, C., Diaz, Z., DeMelfi, T., Wang, L., Bready, J., Estrada, J., Cattley, R., Kaufman, S., *et al.* (2006). AMG 706, an oral, multikinase inhibitor that selectively targets vascular endothelial growth factor, platelet-derived growth factor, and kit receptors, potently inhibits angiogenesis and induces regression in tumor xenografts. *Cancer Res* 66, 8715-8721.
- Renhowe, P.A., Pecchi, S., Shafer, C.M., Machajewski, T.D., Jazan, E.M., Taylor, C., Antonios-McCrea, W., McBride, C.M., Frazier, K., Wiesmann, M., *et al.* (2009). Design, structure-activity relationships and in vivo characterization of 4-amino-3-benzimidazol-2-ylhydroquinolin-2-ones: a novel class of receptor tyrosine kinase inhibitors. *J Med Chem* 52, 278-292.
- Roth, G.J., Heckel, A., Colbatzky, F., Handschuh, S., Kley, J., Lehmann-Lintz, T., Lotz, R., Tontsch-Grunt, U., Walter, R., and Hilberg, F. (2009). Design, synthesis, and evaluation of indolinones as triple angiokinase inhibitors and the discovery of a highly specific 6-methoxycarbonyl-substituted indolinone (BIBF 1120). *J Med Chem* 52, 4466-4480.

- Sharma, K., Weber, C., Bairlein, M., Greff, Z., Keri, G., Cox, J., Olsen, J.V., and Daub, H. (2009). Proteomics strategy for quantitative protein interaction profiling in cell extracts. *Nat Methods* 6, 741-744.
- Sonpavde, G., Hutson, T.E., and Rini, B.I. (2008). Axitinib for renal cell carcinoma. *Expert Opin Investig Drugs* 17, 741-748.
- Takaya, K., Yoshimasa, T., Arai, H., Tamura, N., Miyamoto, Y., Itoh, H., and Nakao, K. (1996). Expression of the RET proto-oncogene in normal human tissues, pheochromocytomas, and other tumors of neural crest origin. *J Mol Med (Berl)* 74, 617-621.
- Vlecken, D.H., and Bagowski, C.P. (2009). LIMK1 and LIMK2 are important for metastatic behavior and tumor cell-induced angiogenesis of pancreatic cancer cells. *Zebrafish* 6, 433-439.
- Wedge, S.R., Kendrew, J., Hennequin, L.F., Valentine, P.J., Barry, S.T., Brave, S.R., Smith, N.R., James, N.H., Dukes, M., Curwen, J.O., *et al.* (2005). AZD2171: a highly potent, orally bioavailable, vascular endothelial growth factor receptor-2 tyrosine kinase inhibitor for the treatment of cancer. *Cancer Res* 65, 4389-4400.
- Yoshioka, K., Foletta, V., Bernard, O., and Itoh, K. (2003). A role for LIM kinase in cancer invasion. *Proc Natl Acad Sci U S A* 100, 7247-7252.

Summary

Zusammenfassung

Summary

Protein kinases represent one of the most important target classes for cancer therapy because of their pivotal roles in tumorigenesis and metastasis. Recent advances in chemical proteomics notably the use of immobilized small molecule kinase inhibitors as affinity probes with a mass spectrometry-based readout, has enabled kinase affinity purification under close to physiological conditions. This great advantage of chemical proteomics has attracted massive interests in developing pan-kinase capturing tools that are able to purify as many kinases as possible to serve the purpose of kinome-wide drug selectivity profiling.

In Chapter I, a pan kinase inhibition probe VI16743 was immobilized and its binding profile was characterized by pulldown experiments using cancer cell lysates. This probe allowed the identification of 179 kinases, including 10 members of the phosphoinositide kinase family (PI3Ks and PI4Ks) among a total number of 30 kinases that were out of reach by the kinobeads. When supplemented to the kinobeads, VI16743 enhanced the binding performance of the kinobeads in terms of both the kinase coverage as well as the quantity of the enriched kinases, demonstrating that VI16743 can be a good complementarity to the kinobeads. Besides that, there are still a number of kinases that are beyond kinobeads coverage, notably the angiogenesis related receptor kinases VEGFRs and FGFRs. For this purpose, under the guidance of molecular modelling, three probes (F1 and F2 in Chapter III, Compound 18 in Chapter IV), aiming of VEGFRs and FGFRs, were carefully designed and synthesized. Probe F2 was capable of enriching all members of the FGF receptor family as well as other kinases involved in cancer such as KDR, FLT4 and RET from cancer cell lysates or human placenta tissue. In combination with the kinobeads approach, probe F2 facilitated the identification of the target spectrum of two angiogenesis inhibitors (Dovitinib and Orantinib), confirming many of the previously identified (off-) targets such as AURKA, FLT4/VEGFR3, IKBKE and PDGFR β . Compound 18 is capable of enriching more than 130 protein kinases, including multiple angiokinases (VEGFRs and PDGFRs) which had not been previously detected by other broad-spectrum kinase inhibitors. Combining compound 18 with kinobeads in competitive binding assays, several off-targets of Pazopanib (DDR1/2 and RET) and Axitinib (AURKB, RET) were confirmed.

Zusammenfassung

Aufgrund ihrer bedeutenden Rolle in der Tumorgenese und Metastasierung repräsentieren Proteinkinasen eine der wichtigsten Klasse von Zielmolekülen in der Krebstherapie. Jüngste Fortschritte in der chemischen Proteomik, insbesondere die Verwendung von niedermolekularen Kinaseinhibitoren als Affinitätssonden gekoppelt mit massenspektrometrischer Analytik ermöglicht die Affinitätsreinigung von Kinasen unter nahezu physiologischen Bedingungen. Dieser Vorzug der chemischen Proteomik weckte massives Interesse an der Entwicklung von Strategien, die eine Isolierung möglichst vieler Kinasen für ein Kinom-weites „Profiling“ von Wirkstoffen gestatten. In Kapitel I wurde als Sonde der pan-Kinase Inhibitor VI16743 immobilisiert und das Bindungsprofil von Lysaten aus Krebszellen in „Pull down“-Experimenten charakterisiert. Die Sonde ermöglichte den Nachweis von 179 Kinasen, wovon 30 Kinasen einschließlich 10 Mitgliedern der Phosphoinositolkinase-Familie (PI3K und PI4K) nicht von den Kinobeads erfasst wurden. Da bei Kombination der Kinobeads mit der Sonde VI16743 sowohl die Anzahl als auch die Quantität der angereicherten Kinasen erhöht wurde, stellt VI16743 eine geeignete Ergänzung für Kinobead-Strategie dar. Daneben existieren noch weitere Kinasen, die mit Kinobeads nicht erfasst werden, namentlich die für die Angiogenese relevanten Rezeptortyrosinkinasen VEGFR und FGFR. Mit Hilfe molekularer Modellierung wurden daher drei Sonden (F1 und F2 in Kapitel III, Compound 18 in Kapitel IV) für VEGFR und FGFR designt und synthetisiert. Die Sonde F2 eignete sich zur Anreicherung aller Mitglieder der FGF-Rezeptorfamilie sowie weiterer, tumor-relevanter Kinasen wie KDR, FLT4 und RET aus Lysaten von Tumorzellen und humanem Plazentagewebe. In Kombination mit Kinobeads deckte die Sonde F2 das Spektrum der Angiogeneseinhibitoren Dovitinib und Orantinib einschließlich bereits identifizierter Ziel- wie auch „Off target“-Strukturen ab: AURKA, FLT4/VEGFR3, IKBKE und PDGFR β . Compound 18 eignet sich zur Anreicherung von mehr als 130 Proteinkinasen einschließlich mehrerer Angiokinasen (VEGFR und PDGFR), die mit anderen Breitspektrum-Kinaseinhibitoren nicht nachweisbar sind. Eine Reihe von „Off targets“ der Wirkstoffe Pazopanib (DDR1/2 und RET) und Axitinib (AURKB, RET) wurden über Kinobeads in Kombination mit Compound 18 in kompetitiven Bindungstests bestätigt.

Acknowledgements
List of Publications
Curriculum Vitae

Acknowledgements

At the end of my thesis, I would like to thank all those people who made this thesis possible and an unforgettable experience for me.

First of all, I would like to express my sincere gratitude to my supervisor Prof. Dr. Bernhard Küster for the continuous support of my doctoral study and research, for his patience, motivation, and immense knowledge. His guidance helped me all the time in the research and writing of this thesis. Besides my advisor, I would like to thank Prof. Dr. Dieter Langosch and Prof. Dr. Dirk Haller for being the rest of my thesis committee.

My sincere thanks also go to Dr. Guillaume Médard, who offered extensive support during the experiments and had provided advices and insight which were priceless to me. His attitude to research inspired me a lot. I also want to thank Dr. Karl Krama for the patient explanation of many background knowledge and techniques in biology.

Also I want to express my gratitude to the excellent technical assistances from Andrea Hubauer, Michaela Krötz-Fahning, and Andeas Klaus. I also want to thank our secretaries Gabriele Kröppelt and Silvia Rötzer for always being supportive and having everything well-organized. In addition, I would like to give a big thank you to my fellow labmates at Chair of Proteomics and Bioanalytics: Barbara Ferreira, Benjamin Ruprecht, Chen Meng, Dominic Helm, Heiner Koch, Huichao Qiao, Mathias Wilhelm, Stefan Maier, Stephanie Heinzlmeir, Susan Kläger as well as Dr. Zhixiang Wu, Dr. Fiona Pachl, Dr. Hannes Hahne and Dr. Amin Moghaddas Gholami for the stimulating discussions, for the beer we had together after work, and for all the fun we have had in the last three years.

Last but definitely not least I want to mention some special people, my family. I want to thank my mom and my dad for having faith in me and encouraging me in every decision I made in my life, always believing in my choices that led me to this place. Words can not express how grateful I am to be in their lives and how much this work was enhanced and made easier by them being in mine.

Publications

1. **Xin Ku**, Stephanie Heinzlmeir, Dominic Helm, Guillaume Médard and Bernhard Kuster. A new affinity probe targeting VEGF receptors for kinase inhibitor selectivity profiling by chemical proteomics. *Journal of Proteome Research*. Accepted.
2. **Xin Ku**, Stephanie Heinzlmeir, Xiaofeng Liu, Guillaume Médard and Bernhard Kuster. A new chemical probe for quantitative proteomic profiling of fibroblast growth factor receptor and its inhibitors. *Journal of Proteomics*. 96 (16), 2014, 44-55.
3. **Xin Ku**, He Huang, Hualiang Jiang and Hong Liu. Efficient Iron/Copper Cocatalyzed S-Arylations of Thiols with Aryl Halides. *Journal of Combinatorial Chemistry*, 2009, 11, 338–340.
4. Wei Zhou, Xiaofeng Liu, Zhengchao Tu, Lianwen Zhang, **Xin Ku**, Fang Bai, Zhenjiang Zhao, Yufang Xu, Ke Ding, Honglin Li. Discovery of pteridin-7(8H)-one-based Irreversible Inhibitors targeting Epidermal Growth Factor Receptor (EGFR) Kinase T790M/L858R mutant. *Journal of Medicinal Chemistry*. 2013, 56, 7821–7837.
5. Jiayu Gong, Chaoqian Cai, Xiaofeng Liu, **Xin Ku**, Hualiang Jiang, Daqi Gao and Honglin Li. ChemMapper: a versatile web server for exploring pharmacology and chemical structure association based on molecular 3D similarity method. *Bioinformatics*, 2013. 29(14) : 1827-1829
6. He Huang, Qin Chen, **Xin Ku**, Linghua Meng, Liping Lin, Caihua Zhu, Zhi Chen, Ming Li, Hualiang Jiang, Kaixian Chen, Jian Ding and Hong Liu. A class of Novel alpha-Heterocyclic Carboxaldehyde Thiosemicarbazones Inhibit Topoisomerase II-alpha catalytic activity. *Journal of Medicinal Chemistry*. *Journal of Medicinal Chemistry*, 2010, 53(8), 3048–3064

Oral Presentation

1. 2nd Annual Conference of the International Chemical Biology Society (ICBS 2013: Session VII: Chemical Genetics/Chemoproteomics). New affinity probes for proteomic selectivity profiling of FGFR inhibitors. Oct 7-9, 2013. Kyoto, Japan.

Curriculum Vitae Xin Ku

Persönliche Daten

Familienname	Ku
Vorname	Xin
Geboren am	21.02.1985
Geburtsort	Liaoning
Nationalität	Chinesisch
Wohnhaft in	Helene-Mayer-Ring 7, 80809, München
Familienstand	Ledig
Handy	+49 176 99654955
Email	kuxin0331@gmail.com

Studium

09/2003 - 06/2007	Studium der Pharmazie an der Huazhong Univeristy of Science and Technology, Wuhan, China Abschluss: Bachelor of Science (B.Sc.)
09/2007 - 07/2010	Studium der Medizinische Chemie am Shanghai Institute of Materia Medica, Chinese Academy of Sciences, Shanghai, China. Abschluss: Master of Science (M.Sc.)
Seit 09/2010	Doktorandin am Lehrstuhl für Proteomik und Bioanalytik der Technischen Universität München (Betreuer: Prof. Dr. Bernhard Küster) Titel der Dissertation: „Development and application of small molecule probes for kinase affinity purification and quantitative chemical proteomics“

